INFLUENCE OF SOIL-STRUCTURE INTERACTION ON THE SEISMIC RESPONSE OF ABOVE-GROUND PIPELINES

BetelhemAsmare

A Thesis submitted to

The School of Civil & Environmental Engineering

Presented in Partial Fulfillment of the Requirements for the Degree of Master of Science in Civil Engineering

(Structure)

Addis Ababa University

Addis Ababa, Ethiopia

October, 2017

Addis Ababa University

Addis Ababa Institute of Technology

School of Civil and Environmental Engineering

This is to certify that the thesis prepared by Betelhem Asmare, entitled*: Influence of Soil-Structure Interaction on the Seismic Response of Above-Ground Pipelines* and submitted in partial fulfillment of the requirements for the degree of Master of Sciences in Civil Engineering (Structures) complies with the regulations of the University and meets the accepted standards with respect to originality and quality.

Signed by the Examining Committee:

Dr. Shifferaw Taye		24.10.2017
Advisor	Signature	Date
Dr. –Ing. Asrat Worku		24.10.2017
External Examiner	Signature	Date
Dr. –Ing. Adil Zekaria		24/10/17
Internal Examiner	Signature	Date
Dr. Agizew Niguse		
Chairman	Signature	Date

Dr. Agizew Nigussie
Dean, School of Civil & Environmental Engineering

Director of Postgraduate Program
Addis Ababa University
Addis Ababa Institute of Technology

ABSTRACT

Lifeline systems are intricately linked with the economic well-being, security, and social fabric of the communities they serve. When earthquakes or other hazards strike lifeline systems, they disrupt the flow of resources and provision of services that sustain communities.

Many Lifeline systems are long-span structure. These structures are extended horizontally to allow people, goods, electric power, gas and other item to move freely between locations. When seismic ground motion strikes, these structures may be affected and, consequently, the economy aspect of a country can be disrupted there by leaving people at risk.

The purpose of this thesis has been to investigate the influence of soil-structure interaction on a dynamic property of above-ground pipeline (as an example of long-span structures and lifeline facilities) for five different support conditions.

Three-dimensional (3D) linear finite element analysis of above-ground pipeline for a different base conditions have been made with the help of general purpose software ABAQUS. For this study, a 12m nominal length of a pipeline with API 5L X80 material grade has been used and models have be studied for Kobe 1995 earthquake ground motion. Dashpot and the spring coefficient for a typical foundation have been establish for use in substructure approach for the analysis. From analysis, it has been noted that, the displacement of pipelines on the soft soil to be larger than the displacement of pipeline laid on other type of soil support. It has also been observed that, when the base condition become more flexible, the values of all response increased.

In a view of these observation, therefore, considering SSI effects in seismic design of above-ground structures resting on flexible support conditions like soft soil deposit is essential to minimize the potential damage of earthquake.

From this thesis, it is recommended that, incorporating SSI for lifeline systems (similar to above-ground pipeline structure) is important in order to assure the safety of the structure.

DECLARATION

I hereby declare that all information in this document has been obtained and presented in accordance with academic rules and ethical conduct. I also declare that, as required by these rules and conduct, I have fully cited and referenced all material and results that are not original to this work.

Name:	Betelhem Asmare
Signature	______________
Place	Addis Ababa Institute of Technology
	Addis Ababa University
Date of Submission	October, 2017

ACKNOWLEDGEMENT

First and foremost I would like to thank Almighty God for his unending blessings. I would like also to express my deepest gratitude and respect to my advisor Dr. Shifferaw Taye for his unreserved assistance, constructive, and timely comments at all stages of my work.

My sincere thanks go to S.L.t Messafint Lissanu from Defense engineering College, department of combat, for allowing high speed computational device to run analysis by ABAQUS software tool.

A special thanks goes as well to my scholarship sponsor, Ministry of Education (Female Scholarship) and I acknowledge that I was provided full academic fee for all course works and thesis with pocket money allowance.

Lastly I express my deepest gratitude to all my family and friends who helped me make this thesis a reality.

TABLE OF CONTENT

ABSTRACT I

DECLARATION IV

ACKNOWLEDGEMENT V

LIST OF TABLE IX

LIST OF FIGURE X

LIST OF SYMBOL AND ABBREVIATION XIII

INTRODUCTION 1

1.1. GENERAL 1

1.1.1. Pipeline Structures 3

1.1.2. B0rief History of Pipeline 3

1.1.3. Pipeline in Ethiopia 5

1.2. MOTIVATION 5

1.3. OBJECTIVE 6

1.3.1. General Objective 6

1.3.2. Specific Objective 6

1.4. SCOPES OF THE RESEARCH 6

1.5. OUTLINE OF THE THESIS 7

THEORETICAL BACKGROUND AND LITRATURE REVIEW 8

2.1. INTRODUCTION 8

2.2. THE NATURE OF EARTHQUAKE GROUND MOTION 8

2.2.1. Seismic Wave 8

2.2.2. Ground Motion Characteristics 10

2.2.3. Interaction between Ground and Structure during Earthquake 11
2.3. SOIL-STRUCTURE INTERACTION MECHANISM.. 12
2.3.1. Kinematic Interaction 14
2.3.2. Inertia Interaction 15
2.4. THE INFLUENCE OF SOIL-STRUCTURE INTERACTION ON DIFFERENT TYPE OF STRUCTURES.. 21
2.5. SEISMIC CONSIDERATION FOR ABOVE-GROUND PIPELINE.................... 22
2.6. FINITE ELEMENT ANALYSIS IN ABAQUS/CAE 23
METHOD, MODELING AND ANALYSIS OF ABOVE-GROUND PIPELINES 27
3.1. GENERAL.. 27
3.2. MODELING FOR STRUCTURAL ANALYSIS 28
3.2.1. Pipeline Material Selection.. 28
3.2.2. Support Material of Pipeline.. 29
3.2.3. Pipeline Length.. 29
3.2.4. Structural Idealization.. 30
3.3. FINITE ELEMENT MODELING.. 31
3.3.1. General and Boundary Condition 31
3.3.2. Natural Frequency of Pipeline Structure 32
3.3.3. Loading Condition 33
3.3.4. Impedance Function.. 35
RESULTS AND DISCUSSION.. 43
4.1. INTRODUCTION AND CONVENTIONS 43
4.2. STRUCTURAL RESPONSE RESULTS 44
4.2.1. Acceleration.. 44

4.2.2. Velocity 48
4.2.3. Displacements 51
4.2.4. Bending moment 63
4.2.5. Principal stresses 65
4.3. DISCUSSION 69
CONCLUSION AND RECOMMENDATION 71
5.1. CONCLUSION 71
5.2. RECOMMENDATION AND FURTHER WORK 72
REFERENCES 73
APPENDIX I
APPENDIX A II
APPENDIX B IX
APPENDIX C XI
APPENDIX D XVI

LIST OF TABLE

Table 1: Typical values for Poisson's ratio 21
Table 2: Pipeline data for this study 29
Table 3: Pipeline support data 29
Table 4: Tolerances of lengths according to API specification... 30
Table 5: Natural frequency of pipeline structure... 32
Table 6: Selected ground type and detail of soil parameter. 35
Table 7: Dashpot and stiffness coefficient for different ground type.................................. 42
Table 8: Peak displacement response quantities and percentage displacement of the pipeline with respect to U1 (Transvers or X). 56
Table 9: Peak displacement response quantities and percentage displacement of the pipeline with respect to U2 (vertical or X)... 62

LIST OF FIGURE

Figure 1: Work approach of the thesis 7
Figure 2: Travel path of body waves: (a) Primary wave, (b) Secondary wave 9
Figure 3: Travel path of body waves: (a) Rayleigh wave, (b) Love wave 10
Figure 4: Wave propagation during SSI 11
Figure 5: Substructure approach to analysis of SSI problem 14
Figure 6: Simplified model for analysis of inertial interaction 15
Figure 7: Frequency-dependent foundation stiffness and damping factors 18
Figure 8: Hypothetical shear stress-strain curve for soils 19
Figure 9: Above-ground support system 23
Figure 10: (a) Finite element model (b) adaptable mesh for API 5L X80 steel pipeline. 31
Figure 11: Mode shapes of pipeline structure 33
Figure 12: (a) Ground motion application in pipeline structure (b) Time history record of Kobe ground motion. 34
Figure 13: Foundation size for pipeline and axis orientation of soil-foundation system 35
Figure 14: Schematic view of above-ground pipeline foundation. 37
Figure 15: Surface foundation for homogenous stratum over bed rock. 38
Figure 16: Soil-foundation system for dense, stiff and soft soil support 40
Figure 17: Presentation module for dashpot and stiffness coefficient for different ground type in ABAQUS 42
Figure 18: Axis orientation for the responses with respect to its nomenclature in ABAQUS. 43
Figure 19: (a) Time history records of Kobe (b) Ground motion application on the pipeline structure. 44
Figure 20: Selected node for acceleration, velocity and displacement response of the pipeline in different views and sections. 44

Figure 21: (a) Time history records of Kobe (1995) , Nodal acceleration history response of the pipeline under (b) fixed base (c) fixed base and rock base with reference to A1 (Transversal or X) Direction.. 45
Figure 22: Nodal acceleration history response of the pipeline under (a) fixed base and dense-soil base (b) fixed base and stiff-soil base with reference to A1 (Transversal or X) Direction 46
Figure 23: Nodal acceleration history response of the pipeline under fixed base and soft-soil base with reference to A1 (Transversal or X) Direction 47
Figure 24: Nodal velocity history response of the pipeline under fixed base with reference to V1 (Transversal or X) direction.. 48
Figure 25: Nodal velocity history response of the pipeline under (a) fixed base and rock base (b) fixed base and dense-soil base with reference to V1 (Transversal or X) direction. 49
Figure 26: Nodal velocity history response of the pipeline under (a) fixed base and stiff-soil (b) fixed base and soft- soil base with reference to V1 (Transversal or X) direction. 50
Figure 27: Nodal displacement history response of the pipeline under (a) fixed base (b) fixed base and rock base with reference to U1 (Transversal or X) direction .. 52
Figure 28: Nodal displacement history response of the pipeline under (c) fixed base and dense-soil base (d) fixed base and stiff-soil with reference to U1 (Transversal or X) direction... 53
Figure 29: Nodal displacement history response of the pipeline under fixed base and soft-soil base with reference to U1 (Transversal or X) direction............................. 54
Figure 30: Displacement response contour of the symmetric model of the pipeline in the direction of U1 (transvers) under (a) fixed base (b) rock base (c) dense-soil base condition. 55
Figure 31: Displacement response contour of the symmetric model of the pipeline in the direction of U1 (transvers) under (a) stiff-soil base (b) soft-soil base condition. 56

Figure 32: Nodal displacement history response of the pipeline under fixed base with reference to U2 (Vertical or Y) direction. 57
Figure 33: Nodal displacement history response of the pipeline under (a) fixed base and rock base (b) fixed base and dense-soil base with reference to U2 (Vertical or Y) direction. 58
Figure 34: Nodal displacement history response of the pipeline under (a) fixed base and stiff-soil (b) fixed base and soft- soil base with reference to U2 (Vertical or Y) direction. 59
Figure 35: Displacement response contour of the symmetric model pipeline in the direction of U2 (vertical) under (a) fixed base condition (b) dense-soil (c) stiff-soil base (d) soft-soil base condition. 61
Figure 36: Bending moment diagram along the length of the pipeline (a) fixed base and rock base (b) fixed base and dense-soil base (c) fixed base and stiff-soil base (d) fixed base and soft-soil base condition. 63
Figure 37: Section bending moment value of pipeline (a) support moment under soft-soil base (b) span moment under soft soil (c) support moment under dense-soil base (d) span moment under dens-soil... 64
Figure 38: Principal stress response contour of the pipeline and selected element............ 65
Figure 39: Nodal principal stress history response of the pipeline under (a) fixed base (b) fixed base and rock base. 66
Figure 40: Nodal principal stress history response of the pipeline under (a) fixed base and dense-soil base (b) fixed base and stiff-soil.. 67
Figure 41: Nodal principal stress history response of the pipeline under fixed base and soft-soil base. 68
Figure 42: Presentation of 2D beam-element...XII
Figure 43: The lumped element mass matrix. XIII

LIST OF SYMBOL AND ABBREVIATION

a_o	dimensionless frequency factor
B	width of the foundation
C_x, C_y, C_z	radiation dashpot coefficient of the foundation in longitudinal, transverse and vertical direction of a foundation.
D_f	total foundation height
D_p	specified outside diameter of pipe
d	height of effective side wall
E	Young modulus
f_n	natural cyclic frequency
f_c	natural cyclic frequency of stratum for compressing mode of vibration
f_s	natural cyclic frequency of stratum for shearing mode of vibration
G	shear modulus of soil
I	moment of inertia
[K]	element stiffness matrix
K_x, K_y, K_z	dynamic stiffness of the foundation in longitudinal, transverse and vertical direction of a foundation
L_f	length of foundation
[M]	element mass matrix

$[M_{ec}]$	consistent element mass matrix
$[M_{el}]$	lamped element mass matrix
t	specific wall thickness
$V_{s\,30}$	average shear wave velocity over the top 30m soil.
υ_s	Poisson ratio of Soil
υ_p	Poisson ratio pipe
ω_n	natural circular frequency
API	American Petroleum Institute
ASME	American Society of Mechanical Engineers
ANS	American National Standards Institute
ASTM	American Society of Testing Materials
FFM	free-field ground-motion
FIM	foundation input ground-motion
SSI	soil-structure interaction

CHAPTER ONE

INTRODUCTION

1.1. GENERAL

Pipeline structures are one of lifeline structures and they are used to convey water and fuel. They are among civil engineering lifeline structures. Lifeline facilities are infrastructures that are vital to the development and suitability of modern economy and quality of life which satisfy fundamental needs for individuals and communities. They are often grouped into four principal systems; thus are: (i) supplying energy (electric power, gas and petroleum), (ii) govern the water cycle (potable water treatment and supply, wastewater and storm water collection and treatment), (iii) civilian communication (telephone, television and internet), and (iv) transportation (roads, railroads, airports, and harbors). Gas pipeline, bridge structure and power transmitters are some examples of lifeline structures. These systems are intricately linked with the economic well-being, security, and social fabric of the communities they serve and the country at large. When earthquakes or other hazards strike lifeline systems, they disrupt the flow of resources and provision of services. In worst case scenario, these disruptions can lead to regional, national and even global social and economic impacts [22].

Many lifeline facilities are long-span structures. These structures allow people, goods, electric power, gas and other item to move freely between locations. Of these structures, pipeline is one of the cost-effective means for the transportation of water supply and sewers, in addition oil and gas from their sources to desired points. The seismic design and assessment of these structures have become an essential issue for sustainable development in recent years [5].

The suitable assessments of response to seismic loading for structures must appropriately characterize a number of factors including [17]: a) earthquake source effect: these effects generally refer to the earthquake magnitude, rupture mechanism, and location relative to the site, b) travel path effects: refer to the attenuation of seismic waves as they travel from the source through bedrock towards the site, c) local site effects: refer to the frequency-dependent amplification or attenuation experienced by seismic waves propagating towards the surface through soil.

The result of these first three effects is a free-field seismic ground motion at the ground surface. Free-Field Motion (FFM) refers to the lack of any influence from structural vibrations on the motion. The last one is d) soil-structures interaction effects: account for the flexibility of the foundation support beneath the structure and potential variations between the foundation and free-field motions [17].

For determining the seismic response of structures, it is a common practice to assume the structure to be fixed at its base. In fact, if the ground is stiff reasonably such as, structures founded on solid rock, it is reasonable to assume that the input motion of the structure due to a design earthquake is essentially identical to the motion of the free field, which is defined as the motion experienced at the same point before the structure is built. On the other hand, for structures constructed on soft soil, certain adjustment that account for determining the seismic response is necessary [1].

Long-span structures are structures whose structural components are extended for a very long distance. Most of these structures share a few common characteristics; thus are (i) spatial extent, (ii) generally varying soil condition at different supports, and (iii) possible incoherence in the seismic input. These structures are more susceptible to relatively severe soil-structure interaction effect during earthquakes when compared to buildings due to the above shared characters [24].

This thesis investigates the influence of soil-structure interaction on the dynamic properties and seismic response behavior of long-span above-ground pipelines and findings from this study are believed can be adapted to work on other structures in order to understand the influence of these shared characters. The study will be made using finite element software ABAQUS/ CAE [25].

Above-ground pipeline structures are relatively large pipe spanning a long distance of connected segments of pipe with pumps, valves, control devices, and other facilities needed for operating the system [5]. This thesis focus on the response behavior analysis of above-ground pipeline structures in view of the fact that, earthquake impact on pipelines may result in the release of hazardous materials and possibly major accidents leading to injuries and fatalities in nearby areas. The seismic response of pipelines is dominated by soil deformation so that vulnerability assessment strongly depends on the ground-pipeline interaction [5].

1.1.1. Pipeline Structures

Pipelines are safe and economical means of transporting gas, water, sewage and other fluids. Failure of an oil and gas pipeline can cause serious economic and environmental damage and in some circumstances it may lead to gas explosions resulting fatalities and severe loss of property. Furthermore, a large amount of money is being spent annually in repair and replacement of pipelines. In terms of property damage, PHMSA (Pipeline and Hazardous Material Safety Administration) records indicate that the 20-year average (1993-2012) cost of significant pipeline incidents is over 318 million dollars, the 10-year average (2003-2012) cost is over 494 million dollars, and the 5-year average (2008-2012) cost is over 545 million dollars. To minimize the risk of any accident, injury and material loss and to prevent the damages that cause a great hazard to the environment, the pipeline industry has been interested in predicting soil and pipe behavior when the pipeline is subjected to external loadings [21].

1.1.2. Brief History of Pipeline

Pipelines have been used for thousands of years but modern day pipelines have their origins in Pennsylvania, USA in the mid 1800s. As technology improved, larger and longer pipelines were built, and the demand for energy during World War II increased both the need and extent of pipelines in the USA and, subsequently, then around the world most countries now have large oil and gas pipelines systems. Worldwide, there are about 3,500,000km of pipelines transporting oil and gas [13].

‘Transmission’ pipelines are the main ‘arteries’ of the oil and gas business working none stop and continuously supplying energy needs. They are critically important to the economies of most countries'. The oil and gas are transported in these large transmission pipelines to refineries, power stations, etc., and converted into energy forms such as gasoline for automobiles, and electricity for homes. The fuels providing the world with its primary energy needs are [13]:

Oil = 34%	Coal = 24%
Gas = 21%	Nuclear = 7%
Hydro = 2%	‘Other’ = 12%

Without the service of such pipelines, it would not be possible to satisfy the huge oil and gas demands. These pipelines are also very safe forms of transporting energy: Pipelines are forty times safer than rail tanks, and hundred times safer than road tank [13]. These high pressure, large capacity pipelines carry hazardous products, and consequently, they are designed, constructed and operated using recognized standards that all have a focus on safety. Additionally, these pipelines have to satisfy safety regulations in most countries [13]; these high standards and regulations ensure safe and secure pipelines.

While oil was transported in wooden barrels on rivers by horse-drawn barges in early 1860s. The next major change in pipeline engineering was the construction of long distance pipelines and this was pioneered in the USA in the 1940s; thus was due to the energy demands of the Second World War. ‘Long’ pipelines had been built at the turn of the century; for example, in 1906 a 755km (472mi), 8 in diameter pipeline was built from Oklahoma to Texas; similar length, small diameter (8 in to 12 in) lines were built in Baku at the same time; in 1912, a 272km (170 mi), 16 in diameter manufactured gas pipeline was built in 86 days, in Bow Island, Canada to make it one of the longest pipelines in North America [13].

To support this growth in energy demand, pipeline infrastructure has grown by a factor of one hundred in approximately 50 years. It has been estimated that world pipeline expansion could be up to 7% per year over the next 15 years. Pipelines are energy transporters, and hence their growth in tomorrow’s world will follow future energy demands and the future will test designers and others in the oil business in view of:

- the need to build bigger, safer, better pipelines, quicker and cheaper, will test investors, designers, constructors and regulators;
- the markets will be tested by balancing increasing demand with decreasing supplies, or highly contested supplies [13].

Most of the future pipelines will be the same as today’s pipelines, so the future, in terms of basic engineering, is predictable and conservative as it has been for the past 150 year since their use for conveying oil and gas come to effects. However, maintenance of pipeline safety are recent day concern and along with the security of supply as their assets age.

This ageing expose pipeline to corrosion problems, reduce their capacity to resist impact damage, accelerate fatigue and cracking, in addition to earthquake effects that threaten their integrity.

This will bring major changes and challenges to both the oil and gas companies, and their pipeline operators. The good news is that all these issues, challenges, etc., present real engineering problems and, hence, exciting opportunities for pipeline engineers. This means that anybody entering the business today will be both challenged and rewarded [13].

1.1.3. Pipeline in Ethiopia

The oil pipeline construction project from Djibouti to Ethiopia is planned to begin after the middle of 2017 (Fig. 2) [14]. Black Rhino Group, a subsidiary of the US based Blackstone Group, plans to construct a 550km long line to transport refined diesel, gasoline and jet fuel from port access in Djibouti, Damerjog, to central Ethiopia. According to the plan, the line will reach Awash, 250km east of Addis Ababa in Afar Regional State.

The governments of Ethiopia and Kenya also agreed to construct an oil pipeline from Lamu Port under the transnational project of Lamu-Southern Sudan-Ethiopia Transport Corridor (Lapsset). The Ethio-Kenya line will also transport oil to Ethiopia [14].

1.2. MOTIVATION

Protecting different lifeline facilities from earthquake hazard is important in order to protect the economic demand of a country because damage to one lifeline system may have undesirable effect. For example loss of electricity can affect the flow pressure in the gas system or water system [22].Effects from earthquake are natural phenomena in Ethiopia in general and along both planned pipeline project in particular.

Pipelines are also among the most vital lifeline facilities and one type of long-span structure, which are exposed to different base condition along with their length. For such reason, minimize the effect of earthquake on this kind of structure; examining the behavior of soil-structure interaction (SSI) is one of the most critical scenarios to provide viable and sustainable project facility and this thesis is conserved with this phenomena as in core object.

As mentioned above, Ethiopia has a plan to construct long pipeline, which is 550km in the near future. This pipeline will pass through a seismic region and the technology of this long-span structure is new to the country. This indicates that it is timely act to start investigation regarding the effect of soil-structure interaction of overlying long-span pipeline system.

1.3. OBJECTIVE

1.3.1. General Objective

The main objective of this thesis is to study the effects of soil-structure interaction on dynamic properties and seismic response of above-ground long-span structures with particular reference to pipeline system applying the finite element analysis method. It is believed that the study will help designers established when to account for potential effect of SSI and when it can be neglected in the planning of such system. It can also help the structural engineer to give attention not only to the response of a structure to seismic effects; but also to that of the underlying soil.

1.3.2. Specific Objective

This research has the specific objectives of:

- studying the effect of soil-structure interaction of the pipeline under different base conditions along with is length.
- examining the dynamic response of a gasoil pipeline facility taking in to account possible effect of soil-structure interaction at various degrees.

1.4. SCOPES OF THE RESEARCH

The following assumptions have been made in this study:

— it is assumed that the pipeline rest on a fairly straight terrain;
— the hammering effect of the fluids is not take in to account;
— only the self-weight, the weight of fluid and the seismic excitation are considered;
— no account is taken for kinematic soil-structure interaction effects;
— only the main pipeline is analyzed; no other part of the pipeline or appurtenances are included in modeling for analysis;
— incoherence in the seismic input of above-ground pipeline is not take in to account;

1.5. OUTLINE OF THE THESIS

This thesis has three main portions (Fig. 1). The first part presents detailed state-of-the art review on above-ground pipeline and the mechanism of soil-structure interaction. This followed by the modelling for analysis of a typical above-ground pipeline structure along with precedence for a step by step analysis based on the finite element concept and application of a software system. The results from investigation and analysis are presented and discussed in detail followed by conclusion and recommendation in the last portion of the work.

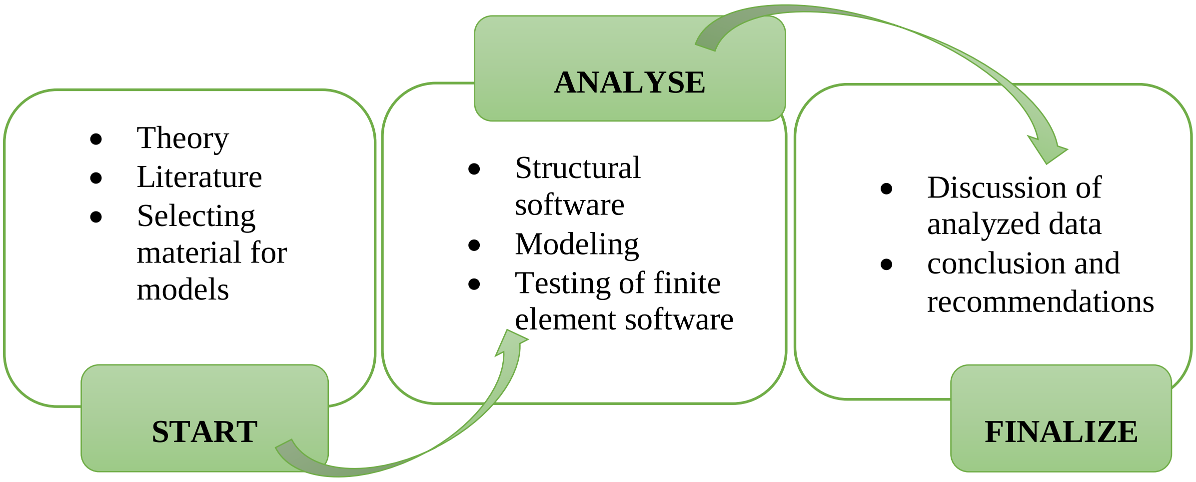

Figure 1: Work approach of the thesis

The above three main portion of the thesis are organized in five chapters. The first chapter includes the background, general information about pipeline, motivations, objectives, and scope of the study. Theoretical background of soil-structure interaction mechanism are presented in Chapter 2. Method, modeling of pipeline, impedance function computation and finite element analysis are reviewed in Chapter 3. Results of the analytical study, discussions and interpretations are presented in Chapter 4. Chapter 5 is devoted to conclusions and recommendations.

CHAPTER TWO

THEORETICAL BACKGROUND AND LITRATURE REVIEW

2.1. INTRODUCTION

Earthquake in populated areas throughout the world causes extensive damage to various structures; this generally results in catastrophic loss of human life and enormous economic damage. However, the damage may also be attributed to the inadequate design of the structures. Earthquake manifestation may be explained by the theory of large scaled tectonic processes, referred as "plate tectonic". Plates are large and stable rigid rock slabs with a thickness of about 100km, forming the crust or lithosphere and part of the upper mantle of the earth. Large tectonic forces take place at the plate edges due to relative movement of the lithosphere–asthenosphere complex. These forces awaken physical and chemical changes and affect the geology of the adjoining plates. However, only the lithosphere has the strength and the brittle behavior to fracture; thus, causing an earthquake [21].

2.2. THE NATURE OF EARTHQUAKE GROUND MOTION

2.2.1. Seismic Wave

The seismic energy that is released during an earthquake radiates outward in all directions in the form of waves. Earthquake shaking is created by two types of elastic seismic waves: body and surface. At small distances from the source, the shaking is mostly a combination of these waves. Body waves travel through the earth's interior layers. They include two waves, longitudinal or primary waves (P- waves) and transverse or secondary waves (S- waves) as shown in Fig. 2. P and S waves are also termed "preliminary tremors" because, in most earthquakes, they are felt first [18, 19].

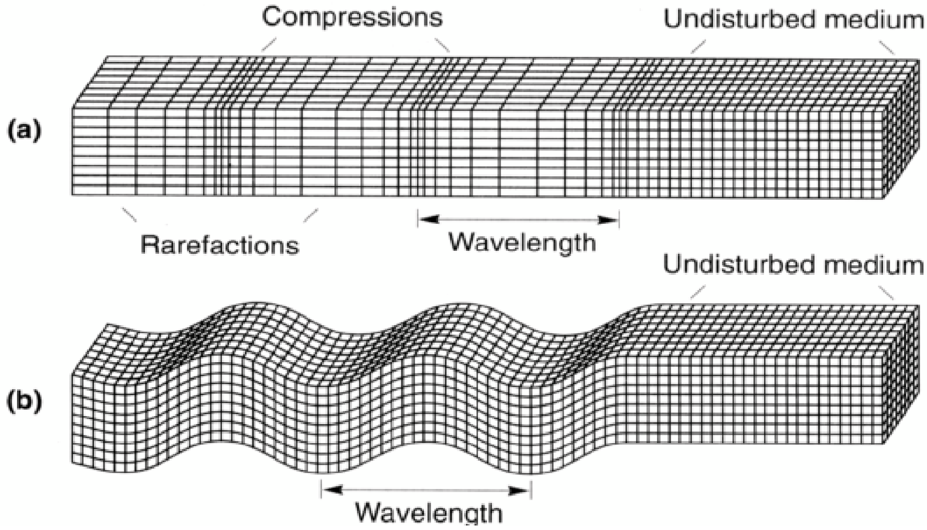

Figure 2: Travel path of body waves: (a) Primary wave, (b) Secondary wave [18].

P-waves generate alternate push (or compression) and pull (or tension) along the rock, where the medium expands and contracts as the waves propagate. P-waves are seismic waves with relatively little damage potential. S-waves propagation causes vertical and horizontal side to side motion, which causes shear stresses in the rock over their paths (also defined as shear waves). Their propagation can be separated into two components, one of them horizontal (SH) and the other vertical (SV), and they both produce significant damage. P-waves travel faster, (1.5-8.0 km/s), while S-wave are slower (50%-60% of the speed of P-waves), where the speed of body waves is governed by the density and elastic properties of the rock and the path in which they pass through [19].

Surface waves, propagate across the outer layers of the earth's crust, are caused by constructive interference of body waves travelling parallel to the ground surface and various underlying boundaries. Such waves are classified into Love (L- waves) and Rayleigh (R-waves) as shown in Fig. 3. These waves stimulate large displacements and hence are also called "principal motion". They are most distinct at distances further away from the earthquake source. Surface waves are most eminent in shallow earthquake while body waves are equally well represented in earthquake at all depths. Because of their long period in earthquake activity, surface waves cause severe damage to structural systems [19].

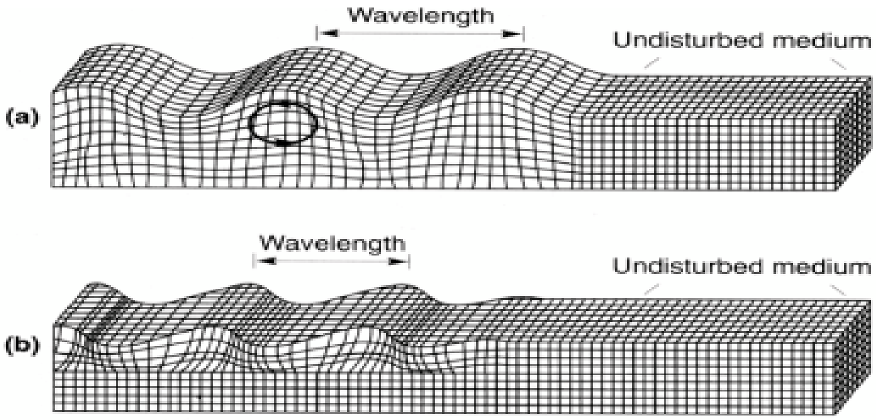

Figure 3: Travel path of body waves: (a) Rayleigh wave, (b) Love wave [19]

Body waves are reflected and refracted at interfaces between different layers of rock. When reflected and refracted waves occur, some of the energy transformed among layers. Immaterial whether the incident wave was P or S, the reflected and refracted waves, also describe as "multiple phase waves" each consists of P and S waves, such as PP, SS, PS and SP. Their name referred to the travel path and mode of propagation. For example, SP starts as S and then continues as P. However, when P and S waves reach the ground surface, they are reflected back to move upwards and downwards, which leads to significant local amplification of the shaking at the surface. It was shown that seismic waves are affected by soil properties and local topography [19].

2.2.2. Ground Motion Characteristics

Earthquake engineers are interested in order to assert soil-structure interaction phenomena, it is important to identify the variable and parameter of an earthquake that influence the nature of the interaction. The ground motion produced by earthquake is generally complicated phenomena. At a given point, those motion can be completely described by three component of translation and three component of rotation. In practice, the rotational component are usually neglected; three orthogonal component of translation motion are most commonly measured. Typical ground motion records such as acceleration-time history, large amount of information. To express all of this information precisely, every detail in each plot must be described.

It is not necessary to reproduce each time history exactly to describe the ground motion adequately for engineering purposes. It is necessary, however, to be able to describe the characteristics of the ground motion that are of engineering significance and to identify a number of ground motion parameters that reflect those characteristics [19].

A number of different ground motion parameters have been proposed, each of which provides information about one or more of these characteristics. In practice, it is usually necessary to use more than one of these parameters to characterize a particular ground motion adequately [18].

2.2.3. Interaction between Ground and Structure during Earthquake

When the seismic wave E_0 generated by an earthquake fault reaches the bottom of the foundation, they are divided into two types as shown in Fig. 4 these are;

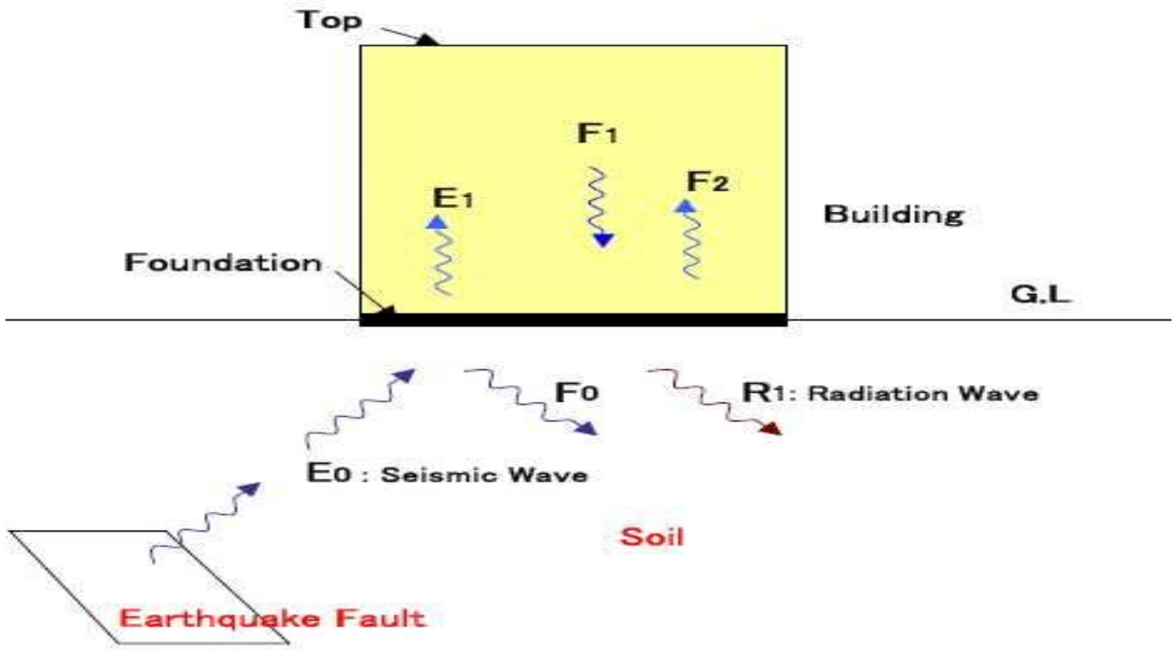

Figure 4: Wave propagation during SSI [17].

transmission waves, E_1, which are approaching a structure and reflection waves, F_o, which are reflected back in to the ground. When the transmission waves enter in to the building, they travels in upward direction due to which the structure is subjected to motion. Then, they are reflected at the top and travel back down to the foundation of the structure these are designated F_1.

At this stage, SSI phenomenon takes place. Again a part of waves is transmitted into the grounds, while the rest are reflected back again and starts to move upwards through the structure, these are designated F_2 as shown in Fig. 4. The waves that are transmitted to the ground are known as radiation waves, these are designated R_1. When the radiated waves are in small amount, the seismic waves once transmitted into the structure continue to stay trapped in the building, and the structure starts to vibrate continuously for a long period of time, similar to the lightly damped structure [17].

The damping caused by radiation waves is popularly known as Radiation Damping of the soil [16]. The radiation damping results in increase of total damping of the soil-structure system in compare to the structure itself. In addition, under the influence of SSI the natural frequency of a soil- structure system shall be lower than the natural frequency of the soil alone. These interactions also increase the overall displacement of the structure and foundations may translate and rotate [17].

2.3. SOIL-STRUCTURE INTERACTION MECHANISM

When a structure is founded on a solid rock and it is subjected to an earthquake load, the extremely high stiffness of the rock constrains the rock motion to be very close the free-field motion. On the other hand, the same structure would respond differently if it supported on a soft soil deposit. In the latter case, the inability of the foundation to conform to the deformation of the free-field motion would cause the motion of the base of the structure to deviate from the free-field motion. Furthermore, the dynamic response of a structure itself would induce deformation of the supporting soil. These two aspects are called kinematic interaction and inertial interaction; respectively. The sum of both effects, in general, is known as dynamic Soil-Structure Interaction (SSI) [19].

Evaluation of effects of dynamic SSI requires proper modeling of soil-structure analysis system in a view of the involved uncertainties in system’s parameters and randomness in the input earthquake motions. Modeling of SSI for dynamic analysis falls into two main categories, namely; direct methods and multistep methods (substructure approach) [17].

The direct method approach, the soil and structure are included within the same model and analyzed in a single step. The soil is often discretized with solid finite elements and the structure with finite beam elements. Hence, a true non-linear analysis is possible in addition to linear analyses. In this case, coupled nonlinear equations are solved using standard step-by-step numerical integration procedures. However, results from nonlinear analysis can be quite sensitive to poorly-defined parameters in the soil constitutive model and, consequently, the analyses remain quite expensive from a computational standpoint [17].

In the substructure method of analysis, the two systems, that is, the superstructure and foundation medium are treated as two independent models. The connection between the two models is established by the interaction forces acting on the interface. The dynamic equilibrium equations are finally written in terms of interface degrees of freedom and solved either in the time domain or in the frequency domain [17].

A complete solution of SSI under seismic excitation, therefore, can be conveniently performed in three steps (Fig. 5) [17].

1. The motion of the foundation is modified in the absence of superstructure; the resulting motion is called Foundation Input Motion (FIM). Since inertial effects are neglected, the FIM represents the effects of kinematic interaction only.
2. Dynamic impedance of the foundation (spring and dashpot coefficients) associated with translation, rocking, and cross-rocking oscillations are determined.
3. The seismic response of the superstructure supported on springs and dashpots is computed, which is subjected to foundation input motion of Step1 above.

The principal advantage of the substructure method is its flexibility. Because each step is independent of the others, the analyst can focus resources on the most significant part of the problem.

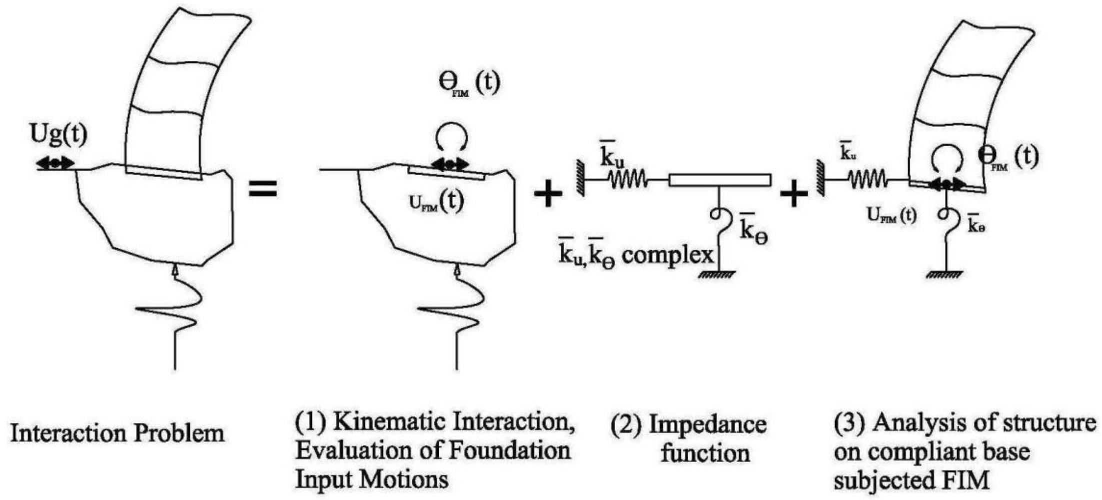

Figure 5: Substructure approach to analysis of SSI problem [17].

Soil-structure interaction provisions in the recent seismic design codes are based on simplified analytical formulation of substructure method. This simplified analysis predicts the variation of first-mode period and damping ratios between the flexible cases, which incorporates the flexibility of both the foundation-soil system and the structure, and the fictional “fixed-base” case. For the purpose of this study substructure method of approach is used in order to investigate effect of SSI for above ground pipeline structure.

2.3.1. Kinematic Interaction

The presence of stiff foundation elements on or in soil will cause foundation motions to deviate from free-field motions. Three mechanisms can potentially contribute to such deviations; these are [19]: (a) base-slab averaging; free-field motions associated with inclined and incoherent wave fields are “averaged” within the footprint area of the base-slab due to the kinematic constraint of essentially rigid-body motion of the slab, (b) embedment effects; the reduction of seismic ground motion with depth for embedded foundations, and (c) wave scattering; scattering of seismic waves off corners and asperities of the foundation. These effects can be, however, neglected if the dimensions of the foundation are small compared to the wavelength of FFM in interested frequency range [19].

2.3.2. Inertia Interaction

General

The mass of structure and foundation causes them to respond dynamically. The SSI effect, which is associated with the mass of the structure, is termed as inertial interaction. It is purely caused by the inertia forces (seismic acceleration times mass of the structure) generated in the structure due to the movement of masses of the structure during vibration. The inertial loads applied to the structure lead to an overturning moment and a transverse shear. If the supporting soil is compliant, the inertial force transmits dynamic forces to the foundation causing its dynamic displacement that would not occur in case of a fixed-base structure. The degree of Influence of SSI on response of structure depends on the following factors: Stiffness of soil, dynamic characteristics of structure itself i.e. natural period and damping factor, stiffness and mass of structure.

Fig. 6 illustrate a system consists of a SDOF structure with height h, mass m, stiffness k, and viscous damping coefficient c. The base of the structure is allowed to translate relative to the free-field by an amount of u_f and rotate an amount θ. The impedance function is represented by lateral and rotational springs with complex stiffness $\bar{k}_u$ and $\bar{k}_\theta$ respectively.

This model can be viewed as a direct model for a single-story building; or more generally, as an approximate model for a multi-mode multi story structure that is dominated by the first mode response. h is interpreted as the distance from the base to the centroid of the inertial forces associated with the first mode response [16].

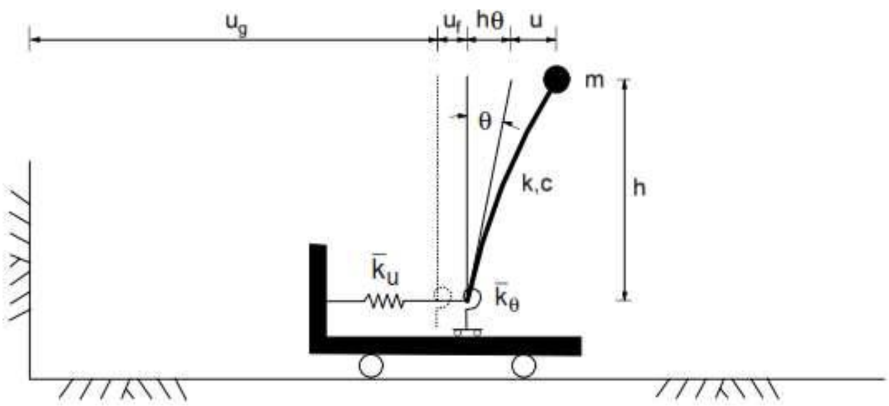

Figure 6: Simplified model for analysis of inertial interaction [18]

Impedance function

(Gazetas & Tassoulas, 1987) and (Fotopoulou, et al., 1989) have published a comprehensive series of studies on the static and dynamic response of embedded rigid foundations having various plan shapes. Among others they developed closed form semi-analytical expressions and charts for stiffness and damping of horizontally and rotationally loaded arbitrarily-shaped rigid foundations embedded in homogeneous soil. These expressions are based on some simple physical models calibrated with the results of rigorous and efficient boundary-element and finite-element elasto-dynamic formulations as well as with numerous results from the published literature [10].

The impedance function of a foundation depends on number of factors including soil profiles, foundation embedment, foundation shape, foundation flexibility and other. As the result the expression which is used to define impedance function must comprise these entire factors [9]. Mathematically, an impedance function is a matrix which relates the forces (e.g., base shear and moment) at the base of the structure to the displacement and rotations of the foundation relative to the free-field. The term in the impedance function are complex-valued and frequency dependent. When the value of impedance parameters at a single frequency must be used (as in case in model in Fig. 6), values at the predominant frequency of the soil- structure system are selected.

A complete set of simplified impedance functions for rigid circular or rectangular foundations located on ground surface and underlain by homogenous visco-elastic half space associated with swaying, vertical, rocking, and cross-swaying-rocking oscillations were summarized by Gazetas [10,11].

$$\bar{k}_j = k_j(ao, v) + i\omega c_j(ao, v) \tag{2.1}$$

Where j denotes either deformation mode (horizontal, vertical and rotational deformation), ω is circular frequency, a_o is a dimensionless frequency defined by a= ωr/Vs and v is Poisson ratio of the soil. The real stiffness and damping of the translational and rotational foundation springs and dashpots are expressed by [17].

$$k_u = \alpha_u K_u \qquad C_{u=}\beta_u \,(k_u \times \frac{r_1}{Vs}) \tag{2.1a}$$

$$k_v = \alpha_v K_v \qquad C_{u=}\beta_u \,(k_u \times \frac{r_1}{Vs}) \tag{2.1b}$$

$$k_\theta = \alpha_\theta K_\theta \qquad C_{\theta=}\beta_\theta \,(k_\theta \times \frac{r_2}{Vs}) \tag{2.1c}$$

where α and β in Eq. 2.1a, 2.1b, 2.1c express in the frequency-dependence of impedance function, V_s is shear wave velocity of the soil and r is the foundation translational and rotational radius and K represents the static stiffness of the foundation for the respective mode of deformation.

Typical frequency dependent values of α and β are presented in Fig. 9 for a horizontal motion and rocking motion, while K_u and K_θ for a disk on a half-pace is given by [21]:

$$K_U = \frac{8}{2-v} \times Gr_1 \tag{2.2a}$$

$$K_U = \frac{8}{2-v} \times Gr3_1 \tag{2.2b}$$

Where G is soil dynamic shear modulus, υ is soil Poisson's ratio and *r* is foundation radius. Foundation radii are computed separately for translational and rotational deformation modes as:

$$r_1 = \sqrt{\frac{Ao}{\Pi}} \qquad r_2 = \sqrt{\frac{4.Io}{\Pi}} \tag{2.3}$$

Despite the demonstrated utility of the impedance function formulation shown above, commonly encountered conditions such as non-uniform soil profiles, embedded, non-circular, or flexible foundations and the presence of piles or piers are not directly modeled by these procedures. The effects of such conditions on foundation impedance can be approximately simulated with adjustments to the basic solution [17].Generally, a summary of spring and dashpot values for different types of foundation type and shapes, embedment and soil profile are given in Gazetas [10,11]. These values can be used in response history analysis by directly considering the frequency dependence (Fig. 7) of both spring and dashpot term.

In response spectral and pseudo-static analysis approach, however, values of impedance parameters at a single frequency must be used. Hence, dynamic stiffness dashpot values are determined at the natural frequency of a soil-structure system [16].

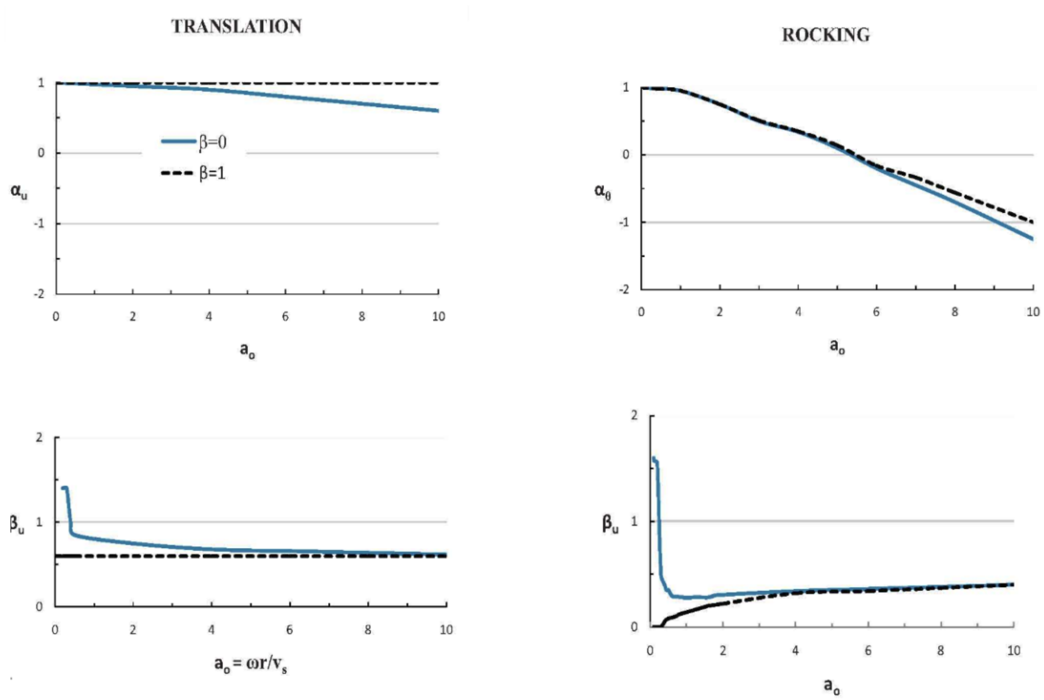

Figure 7: Frequency-dependent foundation stiffness and damping factors [17].

Design parameters for computation impedance function

In the design of foundation, the geometric properties of the foundation and the physical properties of the underlying soil are the basic properties, which should be determined first.

The geometric properties of the foundation include: center of gravity, moments of inertia and mass moments of inertia. The physical properties of the soil include damping and stiffness characteristics of the supporting soil formation [20].

Evaluation of soil parameters

In order to evaluate the impedance function (spring stiffness and the corresponding damping ratios) required for analysis of dynamic soil-structure interaction problems, it is necessary to determine relevant values for the soil parameters including dynamic sheer modulus (G), damping ratio (ξ) , Poisson's ratio(ν), and mass density (ρ) [20].

Shear modulus, G

The mechanism governing the stress-strain behavior of soils at small strains involves mainly the stress-deformation characteristics of the soil particle contacts and is not controlled by the relative slippage of particle associated with longer strains. As a consequence, the stress-deformation behavior of soil is much stiffer at very small strain levels than at usual static strain levels.

It is therefore inappropriate to obtain a shear modulus directly from a static stress-deformation test, such as a laboratory triaxial compression test or a field plate-bearing test, unless the stress and strains in the soil can be measured accurately for very small values of strain [20].

Even at very small values of strain, the stress-strain relationship is non-linear. Therefore, it becomes appropriate to define the shear modulus as an equivalent linear modulus having the slope of the line joining the extremities of a closed loop stress-strain curve shown in Fig. 8.

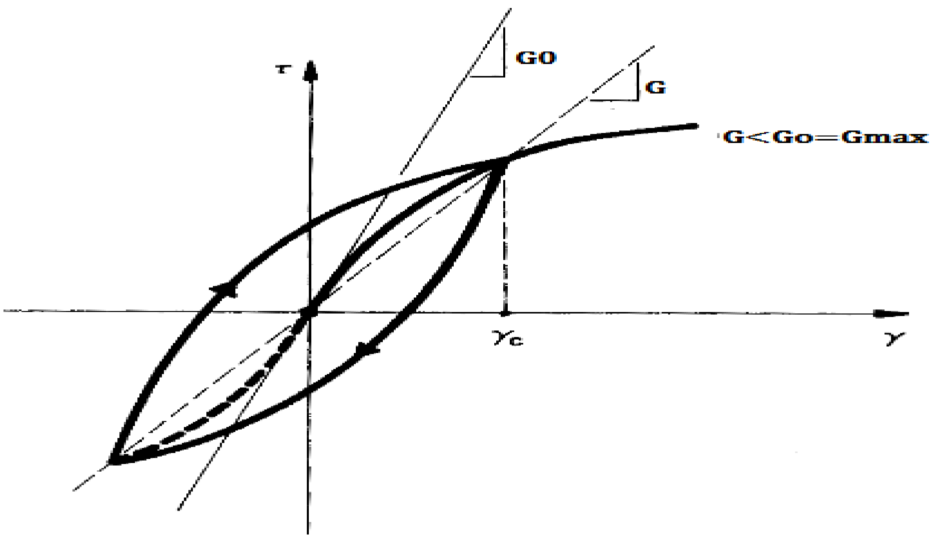

Figure 8: Hypothetical shear stress-strain curve for soils [11].

It is obvious that the shear modulus so defined is strain dependent, and that in order to conduct an equivalent linear analysis; it is necessary to know the approximate strain amplitude in the soil.

For conditions of controlled applied strain, the ordinates of the shear stress in Fig. 10 and therefore G, will vary (usually decrease) with number of cycles applied until a stable condition is reached.

Hence, only the stable equivalent linear value of shear modules will be considered and will be termed the shear modulus.

The shear modulus of the soil can be obtained from the basic relation in Eq. 2.4:

$$G_{Max} = V_s^{\,2} \times \rho \tag{2.4}$$

where G_{Max}= Shear modulus (at very low strain level occurring in the test)

ρ = Mass density of the soil

V_s =Shear wave velocity.

Damping ratio (ξ)

The soil-foundation system consists of two source of damping.

Material "or hysteretic damping"

This kind of damping is an internal property of the soil material. It is a measure of energy lost as a result of hysteretic effects, in which caused by inelastic behavior of soil supporting the foundation and it will depend on the level of strain induced in the soil. If strain is high material damping, can be sustained but if strain is low it can be neglected [15].

Geometric "or radiation damping"

This kind of damping is not an internal property of the soil material that occurs as dynamic force in the structure, in which case the foundation tend to deform the soil and produce stress wave that travel away from the foundation. For a typical foundation radiation damping is often much greater than material damping [15].

Shear wave velocity

The shear waves, denoted S-waves, propagate with a velocity V_s, that is controlled by the shearing stiffness G and the mass density ρ of the soil.

Poisson's ratio, ν, and Soil density, ρ

Soil-foundation interaction problems are relatively insensitive to the values chosen for ν and ρ. Generally, Poisson's ratio can be selected based on the predominant soil type using Table 1.

Table 1: Typical values for Poisson's ratio [4]

Soil Type	Poisson's ratio of soil (v_s)
Saturated clay	0.45-0.50
Partially saturated clay	0.35-0.45
Dense sand or gravel	0.40-0.50
Medium dense sand or gravel	0.30-0.40
Silt	0.30-0.40

Soil mass density value should always be calculated from the total unit weight rather than the buoyant unit weight, because the density term in the mass and inertia ratio equations always represents soil undergoing vibration [20].

2.4. THE INFLUENCE OF SOIL-STRUCTURE INTERACTION ON DIFFERENT TYPE OF STRUCTURES

There are many types of long-span structures that which are vital for the sustainable economy development. As presented earlier, these structures share some common characteristics even though they have their own deterministic behavior.

Many researches have been done on the effect of soil-structure interaction for different structures [29]. This section presents an overview of some notable previous work on the influence of soil-structure interaction for different long-span structures.

Modern transportation facilities demand that bridges be constructed across gorges that may be located in seismically active areas and at the same time the site conditions compel the engineers to place the pier foundation on soil.

A parametric study was conducted to investigate the effects of soil flexibility and bearing parameters (such as stiffness and damping) on the response of such bridge systems. The soil surrounding the foundation of pier has been modeled by frequency-independent coefficients and the complete dynamic analysis has been carried out in time domain.

In order to quantify the effects of SSI, the peak responses of bridge were compared with the corresponding bridge ignoring SSI effects.

It was observed that the soil surrounding the pier has significant effects on the response of the bridge structure and, under certain circumstances, the bearing displacements at abutment locations may be underestimated if the SSI effects are not considered in the response analysis of the system [29].

2.5. SEISMIC CONSIDERATION FOR ABOVE-GROUND PIPELINE

Large diameter pipelines carrying fluid or gas in urban areas are placed above-ground under certain cases. These pipelines are generally supported along with their length by friction block supports. The determination of seismic stresses in the straight segments of such pipelines or at the intersections of the pipelines for ground motion input is, therefore, important in relation to their safety of design and seismic risk analysis [27].

Publish material on the seismic response of pipelines shows that the study of above-ground pipelines for seismic excitation is relatively less reported compared to underground pipeline [27].

The study of transportation of crude oil across active seismic regions is becoming of increasing importance. The recently completed Trans-Ecuadorian pipeline and the Trans-Alaskan pipeline are examples of major pipelines which transport crude oil across areas of high seismic activity. While crude oil pipelines are usually buried below ground. In some cases, however, conditions dictate the use of an above-ground pipeline system supported on either a gravel berm, shown in Fig. 9. This type of system offers the advantage of being readily available for inspection either during normal operation or following a seismic disturbance.

There are a number of construction details of above-ground support system that can be implemented to control the environmental effects i.e. thermal and earthquake ground motion. Such support system are designed in such a way that allow movement due to thermal expansion and contraction and resist the inertial forces, which general develop during an earthquake. An attractive means of doing this is to utilize the friction forces which develop if the pipe is allowed to slide back and forth on the support [16].

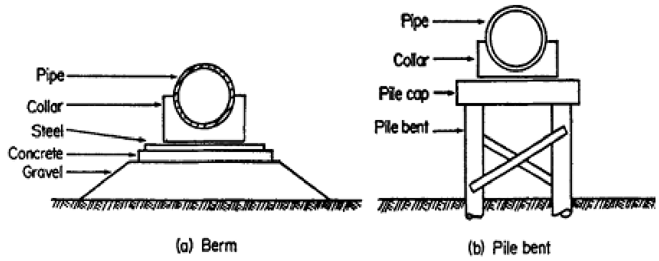

Figure 9: Above-ground support system [16]

Through the selection of surface materials, some degree of control can be imposed on the coefficient of friction and, hence, on both the amount of displacement and level of stress in the pipeline. Gross displacement of the pipeline is prevented by a system of widely spaced anchors [16].

The pipeline must be firmly fixed to the ground by anchors at intervals along its length. Between anchors, however, it must be allowed to slide on its supports to avoid excessive restraint of movements. Hence, the pipe can also slide on its supports during an earthquake [12].

2.6. FINITE ELEMENT ANALYSIS IN ABAQUS/CAE

For selecting an appropriate element type for pipe-soil finite element model, several element parameters should be included and ABAQUS provide all the parameter listed below in order to crate consistent model for the particular analyses type [25]:

- family (continuum, shell, beam, rigid elements…),
- degrees of freedom (directly related to the element family),
- number of nodes,
- formulation and,
- integration,

ABAQUS/CAE is the complete ABAQUS environment that provides a simple, consistent interface for creating ABAQUS models, interactively submitting and monitoring ABAQUS jobs, and evaluating results from ABAQUS simulations.

ABAQUS/CAE is divided into modules, where each module defines a logical aspect of the modeling process; for example, defining the geometry, defining material properties, and generating a mesh. As one moves from module to module, the model will build up. When the model is complete, ABAQUS/CAE generates an input file that you submitted to the ABAQUS analysis product [26].

ABAQUS/Standard and ABAQUS/Explicit are analysis product of ABAQUS/CAE. Both read the input file generated by ABAQUS/CAE, performs the analysis, sends information to ABAQUS/CAE to allow you to monitor the progress of the job, and generates an output database.

The simulation, which normally is run as a background process, is the stage in which ABAQUS/Standard or ABAQUS/Explicit solves the numerical problem defined in the model. Depending on the complexity of the problem being analyzed and the power of the computer being used, it may take anywhere from seconds to days to complete an analysis run [26].

For the structural system consider in this study, the dynamic excitation is the result of time dependent support motion. The equation of motion which is formulate in the subsequent section is the same with that of equation of motion that will be used by ABAQUS. This is due to the inputs provide and the equation of motion formulate here in are consistence and the inputs provide in the software are important to recognize the type of equation which will be used by ABAQUS. The following notation and expression are adapted in this work for the purpose of evaluation of equation of motion of above ground-pipeline.

1. $\{r_a\}$,$\{\dot{r}_a\}$and $\{\ddot{r}_a\}$ vectors of nodal displacement, velocity and acceleration, respectively, with respect to a fixed co-ordinate system (i.e., absolute quantities).
2. $\{r_g\}$,$\{\dot{r}_g\}$and $\{\ddot{r}_g\}$ vectors of displacement, velocity and acceleration, respectively, of the ground immediately beneath the corresponding node.
3. $\{r_r\}$,$\{\dot{r}_r\}$and $\{\ddot{r}_r\}$ vectors of nodal displacement, velocity and acceleration, respectively, relative to the ground. That is

$$\{r_r\} = \{r_a\} - \{r_g\} \tag{2.5a}$$

$$\{\dot{r}_r\} = \{\dot{r}_a\} - \{\dot{r}_g\} \tag{2.5b}$$

$$\{\ddot{r}_r\} = \{\ddot{r}_a\} - \{\ddot{r}_g\} \tag{2.5c}$$

4. [M] = diagonal mass matrix, assumed to be constant.

5. $[F_m]$= vector of inertia forces on the nodes, given by

$$\{F_m\} = [M]\{\ddot{r}_a\} \tag{2.6}$$

or in incremental form,

$$\{dF_m\} = [M]\{d\ddot{r}_a\} \tag{2.7}$$

6. $[K_p]$ = structure stiffness matrix for the pipe alone, which is constant because the pipe is elastic and displacements are small.
7. $\{F_p\}$ =vector of nodal forces due to deformation of the pipe alone, given by

$$\{F_p\} = [K_p]\{r_a\} \tag{2.8}$$

or

$$\{dF_p\} = [K_p]\{dr_a\} \tag{2.9}$$

8. $[K_s]$= stiffness matrix for the support elements only.
9. $\{dF_s\}$= increment of nodal forces due to support deformations, given by

$$\{dF_s\} = [K_s]\{dr_r\} \tag{2.10}$$

10. $[K]$ = stiffness matrix for complete structure, given by

$$[K] = [K_p] + [K_s] \tag{2.11}$$

11. $[C]$ = viscous damping matrix
12. $\{dF_c\}$= increment of nodal forces due to viscous damping effects, assumed to be given

$$\{dF_c\} = [C]\{dr_r\} \tag{2.12}$$

Over a time interval d/t, the following dynamic equilibrium equation must be satisfied.

$$\{dF_m\} + \{dF_c\} + \{F_p\} + \{dF_s\} = \{0\} \tag{2.13}$$

Hence, from Eqs. (2.7), (2.9), (2.10) and (2.12) on gets

$$[M]\{d\ddot{r}_a\} + [C]\{d\dot{r}_r\} + [K_p]\{dr_a\} + [K_s]\{dr_r\} = \{0\} \tag{2.14}$$

And, hence, from Eqs (2.5) and (2.11)

$$[M]\{d\ddot{r}_r\} + [C]\{d\dot{r}_r\} + [K]\{dr_r\} = [M]\{d\ddot{r}_g] - [K_p]\{dr_g\} \tag{2.15}$$

$$[M]\{d\ddot{r}_r\} + [C]\{d\dot{r}_r\} + [K]\{dr_r\} = \{dp\} \tag{2.16}$$

in which

$$\{dp\} = -[M]\{d\ddot{r}_r\} - [K_p]\{dr_r\} \tag{2.17}$$

Similar types of equation of motion (Eq. 2.17) will be used by ABAQUS/Standard and results are obtained after the complete analysis of Eq. 2.17 [15]. Application of the above formulation will be presented subsequently.

CHAPTER THREE

METHOD, MODELING AND ANALYSIS OF ABOVE-GROUND PIPELINES

3.1. GENERAL

Soil-structure interaction under a seismic excitation for a 12m high grade (API 5L X80) straight steel pipeline is undertaken and modeled for analysis in ABAQUS. The pipe is assumed to be supported by low friction Teflon interface and the impedance function for a given type of foundation is described and recommended by Gazetas [11]. This thesis undertakes three-dimensional (3D) linear finite element time history analysis of above-ground pipeline for self-weight of structure, weight of fluid and earthquake ground motion (1995 Kobe) is carried out.

The analysis of the pipeline is carried out by considering soil-structure interaction (SSI) on one hand and by neglecting SSI on the other hand. In the latter case, i.e., when the effect soil-structure interaction is not considered, it implies that the support of a pipeline is modeled as fixed base. In the former case, effect of soil-structure interaction is considered means when the support of a pipeline is modeled as a flexible base. Four cases attributed to soil types to represent the flexibility of the underlying support, these are hard rock, dense-soil, stiff-soil, and soft-soil base conditions.

The response quantities of interest are the relative displacements, bending moment and maximum principal stresses of the pipe for different underlying base conditions. Structural responses under different soil conditions are described in the form of percentage variation of support-flexibility with reference to that obtained for fixed base condition. In the subsequent section, the various parameters and variables that constitute the modeling aspect of the analysis are presented.

3.2. MODELING FOR STRUCTURAL ANALYSIS

3.2.1. Pipeline Material Selection

Steel pipe is used in most pipelines transporting hydrocarbons. It is manufactured according to different specification. American Petroleum Institute (API) [3], the American Society of Mechanical Engineers (ASME) [3], the American National Standards Institute (ANSI) [3], and the American Society of Testing Materials (ASTM) [3] are some of them.

American Petroleum Institute (API) is generally adapted standared for gas transportation and it specifies various grades of line pipe based on their yield strength. Grade A line pipe has a minimum yield strength of 207 MPa, (30,000 psi) with Grade B has a minimum yield strength of 241MPa (35,000 psi). Other grade categories may indicate special fabrication methods. For example, Grade X42 indicates a pipe made of steel with 289MPa (42,000 psi) minimum yield strength; X60 pipe has minimum yield strength of 414 MPa (60,000 psi), etc. Newer pipe grades X70 and X80 are available, but are typically used in offshore or high-pressure gas pipelines for Large-diameter or high-pressure applications [3].

API Specification establishes requirements for two Product Specification Levels (PSL 1 and PSL 2). These two PSL designations define different levels of standard technical requirements.

- PSL 1 pipe can be supplied in Grades A25 through X70.
- PSL 2 pipe can be supplied in Grades B through X80 API Specification [3].

For the purpose of this study, PSL 2, API 5L X80 steel grade pipeline is selected with modeling parameter as shown Table 2. Because of its widespread use and the amount of laid lines continuously increased, demonstrating a consolidated trend in adopting X80 steel pipes as a standard solution for high-pressure gas transportation and their size are typical for oil and gas transmission pipelines [29].

Table 2: Pipeline data for this study

Description	Unit	Pipeline
Pipeline material grade	-	API 5L X80
Outside diameter	m	0.762
Wall thickness	m	0.01905
Steel density	kg/m^3	7850
Young's modulus	GPa	200
Poisson's ratio υ_p	-	0.3

3.2.2. Support Material of Pipeline

Pipeline is modeled to be supported on low frictional Teflon interface (Table. 3). Teflon is brand name of Poly Tetra Fluor Ethylene which is a fluorocarbon-based polymer and is commonly abbreviated PTFE. This family (Teflon) offers high chemical resistance, provide good performance both under low and high-temperatures exhibits resistance to weathering, low friction, electrical and thermal insulation, and slipperiness [31].

Table 3: Pipeline support data

Description	Unit	Support
Support type	-	Poly Tetra Fluor Ethylene/ Teflon
Density	kg/m^3	2160
Young's modulus	GPa	90
Poisson's ratio υ_t	-	0.46

3.2.3. Pipeline Length

Unless otherwise agreed between the purchaser and the manufacturer pipes are generally furnished in the nominal lengths and within the length tolerance according to line pipe specification API [3]. It is not practical to analyze long length of pipeline including many of the discrete support for obtaining the desired response. An optimal length of pipeline with a certain end condition is considered for obtaining the desire response [12]. Hence, for the purpose of this study, high-grade straight threaded and coupled end steel pipeline of a nominal length (12m) is considered, which compromise different factors to represent the whole system of pipeline as presented in, Table 4.

Table 4: Tolerances of lengths according to API specification [3]

Nominal length	Minimum length	Minimum average length for order each item	Maximum length
m	M	M	m
		Threaded and coupled end pipe	
16	4.88	5.33	6.86
12	6.71	10.67	13.72
		Plain-end pipe	
6	2.74	5.33	6.86
12	4.27	10.67	13.72
15	5.33	13.5	16.76
18	6.4	16	19.81
24	8.53	21.34	25.91

Threaded and coupled end pipeline have high resistive capacity to any hazard as compare to plain-end steel pipeline. This is due to sufficiently tight connectivity capacity with the adjacent pipe [3].

3.2.4. Structural Idealization

To set up the structural analysis model, a simplified geometry of the pipeline assembly is used. In modeling pipe-soil interaction, a number of aspects need to be considered [8]:

a) The mechanical behavior of pipeline.
b) The behavior of the soil supporting the pipeline.
c) The interaction between the soil and above-ground-pipeline support.
d) The interaction between the support of pipe and the pipeline itself.
e) The geometry and orientation of the pipeline
f) Mass of the fluid inside the pipeline.

The following additional assumptions have been made to set up the structural model [7,8].

a) The pipe lies horizontally in a single plane. As per Eurocode "a pipeline is considered as a single line when its behavior during and after a seismic event is not influenced by that of other pipelines, and if the consequences of its failure relate only to the functions demanded from it".

b) Each nodal point has three degrees of freedom. As per Eurocode “only the three translational components of the seismic action should be taken into account, (i.e., the rotational components may be neglected)”.
c) The pipe is elastic and the foundation of the pipe rests on elastic-half space.
d) Displacements are assumed to be small in comparison to the plan dimensions of the system.
e) The system is pre-stressed by static loads (gravity) before the earthquake begins. This is important because initial loads on the supports substantially affect the subsequent dynamic response.
f) The mass of the fluid in the pipeline is fully effective in developing inertial resistance.

3.3. FINITE ELEMENT MODELING

3.3.1. General and Boundary Condition

A finite element for structural analysis implemented and the analysis model is created in ABAQUS/CAE. A simplified geometry of the pipeline assembly has been used in the simulations. In reality, the pipeline assembly consists of several parts. However, this thesis focuses on the soil-pipe interaction, hence only the pipe (Fig. 10) itself is setup according to the idealization concepts presented in section 3.2.4.

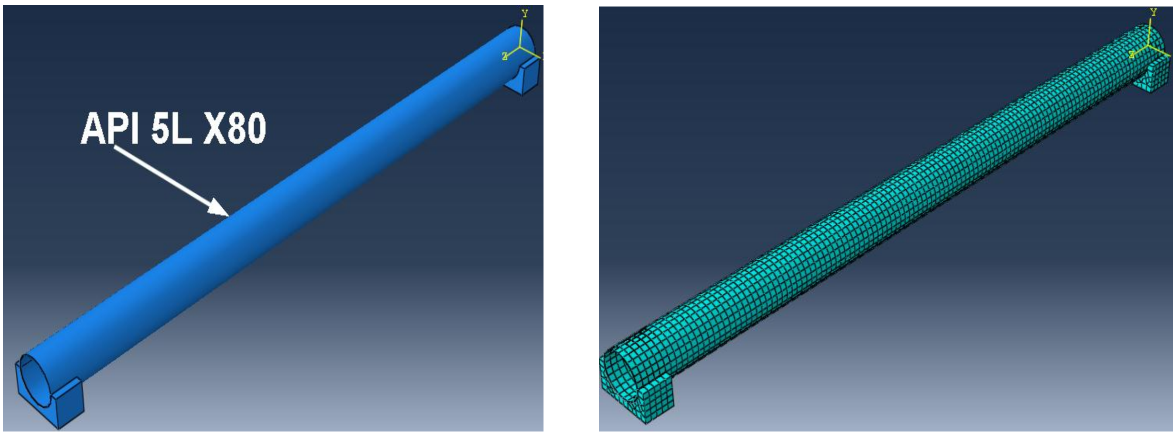

(a) (b)

Figure 10: (a) Finite element model (b) adaptable mesh for API 5L X80 steel pipeline.

The pipeline is modeled with solid elements, entitled C3D20R in ABAQUS/CAE and the elements had a global size of approximately 0.1 meters. The support of a pipeline is constrained in all degrees of freedom to represent fixed base condition. On the other hand, in order to represent flexible base support, the analysis model is constrained again rotational degree of freedom there by allowing only translation displacement. The latter are modelled by using spring and dashpot coefficients.

3.3.2. Natural Frequency of Pipeline Structure

The earthquake ground motion along the pipeline structure can lead to vibration of the pipeline. This kind of vibration may cause fatigue damage to the pipeline. In order to study this kind of vibration on the pipeline structure, computing the natural frequency of the oil pipeline is very important [30].

Resonance phenomenon may occur when the frequency of the exciting forces approach the natural frequency of pipelines. A resonating span can experience significant deflections and associated stresses [30].

Several parameters such as pipeline length, axial forces and boundary conditions influence the natural frequency of the pipeline. Based on the results from validation analysis in appendix C the natural frequency of a 12m length pipelines structure is extracted form a finite element software (ABAQUS /CAE), and the first four frequency and mode shape are tabulated in Table 5 and plotted in Fig. 11.

Table 5: Natural frequency of pipeline structure

Mode	Natural cyclic frequency f_n (Hz)	Natural period $\mathrm{T_n}$ (sec)
1	29.33	0.034
2	29.41	0.034
3	76.58	0.013
4	76.79	0.013

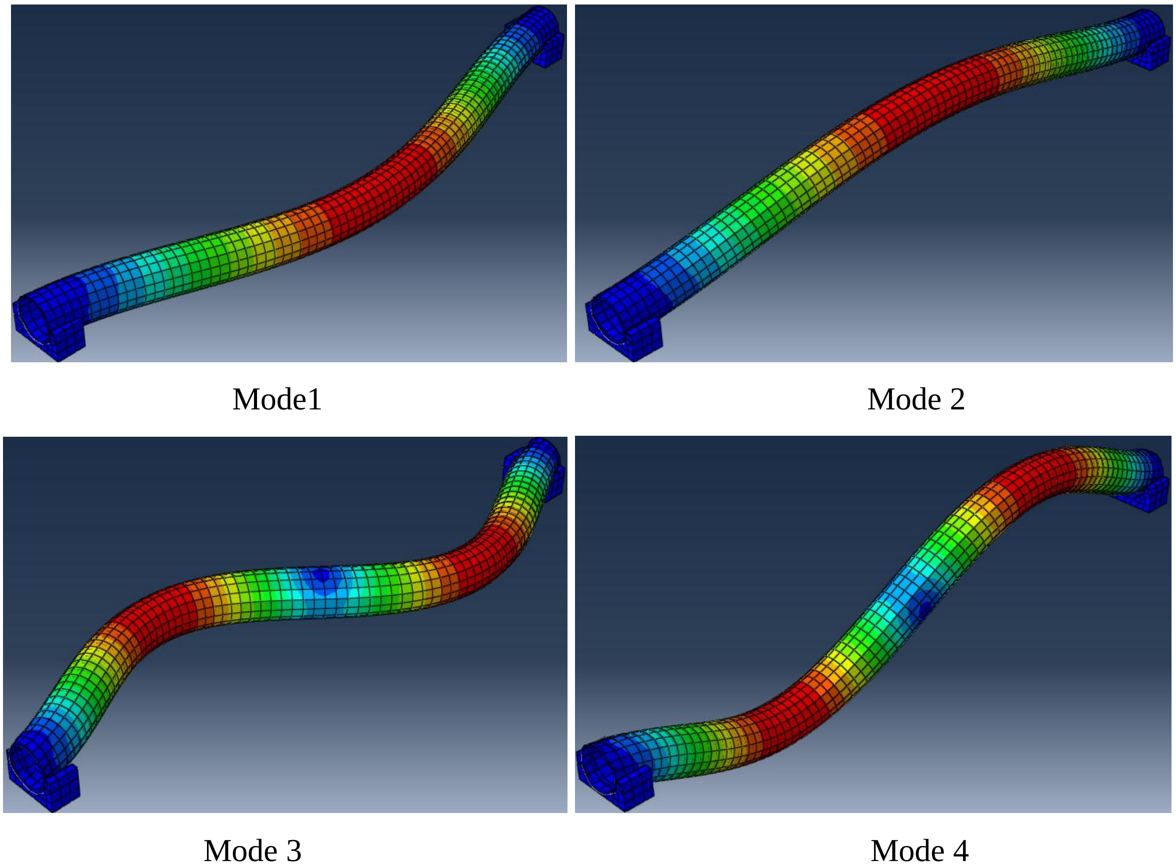

Figure 11: Mode shapes of pipeline structure

3.3.3. Loading Condition

In general, several loads and load combinations affect above-ground pipeline structures. For the purpose of this thesis, seismic ground motion, self-weight of pipe structure and weight of fluid are considered as the load on the system.

Seismic Ground Motion

From many types of external load due to natural hazards that must be considered in the design of structures, the most important by far in terms of its potential for disastrous consequences is the earthquake [18].

The seismic collapse risk of a structure is largely influenced by characteristics of strong ground motion. Amplitude, frequency content and duration are some of the important characteristics of strong ground motion. Amplitude describes the peak magnitude of a single cycle with the ground motion time history and frequency content describes how the amplitude of a ground motion is distributed among different frequency [19].

An earthquake ground motion (1995 Kobe) is intended to be used and is applied at the support of the straight pipeline according to Eurocode [7] and presented in Fig. 12 (a).

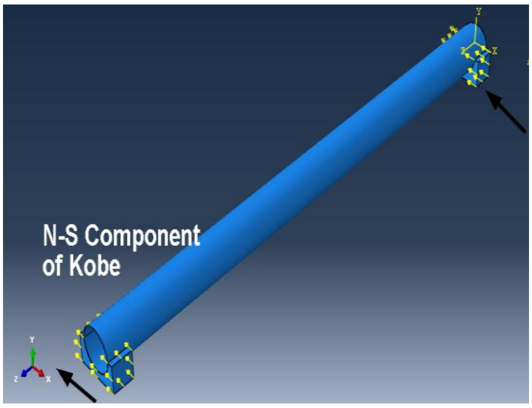

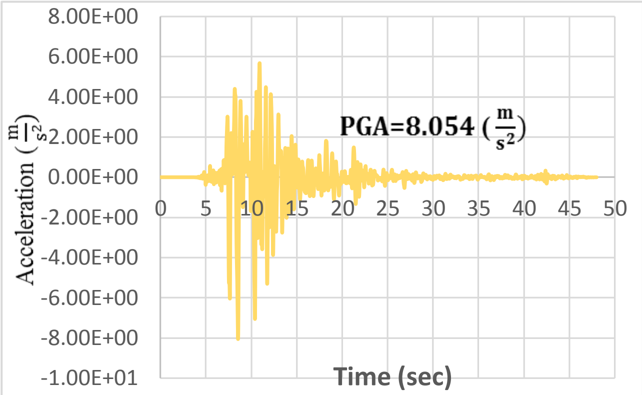

(a) (b)

Figure 12: (a) Ground motion application in pipeline structure (b) Time history record of Kobe ground motion.

Ground motions with high peak acceleration are usually, but not always, more destructive than the motions with lower peak acceleration. Very high peak acceleration that lasts for only a very short period of time may case little damage to many type structures [19].

For the purpose of this thesis, the NS component of Kobe which has a Peak Ground acceleration of 8.054 m/s^2 is used as shown in Fig. 20 (b). During this earthquake, many bridges and many type of long-span structure suffered extensive damage in Abeno [28].

3.3.4. Impedance Function

For the purpose of this thesis, an arbitrarily shaped foundation which is circumscribed by a rectangle of width B and length L (Fig. 13) is assumed under the four base conditions of the pipeline. Gazetas and his co-workers expressed the dynamic impedances for different shape of foundation with respect to the axis orientation.

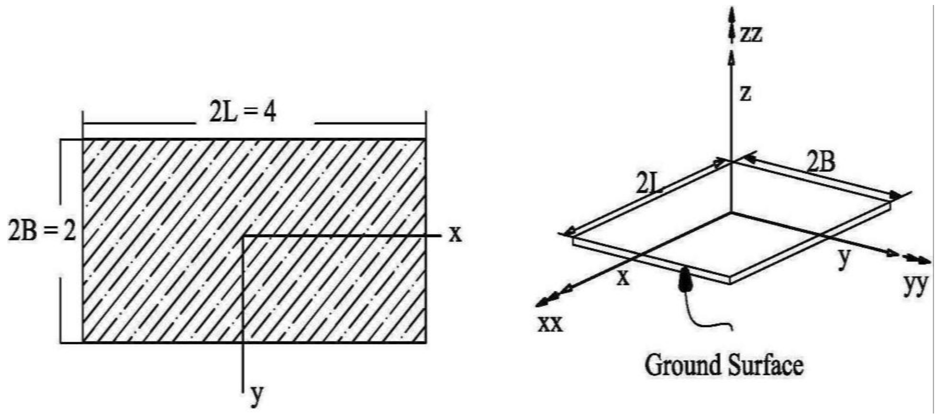

Figure 13: Foundation size for pipeline and axis orientation of soil-foundation system

Four different base conditions based on different soil parameters are selected as support conditions of the pipeline and there are given in Table 6.

Table 6: Selected ground type and detail of soil parameter.

Description	Shear wave velocity V_s. (m/sec)	Poisson's ratio υ_s	Mass density (ρ) kg/m^3
Rock (ground type A)	850	0.30	2200
Dense Soil (ground type B)	450	0.30	2000
Stiff Soil (ground type C)	300	0.35	1800
Soft Soil (ground type D)	100	0.40	1600

To consider the effect of soil-structure interaction, the sub-structure approach (three-step method method), as presented early in section 2.3.2 chapter two, is used. By accounting for different influencing factors, the impedance function for the givens type of foundation is computed.

An equivalent impedance function for the dynamic behavior of the pipeline support resting on elastic-half space under different base conditions and soil parameters are presented in the following section.

Generally, the impedance function for different degree of freedom is represented by Eqs. (3.1) and (3.2.).

$$\tilde{k}(\omega) = k(\omega) + i\omega C(\omega) \tag{3.1}$$

$k(\omega) =$ the dynamic spring coefficient and is equal to:

$$k(\omega) = k_{static} \times x_{(\omega)} \tag{3.2}$$

where K_{static} is the static stiffness and $x_{(\omega)}$ is the dynamic coefficient which is frequency-dependent [12]. Consequently the dynamic spring coefficient is also frequency-dependent, k (ω).

C is the frequency-dependent total damping coefficient, $C(\omega)$. This coefficient includes radiation and material damping. It should be noted that the damping coefficients that are extracted from Gazetas relations do not include the soil hysteretic damping ξ [13]. To incorporate such damping, simply the corresponding material dashpot coefficient should be added to the radiation damping.

The following parameter are important to compute impedance function expressions for the intended foundation (Fig. 14), which will be used for the purpose of this study.

D_f = Total foundation height

d = height of effective side wall

A_w= actual side wall side-soil contact area; for constant height d along the perimeter

$= d \times (\text{perimetr})$

V_{La} is apparent propagetion velocity of compression − extention waves or

$= \frac{3.4}{\Pi \times (1 - v)} \times V_s$ is also called Lysmer's analog" wave velocity

V_S=shear wave velocity for each soil type

L= length of the foundation and B =width of the foundation

$h = D - \frac{d}{2}$

H= Thickness of the ground

L_f= length of foundation

B_f= width of foundation

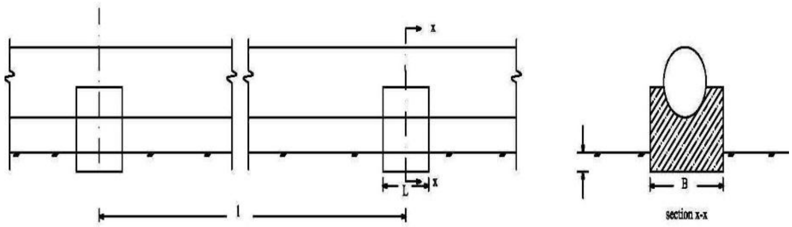

Figure 14: Schematic view of above-ground pipeline foundation.

In the subsequent presentation, the computation of spring and dashpot coefficient for different support formation system are presented.

A. Rock support system

The variation of the dynamic stiffness coefficient with frequency reveals an equally strong dependence on H/B as shown in Fig. 15. On a stratum, k (ω) is not a smooth function, as with a halfspace, but exhibits undulation (peak and vally) of the stratum. In other words, the observed fluctuationsd retur back to the outcome of resonace phenomena: wave emiting from the oscillating foundation reflects at the soil-bed rock interface and retur back to their source at the surface [10].

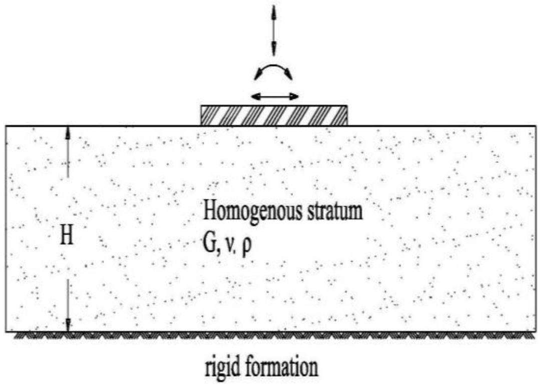

Figure 15: Surface foundation for homogenous stratum over bed rock.

As the result, the amplitude of foundation motion may signifcantly increase at frequncey near the natural frequncy of the deposit. Thus dynamic stiffness (being the invers of displacement) exhibite throug, which are very steep when the hysterstic damping in the soil is small (in fact, in a certain case, k would be exactly zero if the soil were ideally elastic) [10].

For the shearing mode of vabration (swaying and tortion) the natural fundamental frequncy of the stratum, which control the behavior of k (ω), is $f_s = \frac{V_s}{4H}$

While for the compressing mode of vabration (vertical, rocking) the crosponding natural fundamental frequncy of the stratum, is $f_c = \frac{V_{la}}{4H} = \frac{3.4V_s}{\Pi\times(1-v)}$

The shear modulus of the supporting system is determine in Eq. 3.3

$$G = V_s^{\,2} \times \rho \tag{3.3}$$

where G= shear modulus of the supporting soil

ρ = density of soil

V_s= shear wave velocity

The translational dashpot and spring coefficient for rock support condition under different axis orientation are computed in the following section.

i. Dashpot and spring coefficient for transversal (yy) and longitudinal (xx) direction

— Spring coefficient

Dynamic stiffness $\mathrm{k}_{\mathrm{x,y\ sur}}$ = static stiffness $\mathrm{k}_{\mathrm{sur}}$ × dynamical stiffness coefficient $x_{\mathrm{sur}}(\omega)$

Static stiffness $\mathrm{k}_{\mathrm{sur(static)}}$:

$$\mathrm{k}_{\mathrm{x,y\ sur\ (static)}} = \frac{2\mathrm{GL}}{1-\nu}\left[0.73 + 1.54(\tfrac{\mathrm{B}}{\mathrm{L}})^{3/4}\right]\left(1 + \frac{\frac{\mathrm{B}}{\mathrm{H}}}{0.5+\frac{\mathrm{B}}{\mathrm{L}}}\right)$$

Dynamical stiffness coefficient$x_{\mathrm{xy\ sur}}(\omega)$:

$x_{\mathrm{x,y\ sur}} = x_{\mathrm{x,y\ sur}}\left(\frac{H}{B}, \frac{L}{B}, a_o\right)$ is estimated from graph A1 in appendix A in terms of L/B and H/B for the corresponding value of a_o.

where a_o = Dimensionless frequency and defined by $\mathrm{a_o} = \frac{\omega \mathrm{B}}{\mathrm{V_s}}$

— Radiation Dashpot coefficient $\mathbf{C_{sur}(\omega)}$

$\mathrm{C_{xy}}\left(\frac{H}{B}\right) = 0\ at\ frequencies\ f < \frac{3}{4}f_s$; $\mathrm{C_{xy}}\left(\frac{H}{B}\right) \simeq \mathrm{C_{xy}}(\infty)\ at\ f > \frac{4}{3}f_s$;

At intermediate frequencies: interpolate linearly $f_s = V_s/_{4H}$

where f_n = Fundamental natural frequency of the pipeline structure

f_s = Fundamental natural frequency of stratum for the shearing mode of vibration.

ii. Dashpot and spring coefficient for vertical (zz) direction

— Spring coefficient

Dynamic stiffness $\mathrm{k}_{\mathrm{z\ sur}}$ = static stiffness $\mathrm{k}_{\mathrm{sur}}$ × dynamical stiffness coefficient $x_{\mathrm{sur}}(\omega)$

Static stiffness$\mathrm{k}_{\mathrm{sur(static)}}$:

$$\mathrm{k}_{\mathrm{z\ sur\ (static)}} = \frac{2\mathrm{GL}}{1-\nu}\left[0.73 + 1.54(\tfrac{\mathrm{B}}{\mathrm{L}})^{3/4}\right]\left(1 + \frac{\frac{B}{H}}{0.5+\frac{B}{L}}\right)$$

Dynamical stiffness coefficient$x_{\text{xy sur}}(\omega)$:

$x_{\text{z sur}} = x_{\text{z sur}}\left(\frac{H}{B}, \frac{L}{B}, a_o\right)$ is estimated from graph A1 in appendix A in terms of L/B and H/B for the corresponding value of a_o.

— Radiation Dashpot coefficient $\mathbf{C_{sur}(\omega)}$

$\mathrm{C_z}\left(\frac{H}{B}\right) = 0\ at\ frequencies\ f < f_c$; Regardless of foundation shape

$\mathrm{C_z}\left(\frac{H}{B}\right) \simeq 0.8\mathrm{C_z}(\infty)\ at\ f \geq 1.5 f_c$

At intermediate frequencies interpolate

$$f_c = V_{la}/_{4H} = V_{la} = 3.4V_s/\Pi(1-v)$$

$f_{\ c}$= is fundamental natural frequency of stratum for the compressing mode of vibration.

B. Dense, stiff and soft-soil support system

By assuming the same foundation size as above, but with some imbedded depth, the impedance function is computed for dense, stiff and soft soil support condition (Fig. 16).

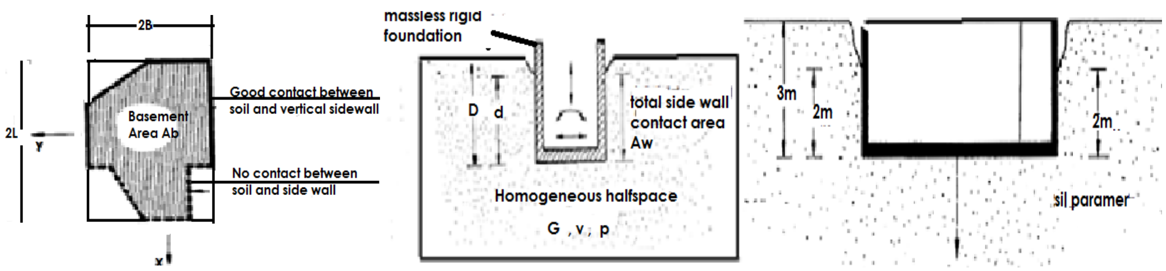

Figure 16: Soil-foundation system for dense, stiff and soft soil support

i. Dashpot and spring coefficient for transversal (yy) and longitudinal (xx) direction

— Spring coefficient

Static stiffness$\mathrm{k_{emb\ (static)}}$:

$$\mathrm{k_{x,y\ emb\ (static)}} = \mathrm{K_{xy\ sur}} \times (1 + 0.15(\frac{\sqrt{\mathrm{D}}}{\sqrt{\mathrm{B}}}) \left[1 + 0.52\left(\frac{\mathrm{h}}{\mathrm{B}} \times \frac{\mathrm{A_W}}{\mathrm{L^2}}\right)^{0.4}\right]$$

Dynamical stiffness$x_{\text{xy emb}}(\omega)$:

The dynamical stiffness coefficient x_{yemb} and x_{xemb} can be estimated in terms of L/B, D/B and d/B for each value of a_o from graph A3 in the appendix A.

— Radiation Dashpot coefficient $\mathbf{C_{emb}(\omega)}$

$$C_{xy\,emb} = 4\rho V_s BLC'_y + 4\rho V_s Bd + 4\rho V_{La} Ld$$

$C'_y = C'_y\,(\frac{L}{B};\ a_o)$ is plotted in graph A2 in appendix A.

$$C'_x \simeq \rho V_s A_b$$

$$V_{La} = \frac{3.4}{\Pi(1-0.3)} x450 = 695.734 \text{ m/s}$$

ii. Dashpot and spring coefficient for vertical (zz) direction

— Spring coefficient

Static stiffness Static stiffness$k_{emb\,(static)}$:

$$k_{z\,emb\,(static)} = K_{z\,sur} \times \left[1 + \frac{1}{21}\frac{D}{B}(1 + 1.3x)\right] \times [1 + 0.2(\frac{A_w}{A_b})^{2/3}]$$

$$K_{z\,sur} = \frac{2GL}{1-v}(0.73 + 1.54X^{0.75})$$

Dynamical stiffness coefficient $x_{xy\,emb}(\omega)$ is computed from appendence A (Table .A1)

— Radiation Dashpot coefficient $\mathbf{C_{emb}(\omega)}$

$$C_{z\,emb} = 4\rho V_{La} BLC'_z + 4\rho V_s (B + L)d$$

$C'_z =\ C'_z$ (L/B, v; a_o) is plotted in graph A2 on the appendix A.

By using the above equations and detailed calculations, impedance functions are employed for analysis and are presented in Table 7. The graph and tables, which are used for computing impedance function, are given in Appendix A.

Table 7: Dashpot and stiffness coefficient for different ground type

Ground type	K_x $(\frac{kN}{m})$	K_y $(\frac{kN}{m})$	K_z $(\frac{kN}{m})$	C_x $(kN.s.m)$	C_y $((kN.s.m)$	C_z $((kN.s.m)$
Rock	26.23×10^6	26.23×10^6	26.23×10^6	61.22×10^3	61.22×10^3	48.88×10^3
Dense	8.90×10^6	9.63×10^6	3.493×10^6	36.66×10^3	36.66×10^3	32.732×10^3
Stiff	3.65×10^6	3.973×10^6	2.896×10^6	23.026×10^3	23.026×10^3	20.153×10^3
Soft	0.367×10^6	0.405×10^6	0.31×10^6	7.18×10^3	7.18×10^3	6.149×10^3

After computing the coefficients of frequency-independent springs and dashpots for different base conditions, they are introduced to the spring-dashpot model enveloped in a FEM model and arranged corresponding to the direction of each degree of freedom of the support as presented in Fig. 17.

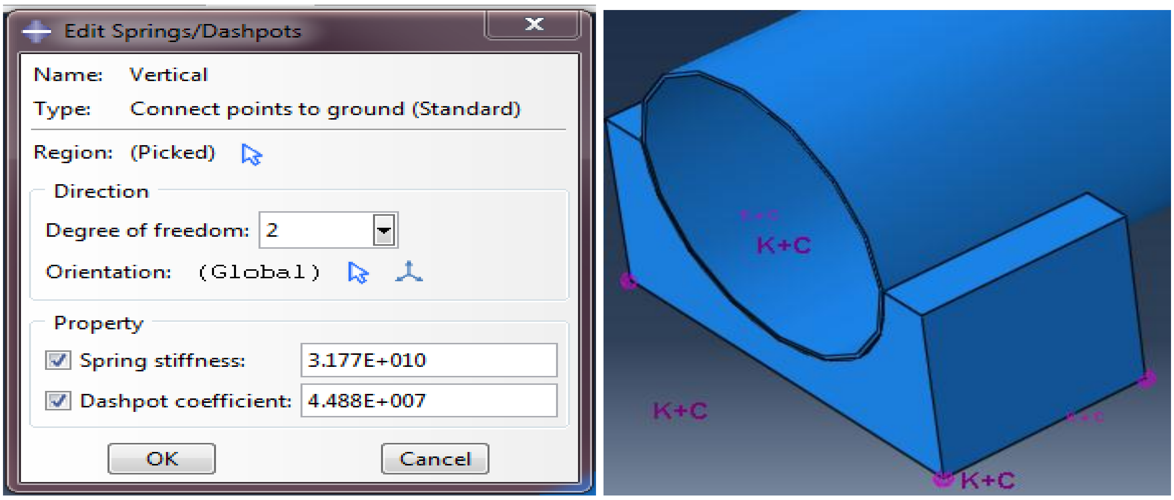

Figure 17: Presentation module for dashpot and stiffness coefficient for different ground type in ABAQUS

Based on the modeling principle presented in the earlier section, several analysis model have been processed using ABAQUS. Due to the demand for extremely large computational time special computational facilities and setup have been implemented. Finding will be discussed in the subsequently.

CHAPTER FOUR

RESULTS AND DISCUSSION

4.1. INTRODUCTION AND CONVENTIONS

In this Chapter, the results from the finite element analysis in ABAQUS software tool are presented. The results show responses; i.e., acceleration, velocity and displacements distribution of the pipeline at a representative node, maximum principal stresses of the pipeline at a representative element and bending moments along the length of the pipeline under five different supporting base condition.

For the purpose of this study, the result outputs are presented using one of or a combination of graphs, figures and tables. The results are presented with respect to axis orientation automatically generated in ABAQUS software tool.

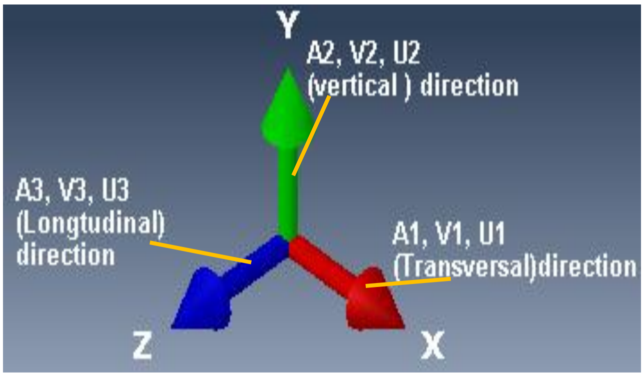

Figure 18: Axis orientation for the responses with respect to its nomenclature in ABAQUS.

Each axis of orientation in ABAQUS has its own nomenclature with regard to structural response of interest, and the orientations are presented in Fig. 18. The transversal acceleration, velocity and displacement of the pipeline in axis X are termed as A1, V1 and U1 respectively. The vertical acceleration, velocity and displacement of the pipeline in axis Y are termed as A2, V2 and U2 respectively. Likewise longitudinal acceleration, velocity and displacement of the pipeline in axis Z are termed as A3, V3 and U3 respectively. Letter 'A' stands for an acceleration response, 'V' for the velocity response and 'U' for the displacement response. Likewise, '1', '2' and '3' orients axis orientation to represents the response in terms of global coordinate system with respect to X, Y, and Z axis in ABAQUS and the analysis result are presented here .

4.2. STRUCTURAL RESPONSE RESULTS

4.2.1. Acceleration

The acceleration result outputs along X axis (Transversal) are presented using graphs for an input ground motion of N-S component of Kobe (Fig. 19a). The ground motion is applied in X axis/Transversal direction of the pipeline as shown in Fig. 19 (b).

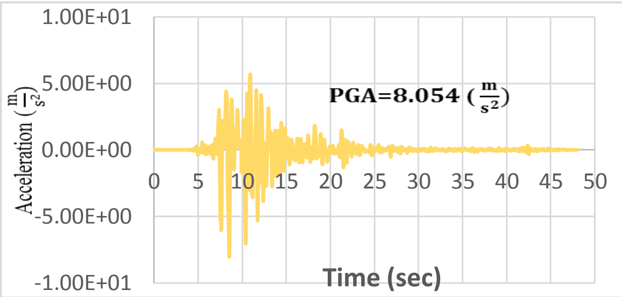

(a)

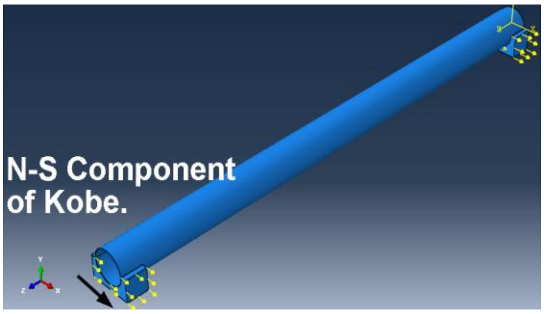

(b)

Figure 19: (a) Time history records of Kobe (b) Ground motion application on the pipeline structure.

Since, each node have different response value, a representative node is selected at the middle length of the pipeline in order to show the acceleration, velocity and displacement response outputs and presented in Fig. 20.

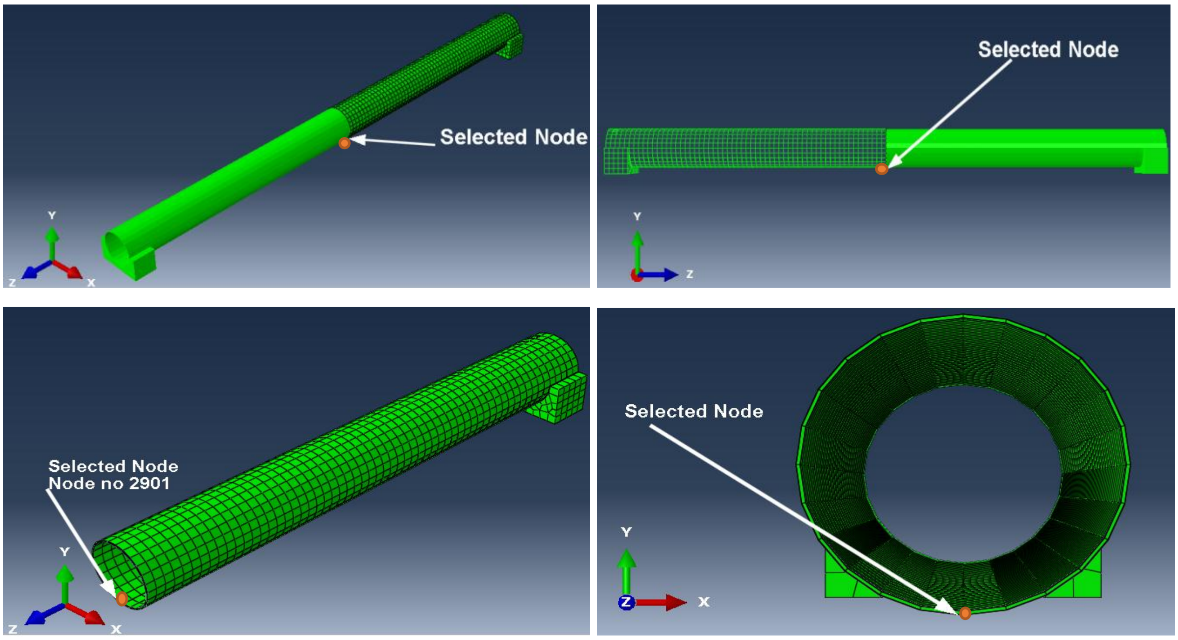

Figure 20: Selected node for acceleration, velocity and displacement response of the pipeline in different views and sections.

The time history records of Kobe 1995, which is used for the purpose of this thesis is shown in Fig. 21 (a) and the seismic horizontal acceleration responses of the straight steel pipeline in the direction of A1 (transverse or X) are presented in Fig. 21, Fig. 22 and Fig. 23.

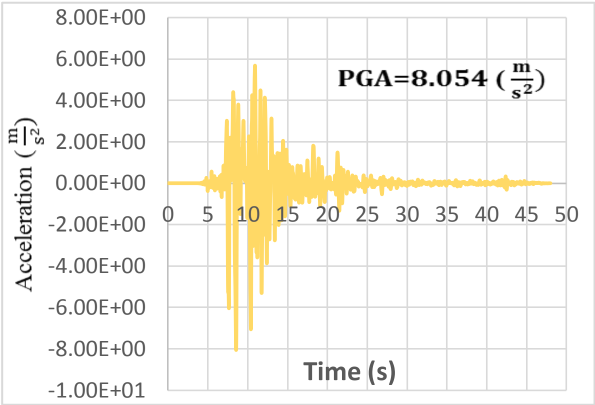

(a)

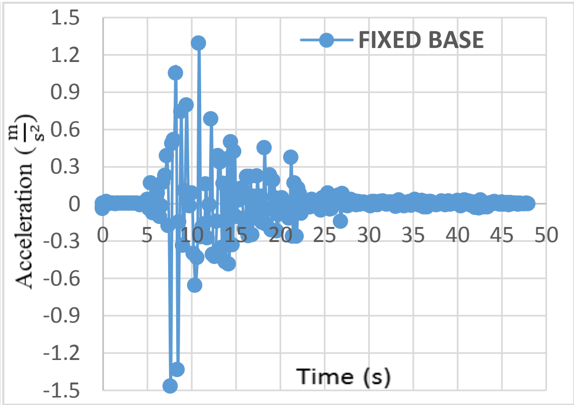

(b)

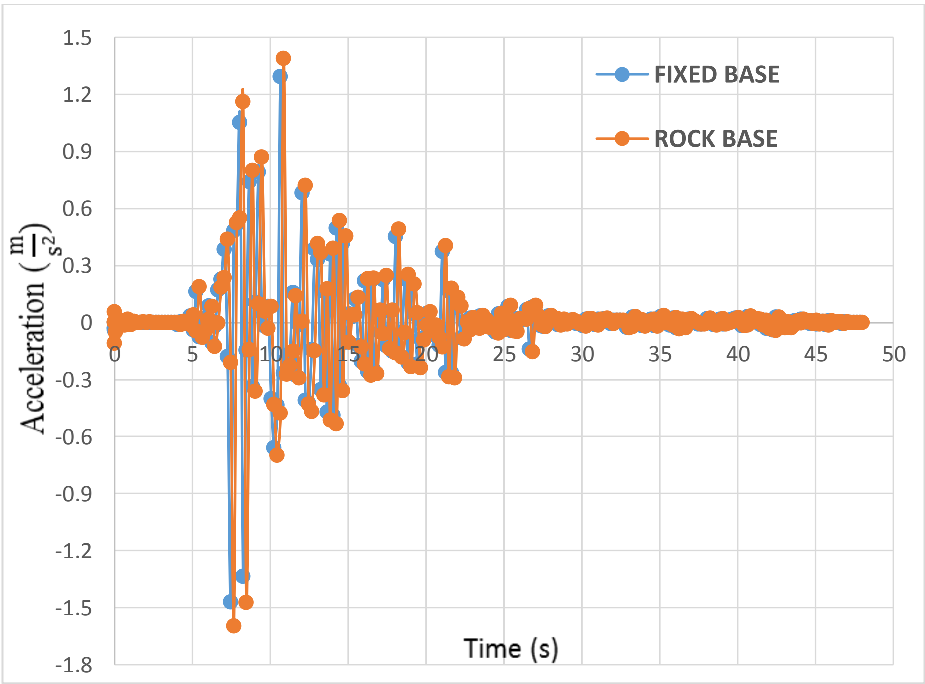

(c)

Figure 21: (a) Time history records of Kobe (1995) , Nodal acceleration history response of the pipeline under (b) fixed base (c) fixed base and rock base with reference to A1 (Transversal or X) Direction

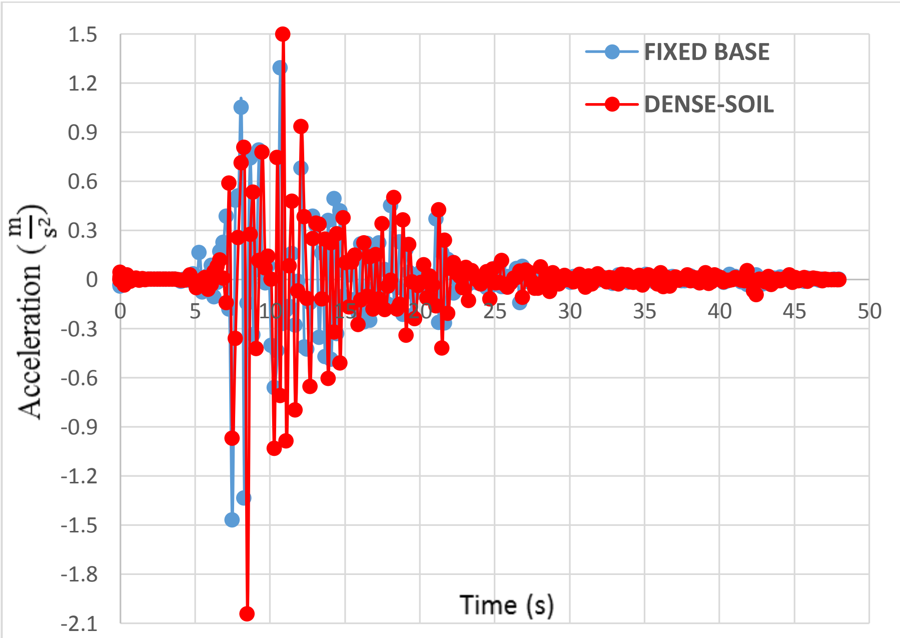

(a)

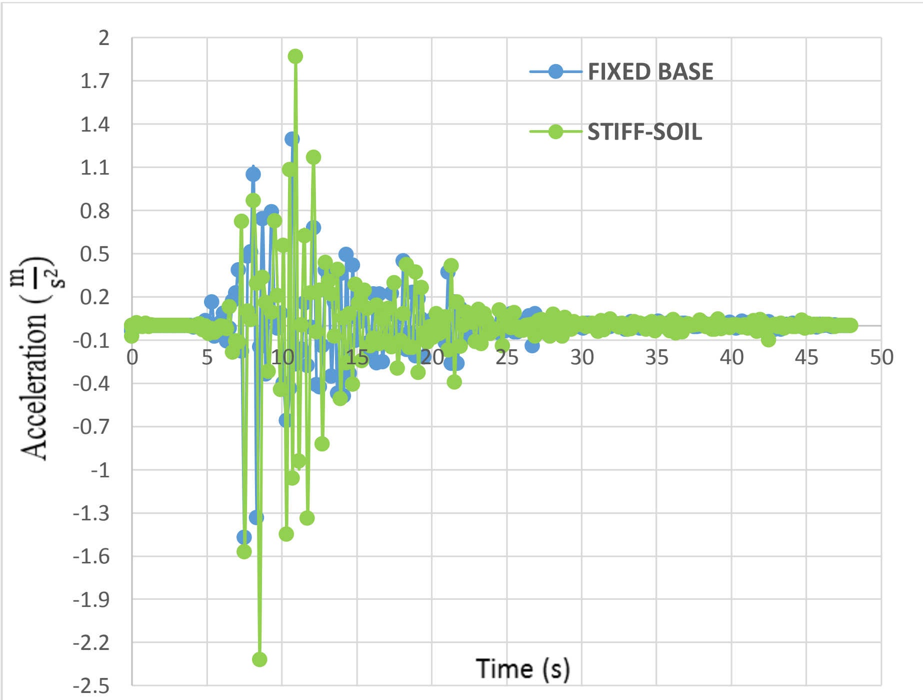

(b)

Figure 22: Nodal acceleration history response of the pipeline under (a) fixed base and dense-soil base (b) fixed base and stiff-soil base with reference to A1 (Transversal or X) Direction

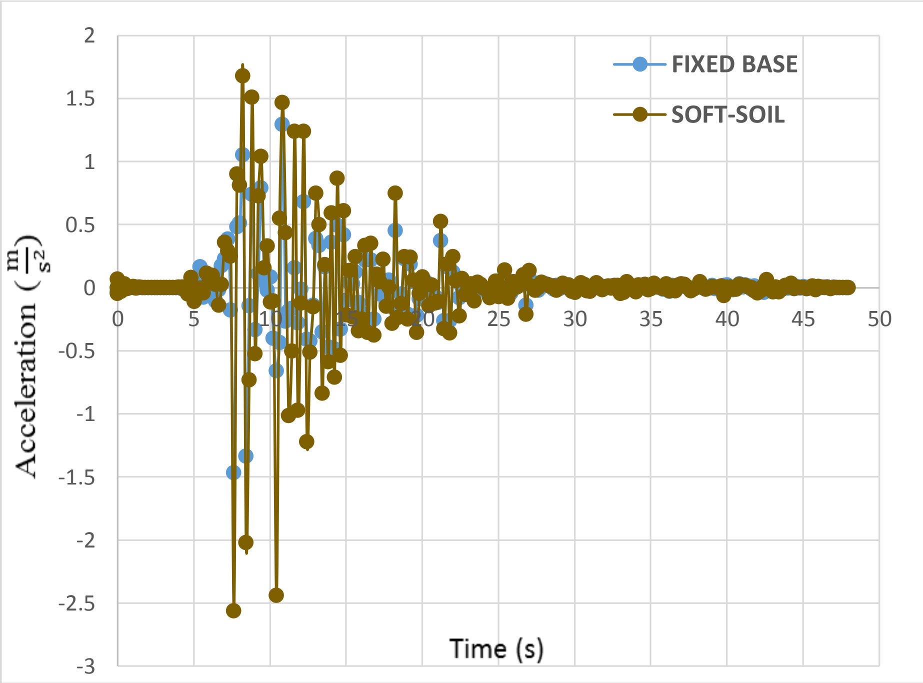

Figure 23: Nodal acceleration history response of the pipeline under fixed base and soft-soil base with reference to A1 (Transversal or X) Direction

The ordinate and abscissa of the graphs represents acceleration response and time respectively. The graphs are presented for the five supporting base conditions and values presented are relative to fixed bases of the pipeline.

In Fig. 21, Fig. 22 and Fig. 23 nodal displacement history responses of the pipeline under the five base conditions are presented. Form these graph it is observed that, the maximum horizontal acceleration of the pipeline under fixed supporting base conditions in the direction of A1 (Transverse or X) is 1.47m/s^2 at 7.66 s. For that of rock supporting base condition the maximum horizontal acceleration of the pipeline in the direction of A1 (transverse or X) is 1.60m/s^2 at 7.66s.

In a case of dense-soil supporting base condition the maximum horizontal acceleration of the pipeline in the direction of A1 (transverse or X) is 2.05 m/s^2 at 8.50s. The maximum horizontal acceleration of the pipeline under stiff-soil supporting base condition in the direction of A1 (transverse or X) is 2.32 m/s^2 at 8.52s. Finally, maximum horizontal acceleration of a pipeline under soft-soil supporting base condition in the direction of A1 (transverse or X) is 2.56m/s^2 at 7.62s.

It is observed that, the horizontal acceleration of the pipeline in the direction of A1 (transverse or X) under the five base condition is maximum at a time range of 7.64s to 8.52 s. On the other hand, the Peak Ground Acceleration (PGA) of the ground motion (N-S component of Kobe) is 8.054m/s^2 at 8.54s. This indicates that, the maximum acceleration of the pipeline under the five base conditions have appeared just before 8.54sec.

4.2.2. Velocity

In order to see the velocity response outputs of the pipeline towards the direction of the application of ground motion, the responses in the direction of X axis (Transversal or V1) are presented and discussed in the following section. For the purpose of this thesis only the velocities in transversal direction will be presented. The velocities in the other direction can be studied in a similar manner. The graphs are presented for the five base conditions and presented relative to fixed bases of the pipeline.

The seismic horizontal velocities response of the straight steel pipeline in the direction of V1 (transverse or X) are shown in Fig. 24, Fig. 25 and Fig. 26. The ordinate and abscissa of the graphs represents velocity response and time respectively. In these plots, a comparison is made between the fixed support condition of the pipeline and the rock base, dense-soil base, stiff-soil base and soft-soil base.

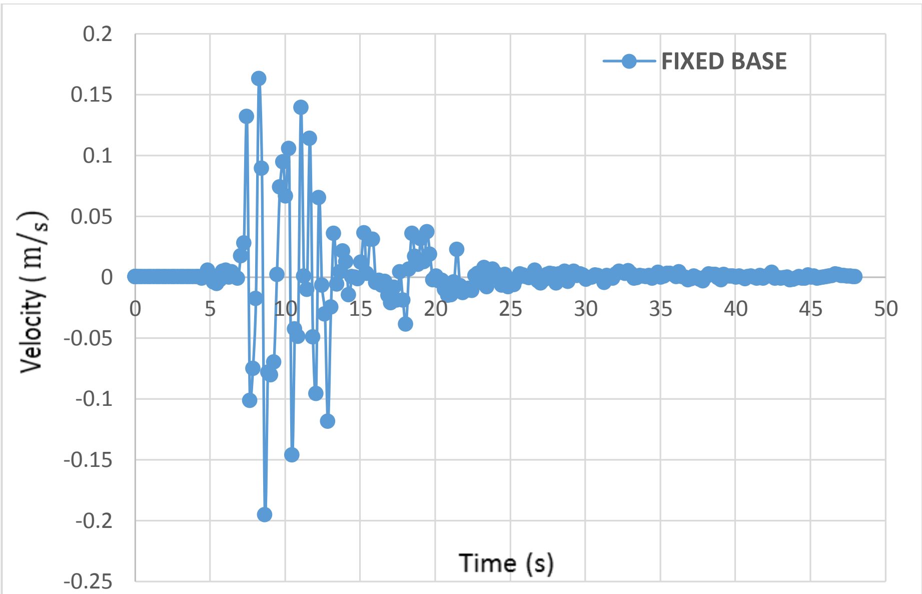

Figure 24: Nodal velocity history response of the pipeline under fixed base with reference to V1 (Transversal or X) direction.

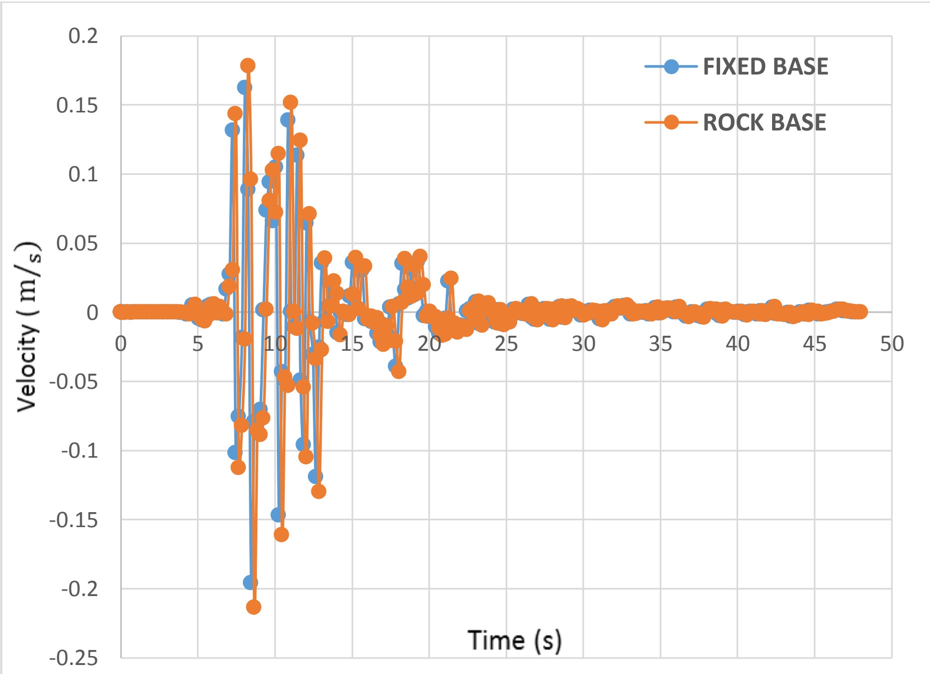

(a)

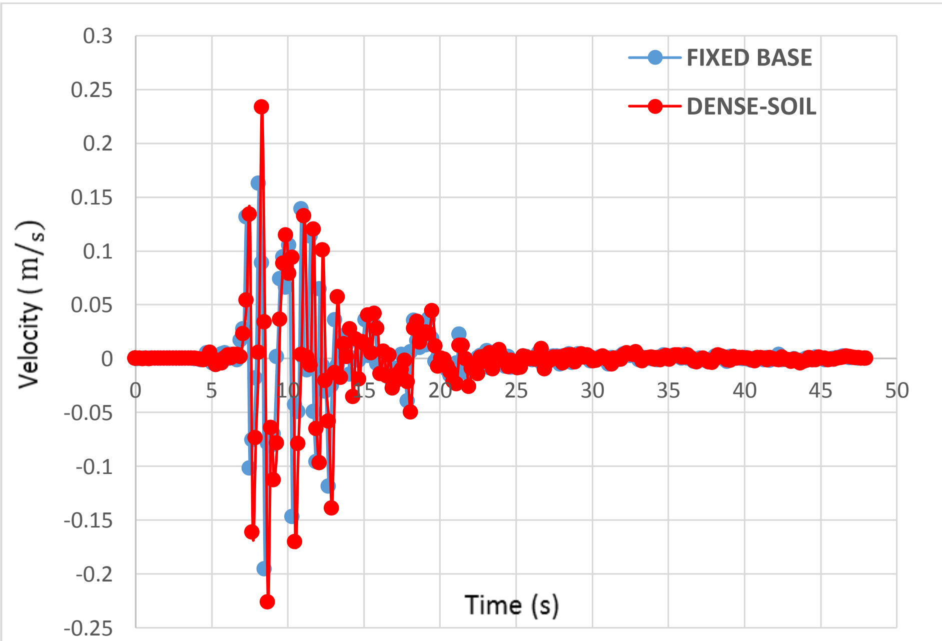

(b)

Figure 25: Nodal velocity history response of the pipeline under (a) fixed base and rock base (b) fixed base and dense-soil base with reference to V1 (Transversal or X) direction.

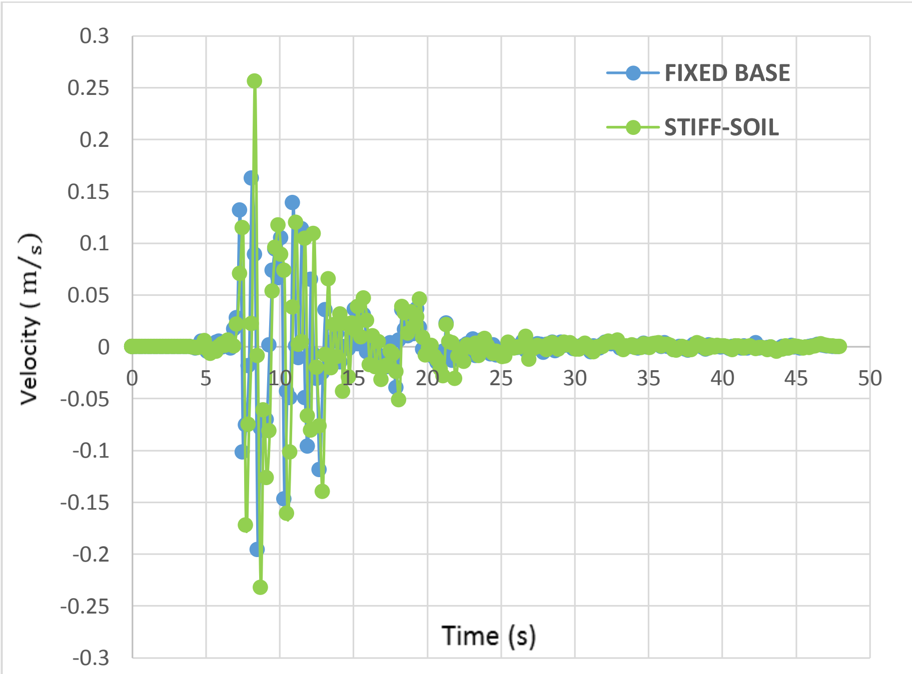

(a)

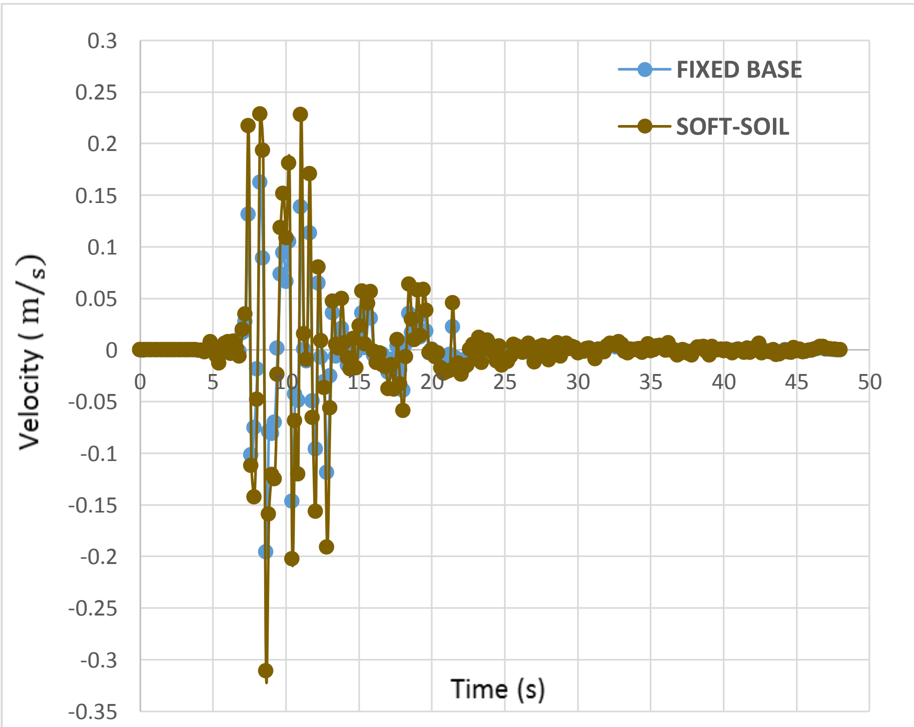

(b)

Figure 26: Nodal velocity history response of the pipeline under (a) fixed base and stiff-soil (b) fixed base and soft- soil base with reference to V1 (Transversal or X) direction.

In Fig. 24, Fig. 25 and Fig. 26 nodal velocity history response of the pipeline under the five supporting base conditions are presented. Form these graph it is observed that, the maximum horizontal velocity of the pipeline under fixed supporting base condition in the direction of V1 (Transverse or X) is 0.2 m/s at 8.66s. For that of rock supporting base condition the maximum horizontal velocity of the pipeline in the direction of V1 (transverse or X) is 0.21m/s at 8.66s.

In a case of dense-soil supporting base condition the maximum horizontal velocity of the pipeline in the direction of V1 (transverse or X) is 0.23 m/s at 8.30s. The maximum horizontal velocity of the pipeline under stiff-soil supporting base condition in the direction of V1 (transverse or X) is 0.26m/s at 8.32s. Finally, maximum horizontal velocity of a pipeline under soft-soil supporting base condition in the direction of V1 (transverse or X) is 0.31m/s at 8.64s.

4.2.3. Displacements

The displacement result outputs along X axis (Transversal or U1) and Y (vertical or U2) direction are presented using graphs for an input ground motion of N-S component of Kobe, 1995. The value of the displacement in the Z axis (Longitudinal or U3) direction is small as compared with the other two directions (U1, U2). For that reason, only the dominant vertical (Y) and transversal (X) displacements are briefly discussed. The ordinate and abscissa of the graphs represents displacement response and time respectively. The result outputs for displacements are presented in the following section.

i. Displacement in U1 (Transverse) Direction

In Fig. 27, Fig. 28 and Fig. 29 are shown, the seismic horizontal displacement response of the straight steel pipeline system in the direction of U1 (transverse or X). The graphs are presented for the five base conditions and presented relative to fixed bases of the pipeline.

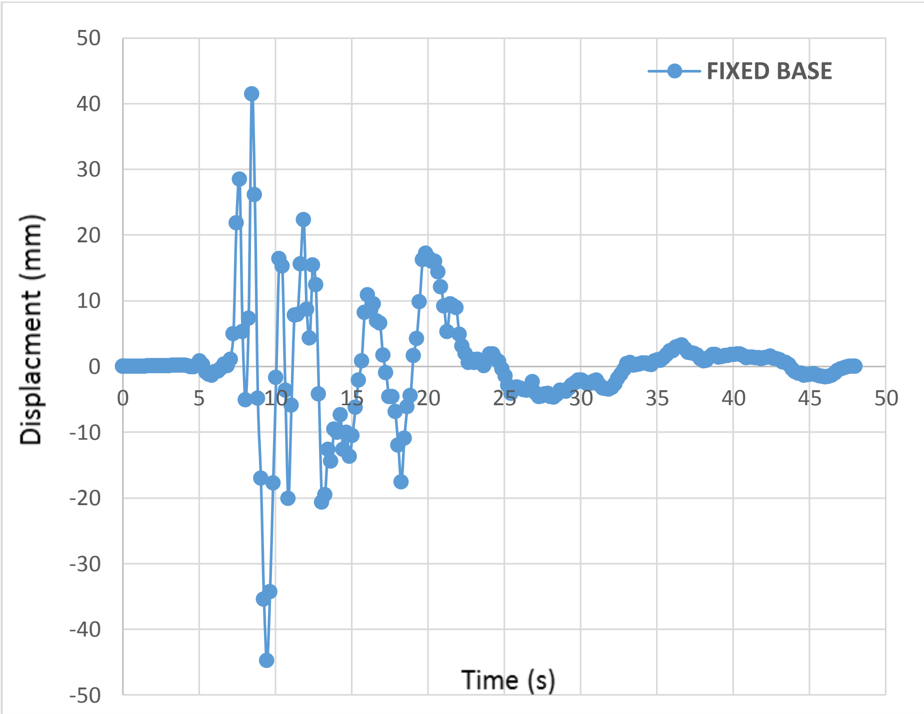

(a)

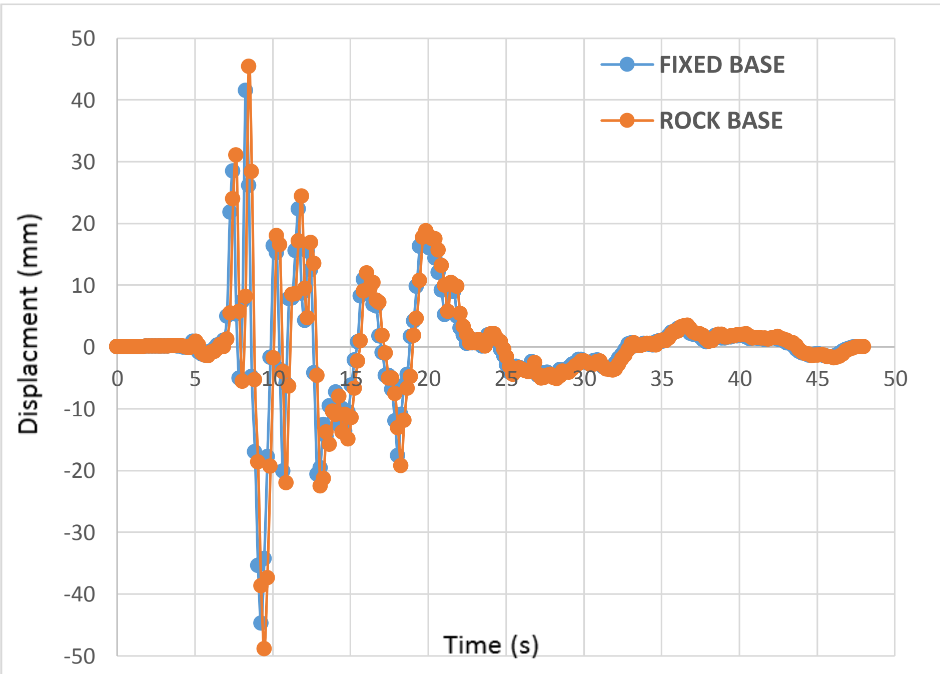

(b)

Figure 27: Nodal displacement history response of the pipeline under (a) fixed base (b) fixed base and rock base with reference to U1 (Transversal or X) direction

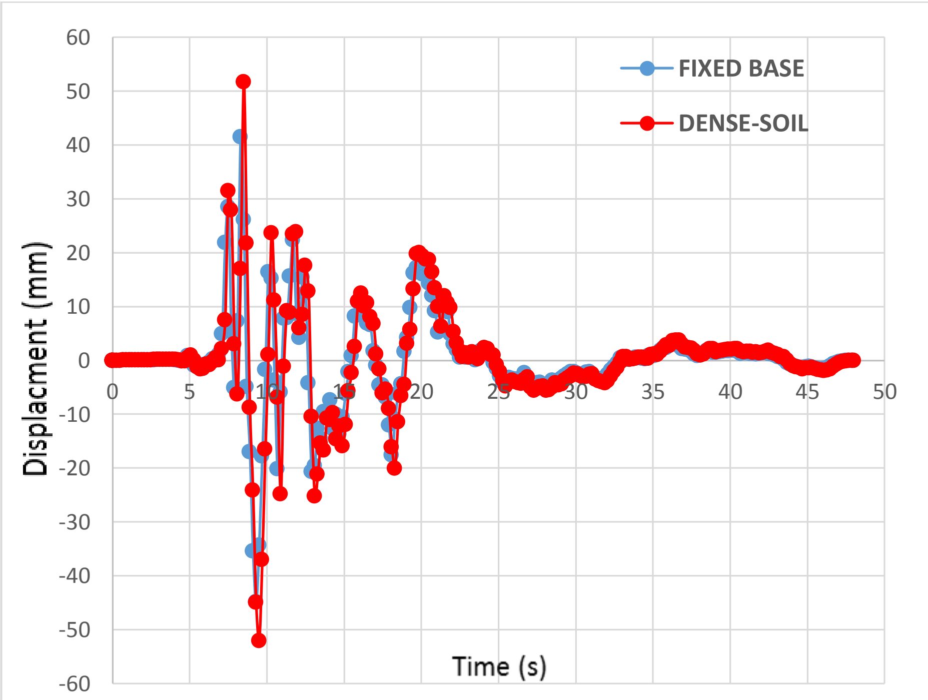

(a)

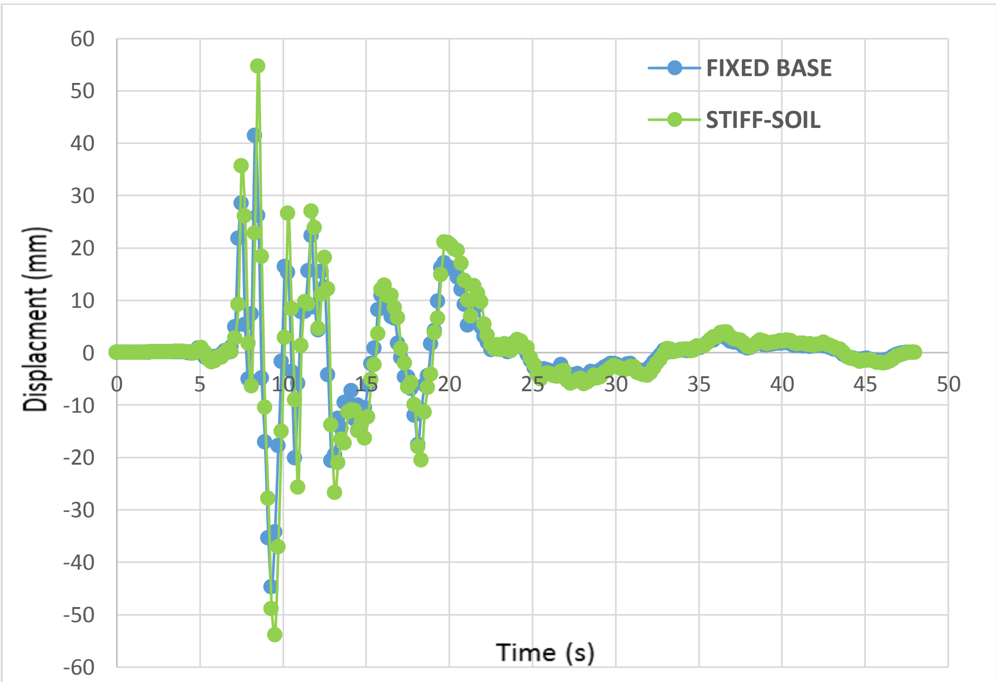

(b)

Figure 28: Nodal displacement history response of the pipeline under (c) fixed base and dense-soil base (d) fixed base and stiff-soil with reference to U1 (Transversal or X) direction

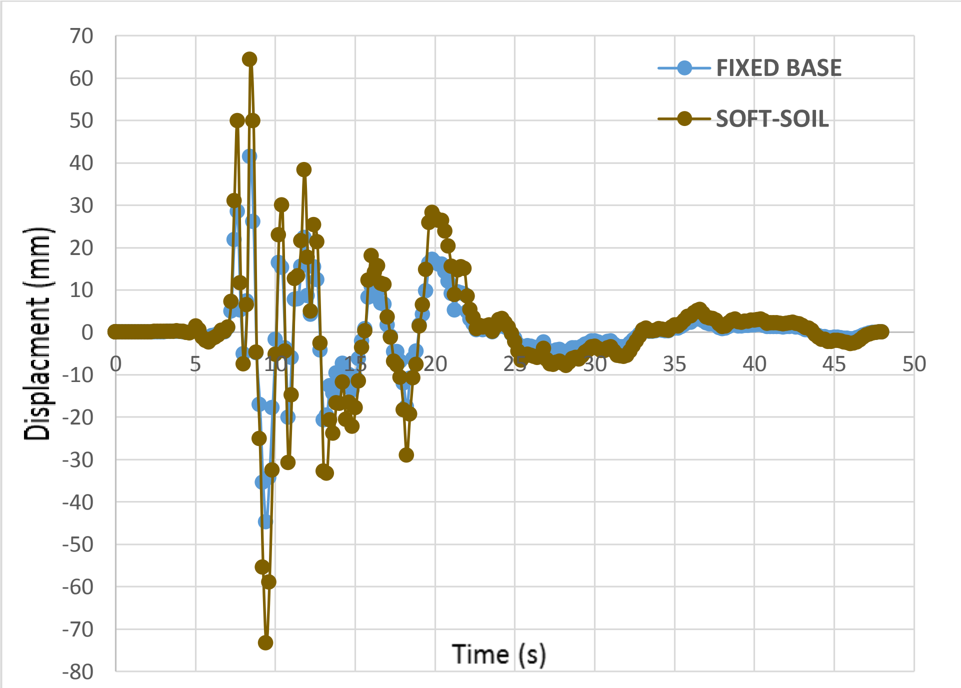

Figure 29: Nodal displacement history response of the pipeline under fixed base and soft- soil base with reference to U1 (Transversal or X) direction

In Fig. 27, Fig. 28 and Fig. 29 nodal displacement history response of the pipeline under the five base conditions are presented. Form these graph it is observed that, the maximum horizontal displacement of the pipeline under fixed supporting base conditions in the direction of U1 (Transverse or X) is 44.80mm at 9.46s. For that of rock supporting base condition the maximum horizontal displacement of the pipeline in the direction of U1 (transverse or X) is 48.92mm at 9.46s. In a case of dense-soil base supporting condition the maximum horizontal displacement of the pipeline in the direction of U1 (transverse or X) is 52.04mm at 9.52s.

The maximum horizontal displacement of the pipeline under stiff-soil supporting base condition in the direction of U1 (transverse or X) is 54.69mm at 8.52s. Finally, maximum horizontal displacement of a pipeline under soft-soil supporting base condition in the direction of U1 (transverse or X) is 73.32mm at 9.44s.

From the above graph and discussion, it is observed that the horizontal displacement of the pipeline in the direction of U1 (transverse or X) under the five base conditions is maximum at a time range of 9.46s to 9.52s. On the other hand, the Peak Ground Acceleration (PGA) of the ground motion (N-S component of Kobe 1995) is 8.054m/s^2.

This indicate that, the maximum displacement of the pipeline under the five base condition are appeared after 8.54s.In addition, Fig. 30 and Fig. 31 show, displacement response contour of the symmetric model of the pipeline at a length of 6m in the direction of U1 (transverse or X). It is observed that, the pipe showed deformation and the value of displacement around the selected node (Node no 2913) is range between 42.25 mm to 46.38mm at a time of 9.46s under fixed supporting base condition.

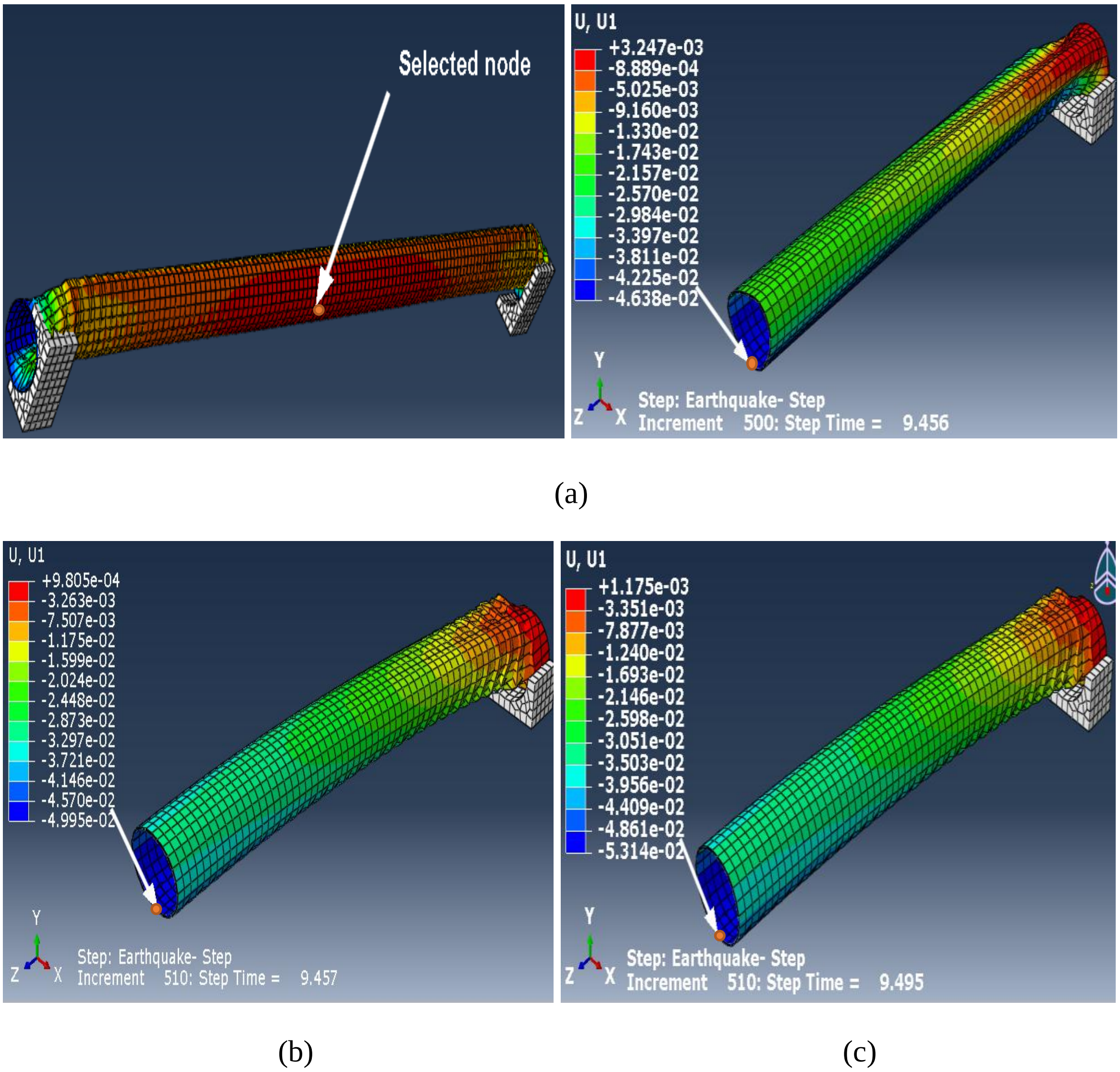

Figure 30: Displacement response contour of the symmetric model of the pipeline in the direction of U1 (transvers) under (a) fixed base (b) rock base (c) dense-soil base condition.

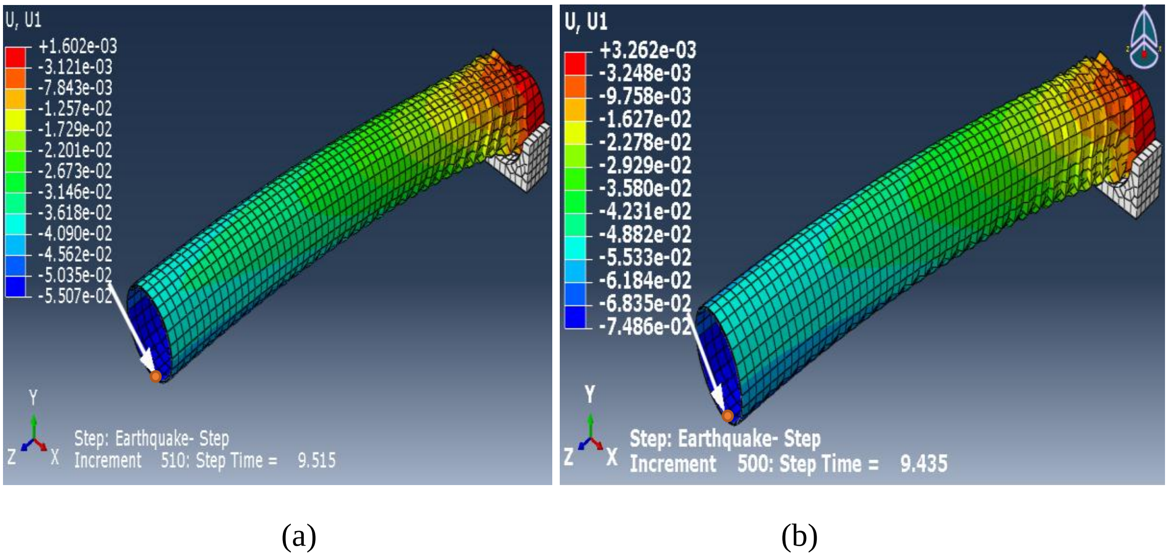

Figure 31: Displacement response contour of the symmetric model of the pipeline in the direction of U1 (transvers) under (a) stiff-soil base (b) soft-soil base condition.

The value of displacement of the pipeline under dense-soil base condition (Fig. 24d) around the selected node is in a range between 48.61 mm to 53.14mm at a time of 9.50s. When the base condition is changed to soft-soil supporting base the value of displacement is in a range between 68.35 mm to 74.86mm at a time of 9.44s.

Table 8 summaries the percentage displacement of different support conditions under Kobe, 1995 earthquake ground motion. Fixed base of structure is kept as a datum case and the response of the pipeline under the other four base conditions are compared with the fixed one.

Table 8: Peak displacement response quantities and percentage displacement of the pipeline with respect to U1 (Transvers or X).

Support condition	Displacement in transversal direction U1	
	U_1 (mm)	% increase relative to fixed
Fixed support	44.80	0.00
Rock support	48.92	9.20
Dense soil support	52.04	16.16
Stiff soil support	54.69	22.08
Soft soil support	73.32	63.66

As the base condition of the pipeline changes from fixed (without SSI) to rock, dense-soil, stiff-soil and soft-soil support conditions, the displacement has increased by 9.20%, 16.16%, 22.08%, and 63.66% respectively.

In general, the percentage variation of displacement (Transverse or X) relative to the fixed support condition increases as the support condition becomes more flexible.

ii. Displacements in U2 (Vertical) Direction

Fig. 32, Fig. 33 and Fig. 34 show, the seismic vertical displacement response of the straight steel pipeline system in the direction of U2 (Vertical or Y). The graphs are presented for five base conditions with relative to fixed bases of the pipeline.

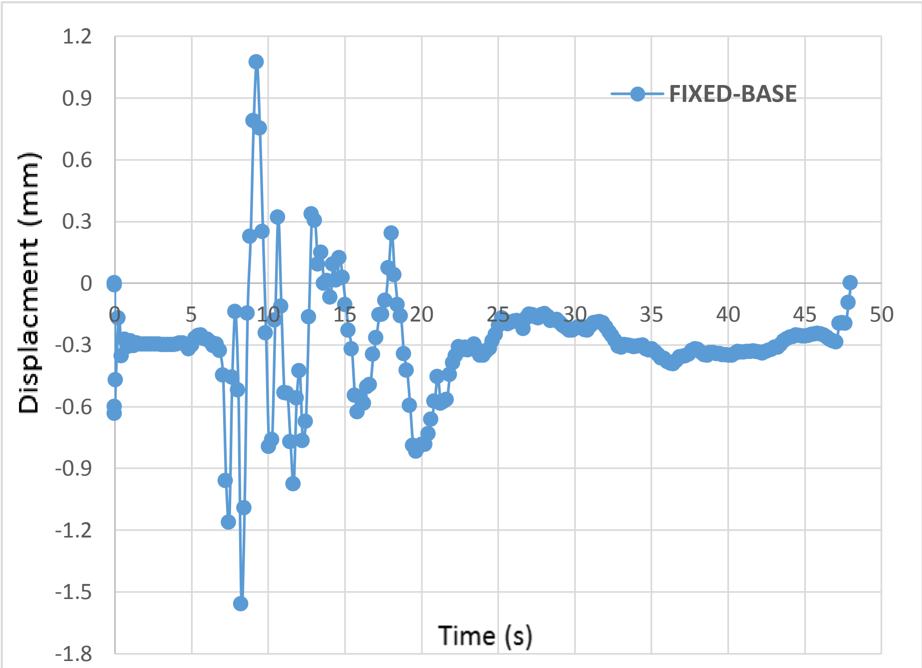

Figure 32: Nodal displacement history response of the pipeline under fixed base with reference to U2 (Vertical or Y) direction.

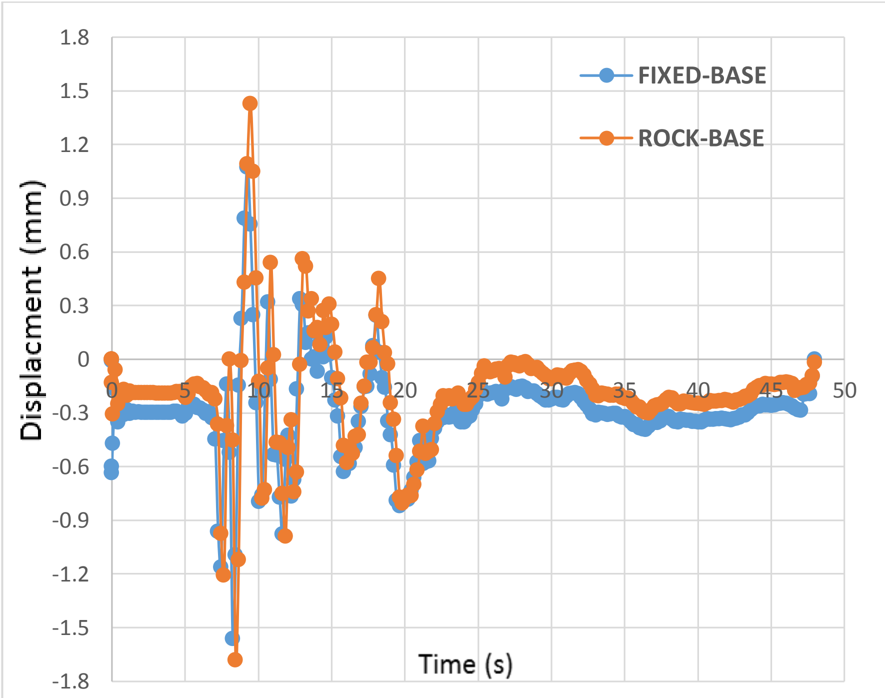

(a)

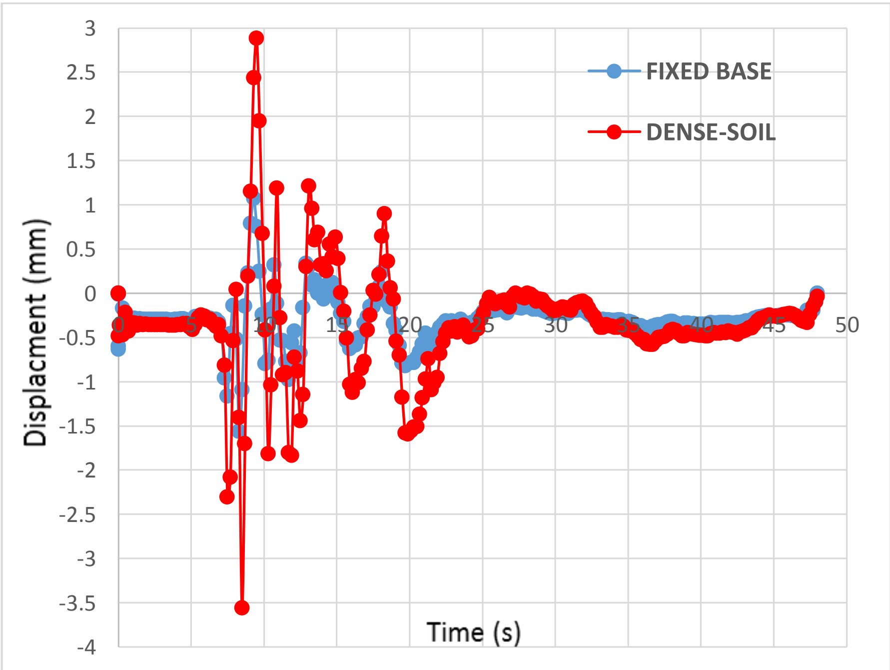

(b)

Figure 33: Nodal displacement history response of the pipeline under (a) fixed base and rock base (b) fixed base and dense-soil base with reference to U2 (Vertical or Y) direction.

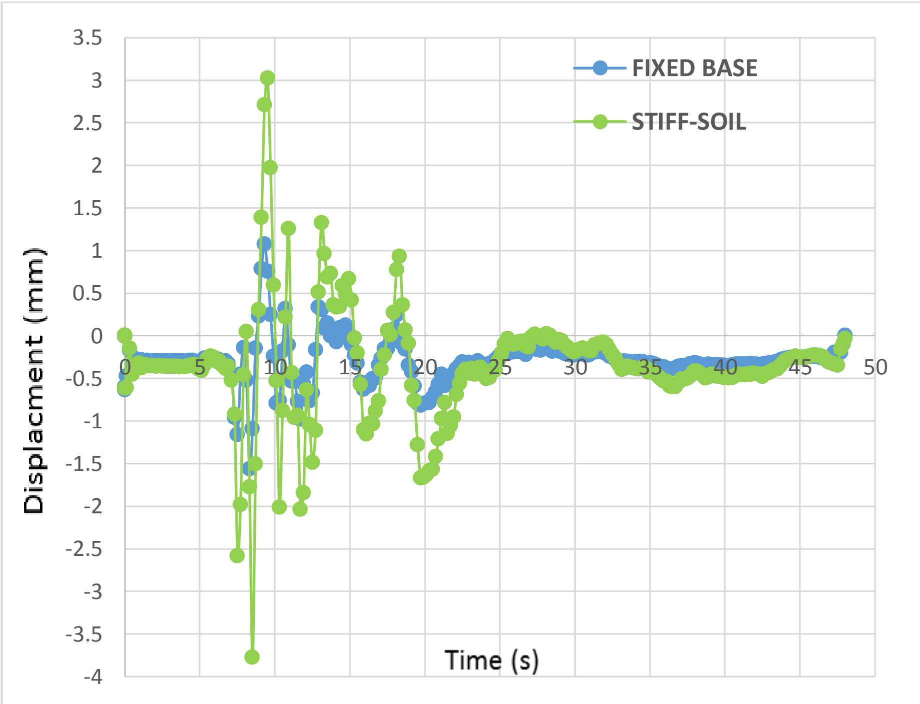

(a)

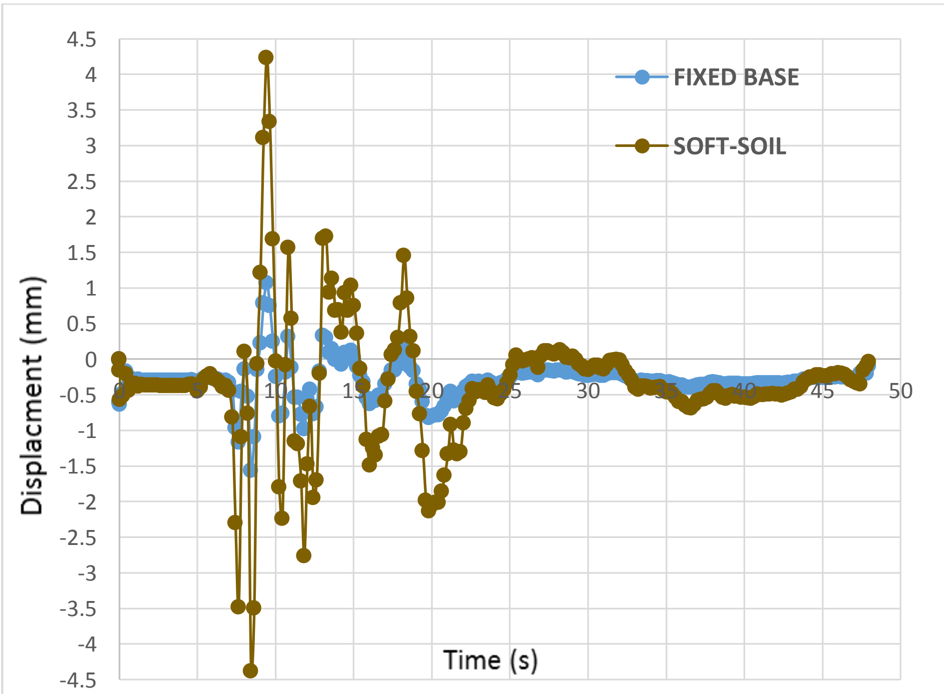

(b)

Figure 34: Nodal displacement history response of the pipeline under (a) fixed base and stiff-soil (b) fixed base and soft- soil base with reference to U2 (Vertical or Y) direction.

From the graphs, figures and table the same behavior is observed for U2 (Vertical) direction similar to that of U1 (transverse) direction i.e., the displacement in U2 direction increases when SSI is considered. Hence, the discussion made for U1 direction is also applied to the results of U2 direction.

In Fig. 32, Fig. 33 and Fig. 34 nodal displacement history response of the pipeline under the five base conditions are presented. Form these graph it is observed that, the maximum horizontal displacement of the pipeline under fixed supporting base condition in the direction of U2 (Vertical or Y) is 1.56mm at 8.26s. For that of rock supporting base condition the maximum horizontal displacement of the pipeline in the direction of U2 (Vertical or Y) is 1.70mm at 8.46s. In a case of dense-soil base supporting condition the maximum horizontal displacement of the pipeline in the direction of U2 (Vertical or Y) is 3.56mm at 8.50s.

The maximum horizontal displacement of the pipeline under stiff-soil supporting base condition in the direction of U2 (Vertical or Y) is 3.77mm at 8.52s. Finally, maximum horizontal displacement of a pipeline under soft-soil base supporting condition in the direction of U2 (Vertical or Y) is 4.38mm at 8.44s.

From the above graph and discussion, it is observed that the vertical displacement of the pipeline in the direction of U2 (Vertical or Y) under the five base conditions is maximum at a time range of 8.457sec to 8.59s. This indicate that, the maximum displacement of the pipeline under the five base condition are appeared just before and immediately after 8.54s.

In addition, Fig. 35. (a), (b), (c) and (d) show, displacement distribution figures of a pipeline system at a length of 6m in the direction of U2 (Vertical or Y) from ABAQUS software tool. In this figure it is observed that, the maximum displacement of the pipeline around the selected node near the mid span is 1.67mm at a time of 8.257 under fixed supporting base condition.

The displacement of the pipeline approximately around the selected node is 4.82mm at a time of 8.50s under dense-soil supporting base condition.

On the other hand, the displacement of the pipeline at same node is 5.14mm at a time of 8.52s under stiff-soil supporting base condition. For soft-soil supporting base, the displacement of the pipeline is 6.1mm at a time of 8.44s.

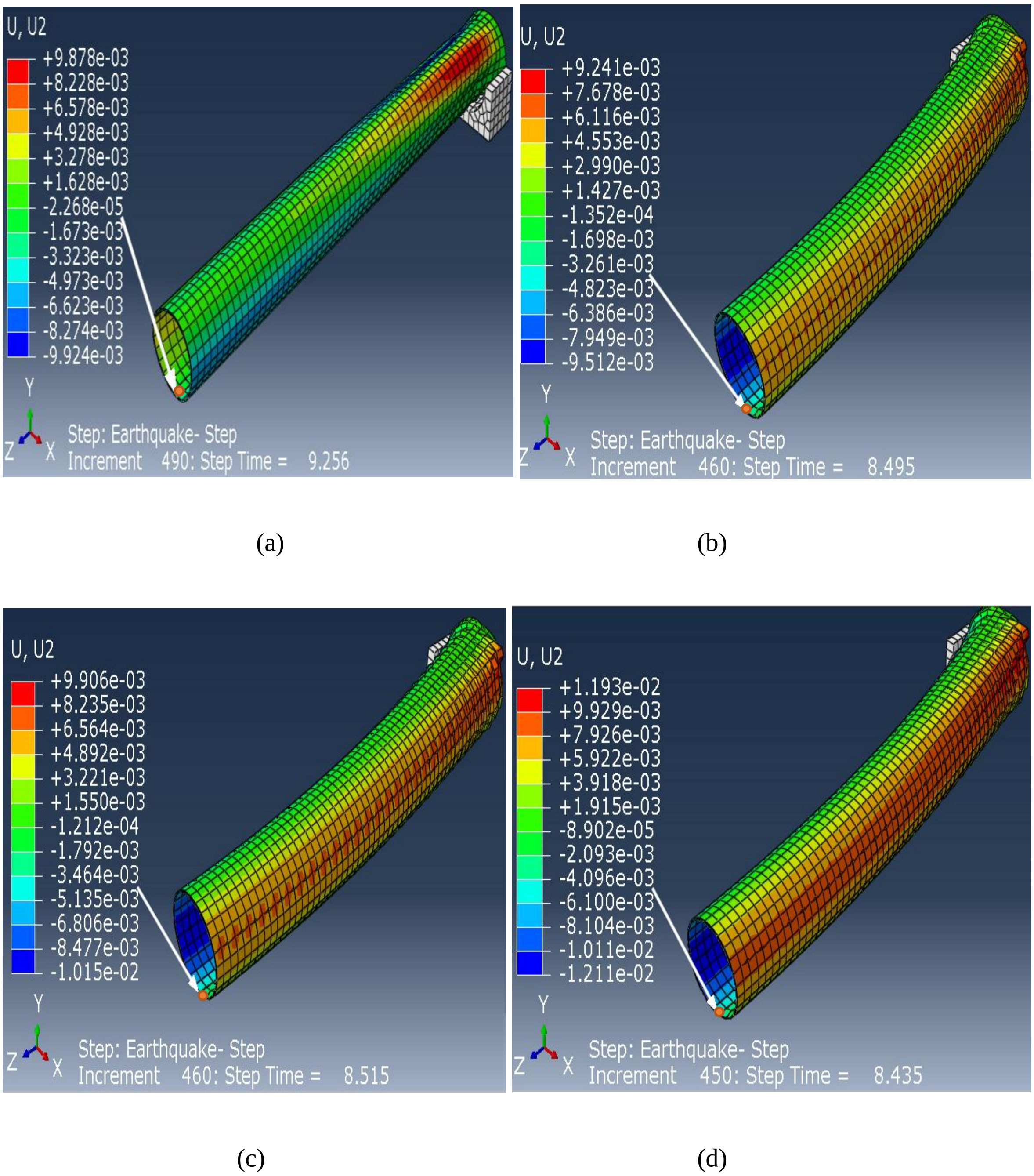

Figure 35: Displacement response contour of the symmetric model pipeline in the direction of U2 (vertical) under (a) fixed base condition (b) dense-soil (c) stiff-soil base (d) soft-soil base condition.

Table. 9 summaries the percentage displacement of different support condition under Kobe, 1995 earthquake ground motion. By keeping fixed supporting base of structure as a datum case, the response of the pipeline under the other four supporting base conditions are compared with the fixed one.

Table 9: Peak displacement response quantities and percentage displacement of the pipeline with respect to U2 (vertical or X).

Support condition	Displacement in vertical direction U2	
	U_2 (mm)	% increase relative to fixed
Fixed support	1.56	0.00
Rock support	1.68	8.97
Dense soil support	3.56	128.2
Stiff soil support	3.80	143.6
Soft soil support	4.38	180.8

As the base condition of pipeline changes from fixed (without SSI) to rock, dense-soil, stiff-soil and soft-soil support conditions, the displacement has increased by 8.97%, 128.2%, 143.6%, and 180.8% respectively.

4.2.4. Bending moment

The variation of bending moment for all the cases along the length of the pipeline (X) are plotted in Fig. 36 (a), (b), (c) and (d). As it can be observed from these graphs, the pipe has both support moment and span moment in all cases, this is due to the fact that support system between the pipe and the support material (Teflon) acts as partially restrained support system.

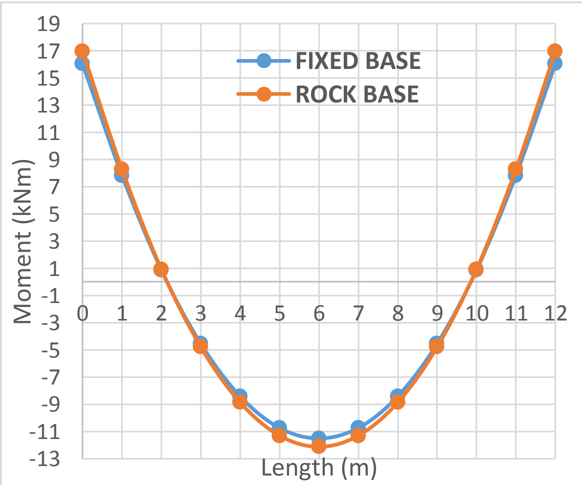

(a)

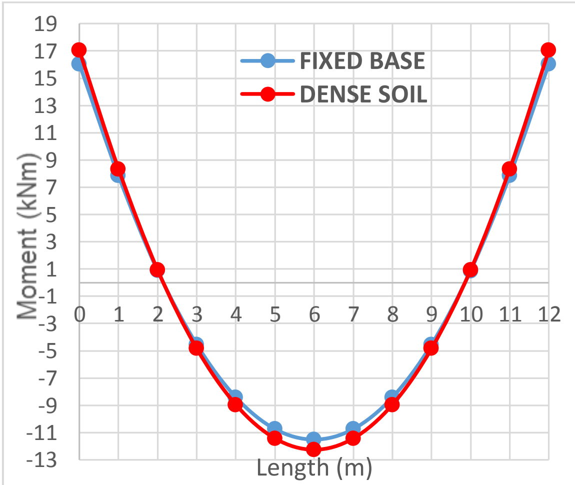

(b)

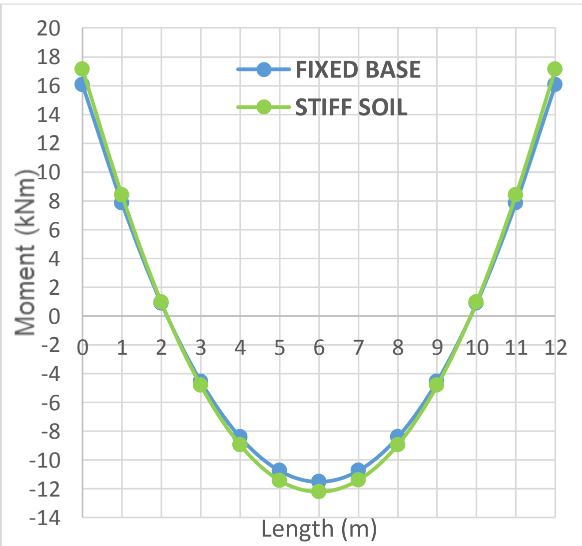

(c)

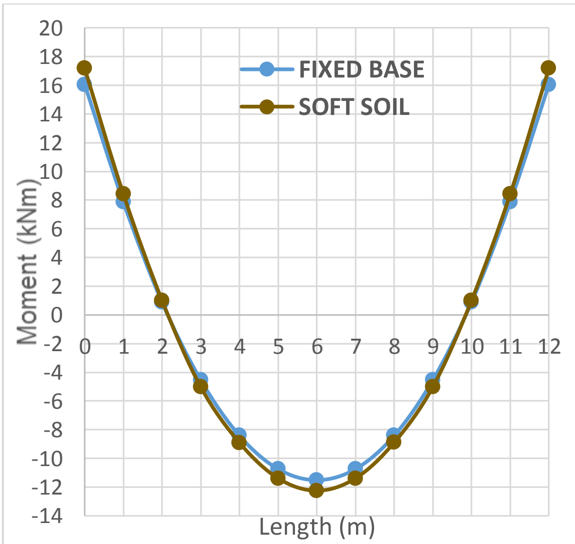

(d)

Figure 36: Bending moment diagram along the length of the pipeline (a) fixed base and rock base (b) fixed base and dense-soil base (c) fixed base and stiff-soil base (d) fixed base and soft-soil base condition.

The values of support and span moment of a pipeline under fixed base condition are 16.06kN.m, and 11.51kN.m respectively. On the other hand, the values of support and span moment of a pipeline under rock base condition are 16.96kN.m, and 12.13kN.m respectively. For that of dense soil base condition the values of support and span moment of a pipeline are 17.04kN.m, and 12.26kN.m respectively and for stiff soil base condition the values of support and span moments are 17.13kN.m, and 12.2kN.m respectively. Finally for soft soil base condition the values of support and span moments are 17.17kN.m and 12.25kN.m respectively.

From the above graph and discussion, it is observed that both the support moment and the span moment is increase as the base condition become more flexible. This indicate that the bending moment of a pipeline will become large as the shear wave velocity and the stiffness of support conditions is small.

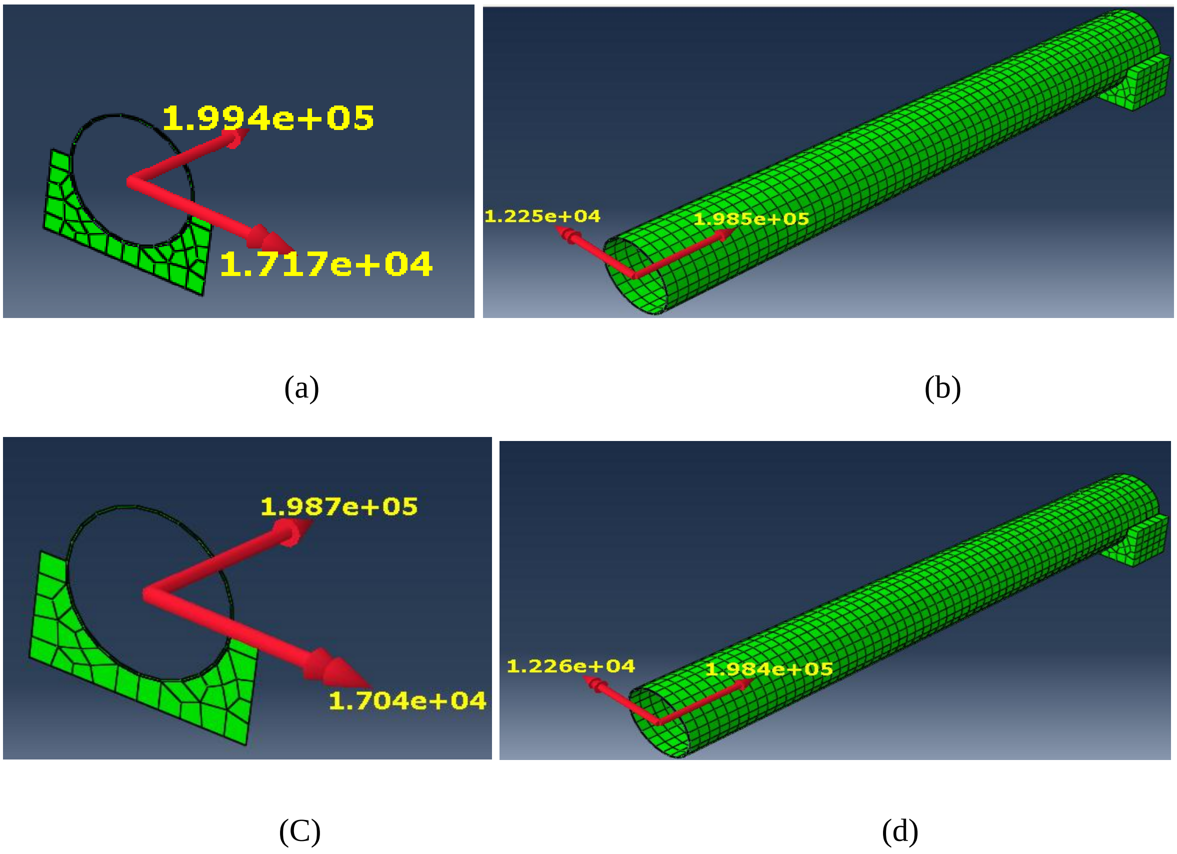

Figure 37: Section bending moment value of pipeline (a) support moment under soft-soil base (b) span moment under soft soil (c) support moment under dense-soil base (d) span moment under dens-soil

Figure. 37 (a), (b), (c) and (d) show that the values of bending moment of a pipeline under soft-soil and dense-soil base condtion, where the plane of section cut the Z-plane of the pipe perpendicularly in ABAQUS cordinate system.

4.2.5. Principal stresses

The finite element models created in chapter three facilities the analysis of a stress distribution of the areas of interest along the pipeline. It is, however, important to notice that the relevant stresses associated with seismic damage are the maximum principal stresses (tension and compression values when the value of the shear is equal to zero) and the first principal stress (maximum Principal stress) are one of special interest [4].

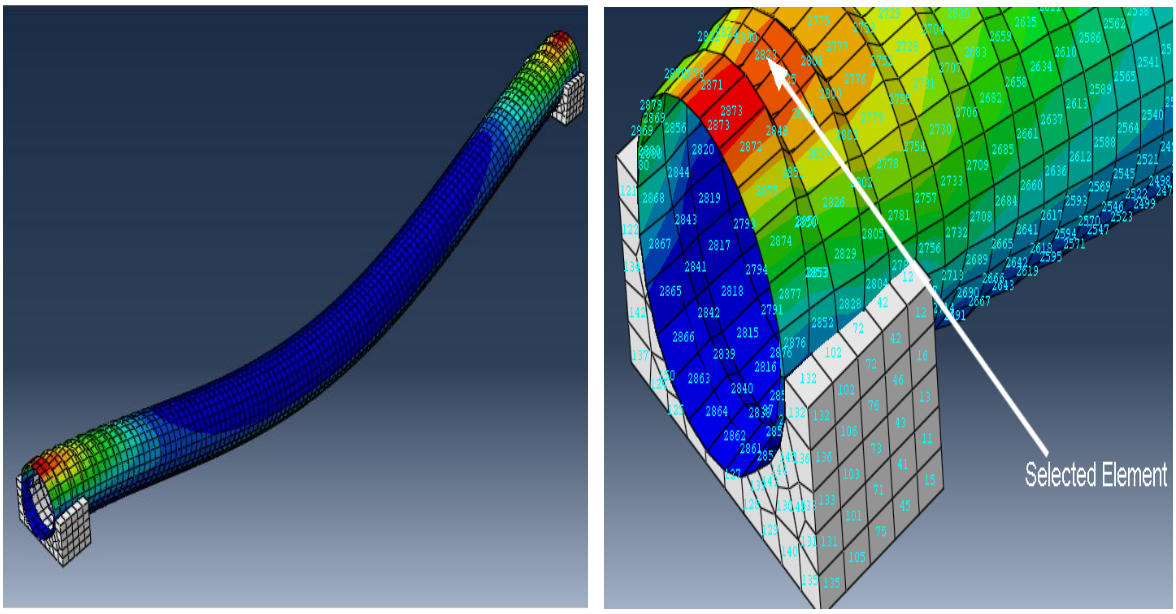

Figure 38: Principal stress response contour of the pipeline and selected element.

As can be seen from the Fig. 38, the nature of distribution of stress along the pipeline is similar under the five base conditions except that the values are different. Accordingly, the highly-stressed region under all the five cases is found at the support of the pipeline and the values of stresses decrease away from the support. As a result, for the purpose of this thesis a representative element is selected around the support of the pipe in order to realize the maximum principal stress on the pipeline.

Fig 39. Fig. 40 and Fig. 41 show, the maximum principal stresses for the five aforementioned cases of a representative element.

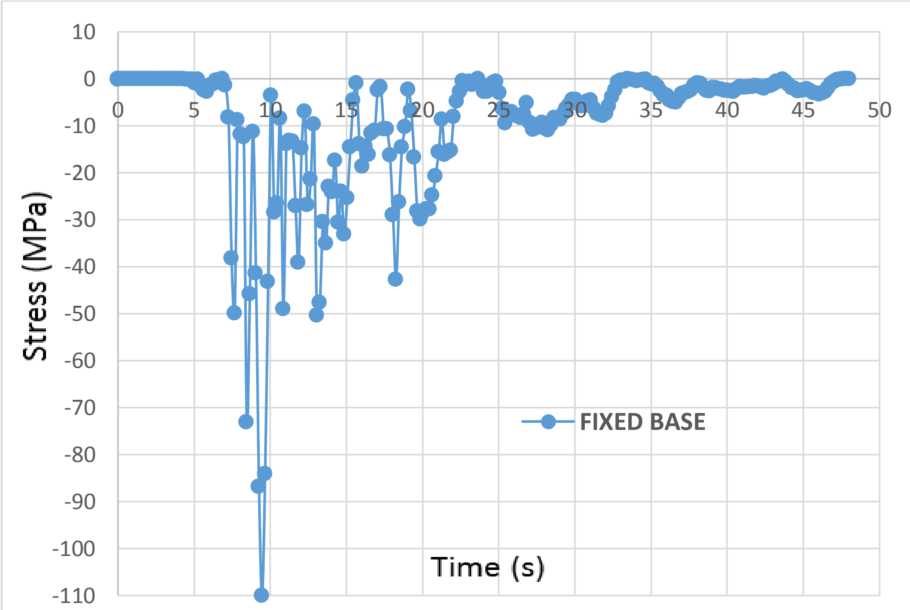

(a)

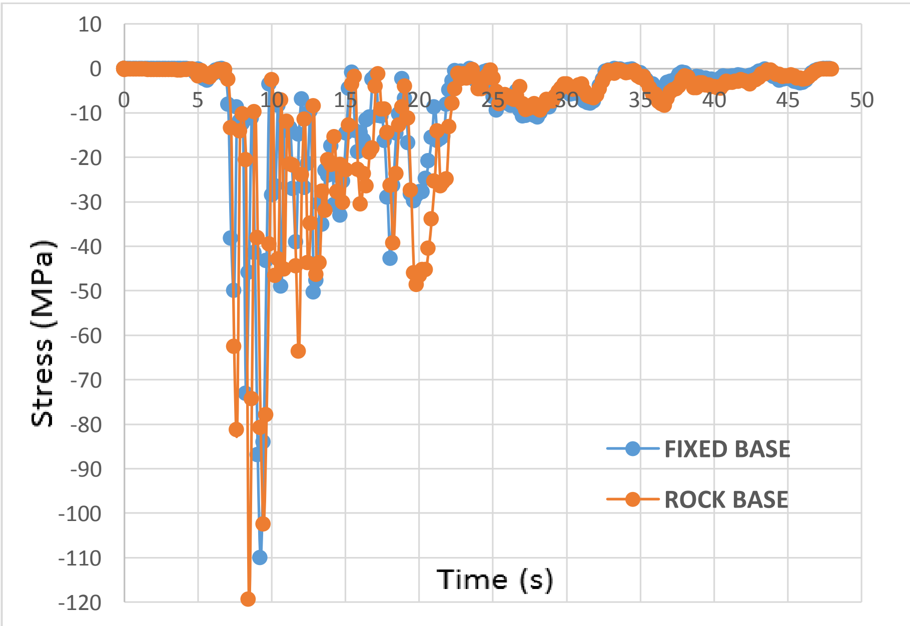

(b)

Figure 39: Nodal principal stress history response of the pipeline under (a) fixed base (b) fixed base and rock base.

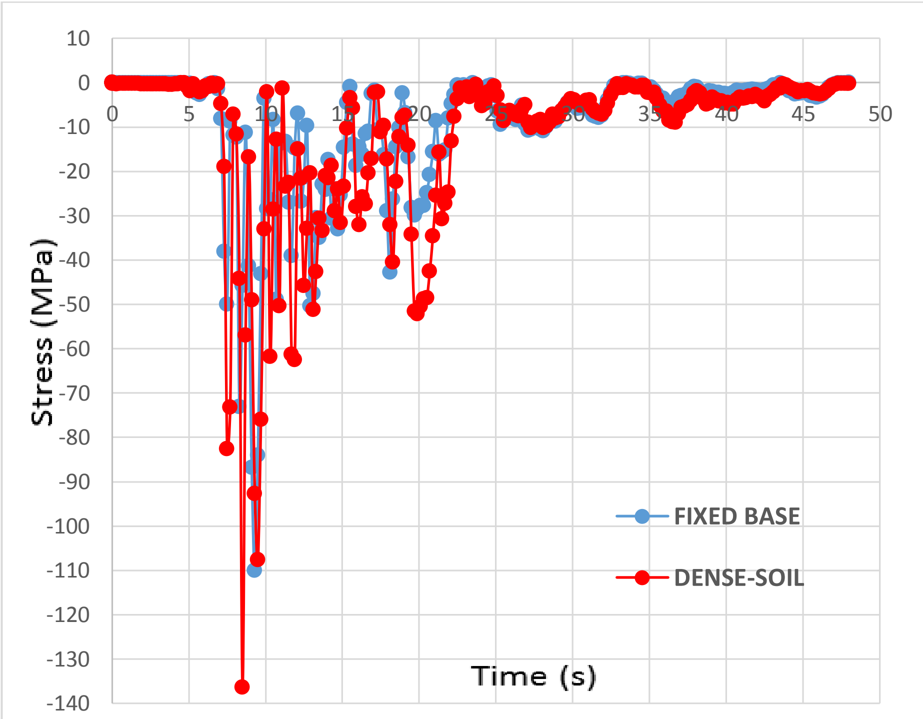

(a)

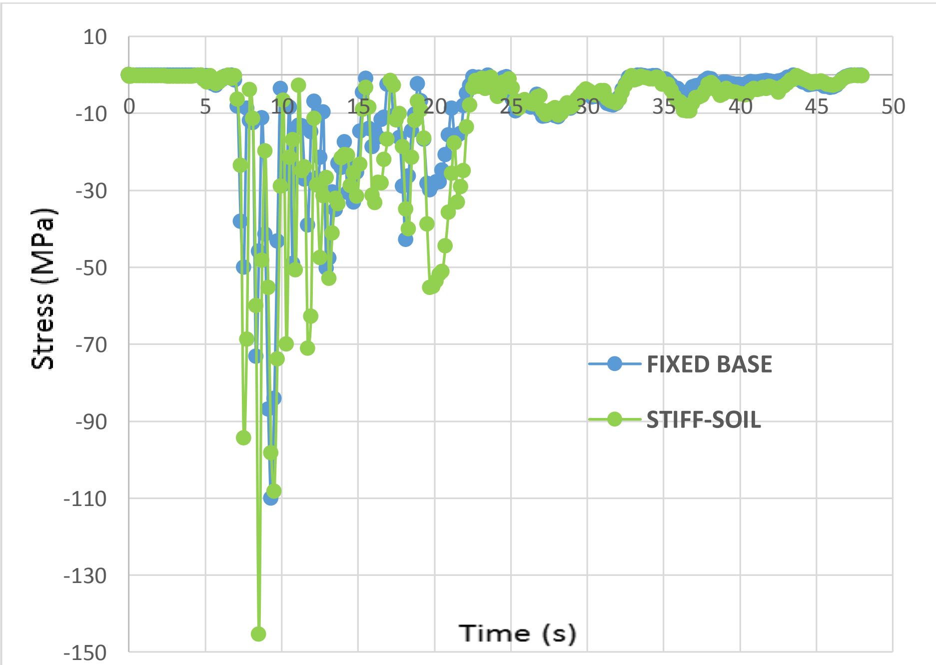

(b)

Figure 40: Nodal principal stress history response of the pipeline under (a) fixed base and dense-soil base (b) fixed base and stiff-soil

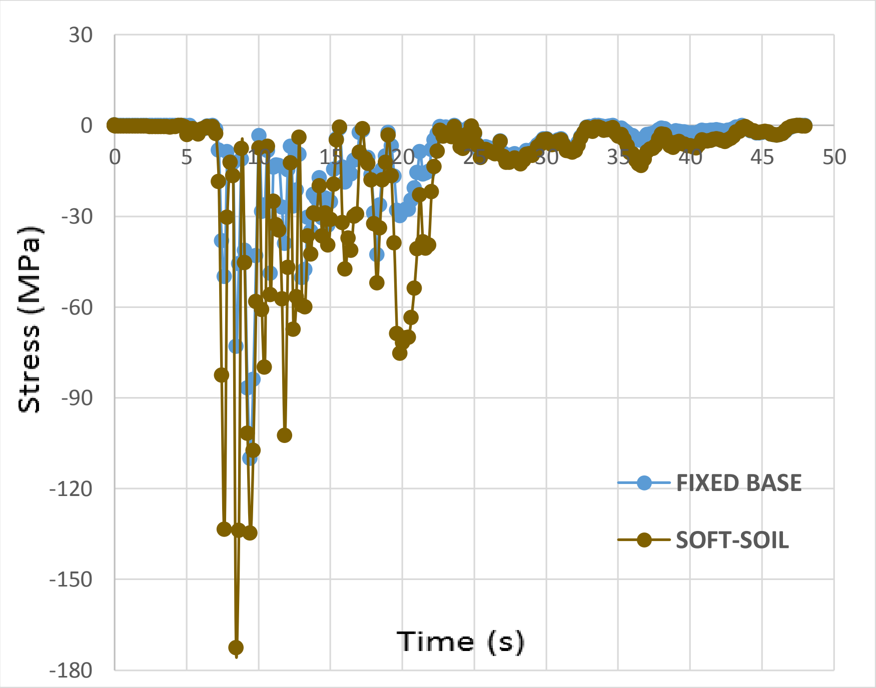

Figure 41: Nodal principal stress history response of the pipeline under fixed base and soft- soil base.

In Fig. 39, Fig. 40 and Fig. 41 the nodal principal stress history response of the pipeline under five supporting base conditions are presented. It is observed that, the maximum principal stress under fixed base condition is 110.00 MPa at 9.46s. On the other hand, the maximum principal stress of the pipeline under rock base condition is 119.42 MPa at 8.48s. For dense-soil base condition, the maximum principal stress is 136.36MPa at 8.50s. For that of stiff-soil base condition, the maximum principal stress is 145.31MPa at 8.52s while the maximal principal stress of a pipeline under soft-soil base condition is 172.57MPa at 8.44s.

4.3. DISCUSSION

In this study, acceleration, velocity and displacement time history have been used to describe the behavioral response of pipelines under seismic action. The acceleration time history has shown a significant portion of relatively high frequencies and exhibited the same pattern with the applied ground motion as shown in Fig. 21 Fig. 22 and Fig. 23. Integration produced a smoothing effect of the graph, therefore, the velocity time history response shows substantially lesser high-frequency response than the acceleration time history response as shown in Fig. 24, Fig. 25 and Fig. 26. The displacement time history, obtained by another round of integration is dominated by relatively low frequency response and is presented in Fig. 27, Fig. 28 and Fig. 29. This smoothing effect shows that the result obtained from finite element analysis conforms to expected finding.

From the above discussion the horizontal acceleration A1 of the pipeline in the Transvers or X direction and which is on soft-soil is larger than the acceleration of the pipeline on all the support conditions. Furthermore, it is observed that the horizontal velocity (V1) and displacement (U1) of the pipeline in the transvers (X) direction and on the soft-soil is larger than the velocity and displacement of the pipeline on the other support conditions.

The maximum principal stress and the bending moment along the length of the pipeline, associated with soft-soil, is larger than the maximum principal stress and the bending moment of the pipeline under other support conditions.

In addition, from the graph and the discussion above it is observed that the displacement of the pipeline has different value at different time under the same loading condition while having different base/support system.

Generally, all the responses vary with the value of dynamic spring and dashpot; as the result, as the base condition becomes more flexible all response value will be larger. The responses is for each case vary due to the soil stiffness being different for each support condition.

The soil stiffness is one of the significant factors which affect the pipe response under seismic load as noted in this study. It is highly influence by soil parameters, i.e., shear wave velocity ($V_{s.}$), density of the soil $\boldsymbol{\rho}$, and void ratio v.

All the above discussions show that the responses of the pipeline are related to the soil parameters. As the shear wave velocity ($V_{s.}$) and the density of the soil increase, the responses tend to decrease.

This leads to conclude that the existence of significant relation of the pipe responses with that of shear modulus (G) of the soil; thus, the shear modulus of the soil increases, the flexibility of the soil will decrease.

Among the factors considered in this study, void ratio is one that contribute to the value of shear modules (G) and shear wave velocity ($V_{s.}$). When void ratio increases, both shear modulus and shear wave velocity decrease. Soft soil has a large value of void ratio, accordingly, it has large responses.

From the above discussion it can be observed that the peak response of above-ground pipeline under the effect of SSI has significant difference with that of the corresponding above-ground pipeline ignoring SSI effect. As a result the soil surrounding the foundation has substantial effect on the response of the pipeline structure and the time-history analyses that neglected the effect of SSI resulted in large underestimation of displacement of the structure particularly for soft soil. Therefor ignoring the effect of SSI for a soil type with small value of shear wave velocity may resulted in a large underestimation of displacement in the response analysis of the system.

The overall point which can be drawn from the above discussion is that the assumption of fixed-base structure in the structural analysis is not always realistic. The earthquake impact of pipelines may result in release of hazardous material. Therefore assuming fixed-base structure is no longer adequate in terms of structural safety. Accordingly, considering SSI effects in seismic design of above-ground pipeline structures resting on flexible support conditions particularly for soft soil deposit is important in order to guarantee the structural safety of above-ground pipeline in particular, long-span lifeline facilities as whole.

CHAPTER FIVE

CONCLUSION AND RECOMMENDATION

5.1. CONCLUSION

The influence of soil-structure interaction for above-ground pipeline is studied using time history analysis for fixed-base, rock, dense, stiff and soft-soil supporting base conditions. After careful analysis and discussion, the following major conclusions are drawn:

- The effect of change of base condition is observed to be of paramount importance. As the base condition become more flexible, displacement, acceleration, bending moment and principal stresses increase significantly. In a view of such development, therefore, such increases in the response will considerably alter the performance level of the above-ground pipeline structures under seismic excitation.
- The displacements, accelerations, bending moments and principal stresses of the pipeline are maximum with soft-soil base condition. This indicates that the response of the pipeline has significant relation with the soil parameter. Hence, particular emphasis should be given in the evaluation of spring and dashpot coefficient for soft-soil base condition in order to reflect the actual base-system scenario.
- As the shear wave velocity of the system increases, the stiffness and dashpot properties of the system will also increase. This implies that as V_S increases, the properties of the system will approach the properties of an equivalently fixed base system. Hence, for soil type with high shear wave velocity property that approaches shear wave velocity of rock, consideration of SSI can be neglected during analysis.
- The overall conclusion which can be drawn from the study is that the classical assumption of fixed-base structure (without the effect of soil- structure interaction) in the structural analysis is not always realistic; this is because the soil under the structure foundation modifies earthquake loading and changes the structural response property. Hence, it can be concluded that in the conventional structural analysis methods assuming fixed-base structure is no longer adequate to guarantee structural safety. Therefore, considering SSI effects in seismic design of long-span above-ground pipeline structures resting on flexible support conditions like soft soil deposit is essential.

5.2. RECOMMENDATION AND FURTHER WORK

It is recommended to incorporate soil-structure interaction (SSI) for long-span above-ground pipeline structure during seismic analysis in order to assure the structural safety. In addition to investigating issues related to the influence of soil-structure interaction effect, on the general understanding of seismic response of long-span above-ground pipeline structure, the following areas are identified for future studies:

- This study focused only on the response of long-span above-ground pipeline under the influence of soil-structure interaction. Similar studies on power transmission lines, bridges and other long-system structures could be an important extension of this work.
- This study has assumed structure placed on a flat terrain; considering the configuration layout of pipelines on different terrain would be an important aspect to study in association with SSI.
- Further study can be conducted by considering hammering effect of the fluids, and differential temperature.
- In this work, only identical spring and dashpot coefficient have been consider along the entire length of the pipeline; but further research work can be pursued by specifying variable spring and dashpot coefficient to simulate variable conditions of pipeline embedment (soil-support heterogeneity along with entire length of the pipeline).

REFERENCES

1. Ahmed, A. and Hamdy, H., “Contribution of Soil-Structure Interaction to Seismic Response of Buildings”, KSCE Journal of Civil Engineering 17(5): 959-971, 2013.
2. Alvaro, D. “Finite Element Modeling of Damage and Failure in Fiber Reinforced composites” aerospace engineering, May 2015.
3. American Petroleum Institute, “Specification for Line Pipe”, API 5L: 49 CFR 192.113, the Executive Director Office of the Federal Register Washington, D.C., 2004.
4. Arora, K., “Soil Mechanics and Foundation Engineering”, 4 Publishers Distributors, India, Delhi Standard, 1997.
5. Douglas, J., William, J. and Vincent, S., “Trans-Alaska Pipeline Seismic Engineering Legacy”, Tenth U.S. National Conference on Earthquake Engineering, Frontiers of Earthquake Engineering, Alaska, July, 2014.
6. Elnashai, A. and Sarno, L., “Fundamentals of Earthquake Engineering”, John W. & Sons, Ltd, Publication, UK, 2008.
7. European Standard Norme “Eurocode 8: Design of Structures for Earthquake Resistance part 1: General rules, Seismic Action and Rules for Building” 1998-1, 2003.
8. European Standard Norme “Eurocode 8: Design of Structures for Earthquake Resistance part 4 Silos, Tanks and Pipeline” 1998-4, 2003.
9. Gazetas, G., “Analysis of Machine Foundation Vibration: State of Art”, Soil Dynamics and Earthquake Engineering, Vol. 2, No. 1, pp. 1-41, 1983.
10. Gazetas, G., “Foundation Engineering Handbook, Foundation Vibrations”, Greece and State University of New York Bufaffalo 1991.
11. George, M. and Gazetas, G., “Seismic Soil-Structure Interaction: Beneficial or Detrimental?” Journal of Earthquake Engineering, Vol. 4, No. 3, 277-301, 2000.
12. Graham, H., “Seismic Response Analyses of Above-ground Pipelines”, University of California, Berkeley, California, U.S.A., Earthquake Engineering and Structural Dynamics, VOL. 6, 157-165, 1978.
13. Hopkins, P., “Pipelines: Past, Present, and Future”, the 5th Asian Pacific IIW International Congress, Australia, March 2007.

14. http://www.bloomberg.com/topics/ethiopia/Djibouti Agree on Blackstone-Backed Fuel Pipeline Bloomberg Business.html
15. Izuru, T., “Closed-Form Sensitivity of Earthquake Input Energy to Soil-Structure Interaction System”, Journal of Engineering Mechanics, vol. 133, No. 4, April, 2007.
16. James, C. and Sterling, B., “Seismic Behavior of Above-Ground Oil Pipelines”, Earthquake Engineering and Structural Dynamics, Vol. 3, 319-336, Los Angeles, 1975.
17. Jonathan, P., Raymond, B and Gregory. L., “Empirical Evaluation of Inertial Soil-Structure Interaction Effects”, PEER-98/07, University of California, Berkeley, November, 1998.
18. Kanai, K., “Engineering Seismology”, University of Tokyo Press, Japan, 1983.
19. Kramer, S. and Stewart, J., “Geotechnical Aspects of Seismic Hazard”, “Earthquake Engineering: From Engineering Seismology to Performance Based Engineering”, CRC Press, 2004.
20. Mulugeta, A. “Vibration Analysis and Design of Block-Type Machine Foundation Interacting with Soil” Masters Thesis, Addis Ababa University, March 2003.
21. National Energy Board, “Focus on Safety and Environment, a Comparative Analysis of Pipeline Performance”, Canada: National Energy Board, 2009.
22. NEHRP Consultants Joint Venture, National Institute of Standards and Technology, Willie, E., Acting Under Secretary of commerce for Standards and Technology, “Earthquake-Resilient Lifelines: NEHRP Research, Development and Implementation Roadmap”, U.S. Department of Commerce, NIST GCR 14-917-33, Gaithersburg, Maryland, October, 2014.
23. Roser, M. “Frequencies Extraction of a Cantilever Beam using Finite Element Modelling” April, 2008.
24. Shehata, E. and Toshiro, H., “Soil-Structure Interaction Modeling Effects on Seismic Response of Cable-Stayed Bridge Tower”, International Journal of Advanced Structural Engineering, 2013.
25. Simula, “Abaqus 6.12, CAE User’s Manual”, A product of Dassault Systèmes Simula Corp., Providence, RI, USA, 2012.
26. Simula, “Abaqus 6.12, Getting Started with Abaqus: Interactive Edition”, A product of Dassault Systèmes Simula Corp., Providence, RI, USA, 2012.

27. Soliman, H. and Datta, T., "Response of Over-Ground Pipelines to Random Ground Motion", Civil Engineering Department, Indian Institute of Technology, New Delhi-110016, India, 1995.
28. Soneji, B. and Jangidi, R " Influence of Soil-Structure Interaction on Response of Seismically Isolated Cable-Stayed Bridge" Civil Engineering Department, Indian Institute of Technology, Munbai, India, 2010.
29. Spinelli, C. and Prandi, L.," High Grade Steel Pipeline for Long Distance Projects at Intermediate Pressure", 7th Pipeline Technology Conference, 2012.
30. Wachel, j. and Kenneth, E "Piping Vibration" Engineering dynamics, incorporated san Antonio, Texas.
31. www.sepbearings.com/Fluorgold Slide Bearings and Fluorotemp Registered Trademarks of Saint-Gobain.html

APPENDIX

APPENDIX A

Table A1: Dynamic stiffness's and dashpot coefficients for arbitrarily shaped foundation on the surface of a homogeneous stratum over bedrock.

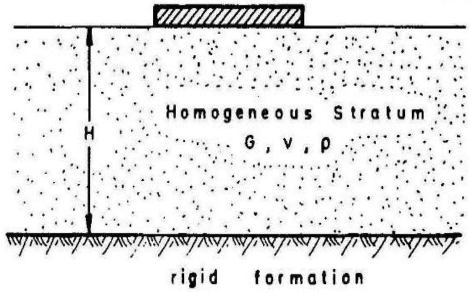

Foundation Shape		Circular Foundation of Radius $B = R$	Rectangular Foundation $2B$ by $2L$ $(L > B)$	Strip Foundation $2L \to \infty$
Static stiffnesses, K	Vertical, z	$K_z = \dfrac{4GR}{1-\nu}\left(1 + 1.3\dfrac{R}{H}\right)$	$K_z = \dfrac{2GL}{1-\nu}\left[0.73 + 1.54\left(\dfrac{B}{L}\right)^{3/4}\right]\left(1 + \dfrac{\frac{B}{H}}{0.5 + \frac{B}{L}}\right)$	$\dfrac{K_z}{2L} \simeq \dfrac{0.73G}{1-\nu}\left(1 + 3.5\dfrac{B}{H}\right)$
	Lateral, y	$K_y = \dfrac{8GR}{2-\nu}\left(1 + 0.5\dfrac{R}{H}\right)$	•	$\dfrac{K_y}{2L} \simeq \dfrac{2G}{2-\nu}\left(1 + 2\dfrac{B}{H}\right)$
	Lateral, x	$K_x = K_y$	•	—
	Rocking, rx	$K_{rx} = \dfrac{8GR}{3(1-\nu)}\left(1 + 0.17\dfrac{R}{H}\right)$	•	$\dfrac{K_{rx}}{2L} = \dfrac{\pi GB^2}{2(1-\nu)}\left(1 + 0.2\dfrac{B}{H}\right)$
	Rocking, ry	$K_{ry} = K_{rx}$	•	—
	Torsional, t	$K_t = \dfrac{16}{3}GR^3\left(1 + 0.10\dfrac{R}{H}\right)$	•	—
Dynamic stiffness coefficients, $k(\omega)$	Vertical, z	$k_z = k_z(H/R, a_0)$ is obtained from Graph III-1	$k_z = k_z(H/B, L/B, a_0)$ is plotted in Graph III-2 for rectangles and strip	
	Horizontal, y or x	$k_y = k_y(H/R, a_0)$ is obtained from Graph III-1	•	$k_y = k_y(H/B, a_0)$ is obtained from Graph III-3
	Rocking, rx or ry Torsional	$k_\alpha(H/R) \simeq k_\alpha(\infty)$, $\alpha = rx, ry, t$	• •	$k_{rx}(H/R) \simeq k_{rx}(\infty)$
Radiation dashpot coefficients, $C(\omega)$	Vertical, z	$C_z(H/B) \simeq 0$ at frequencies $f < f_c$, regardless of foundation shape $C_z(H/B) \simeq 0.8C_z(\infty)$ at $f \geqslant 1.5f_c$ At intermediate frequencies: interpolate linearly. $f_c = \dfrac{V_{La}}{4H}$, $V_{La} = \dfrac{3.4V_s}{\pi(1-\nu)}$		
	Lateral, y or x	$C_y(H/B) \simeq 0$ at $f < \frac{3}{4}f_s$; $C_y(H/B) \simeq C_y(\infty)$ at $f > \frac{4}{3}f_s$ At intermediate frequencies: interpolate linearly. $f_s = V_s/4H$. Similarly for C_x		
	Rocking, rx or ry	$C_{rx}(H/B) \simeq 0$ at $f < f_c$; $C_{rx}(H/B) \simeq C_{rx}(\infty)$ at $f > f_c$. Similarly for C_{ry}		
	Torsional, t	$C_t(H/B) \simeq C_t(\infty)$		

Graph A1: Accompanying table A1

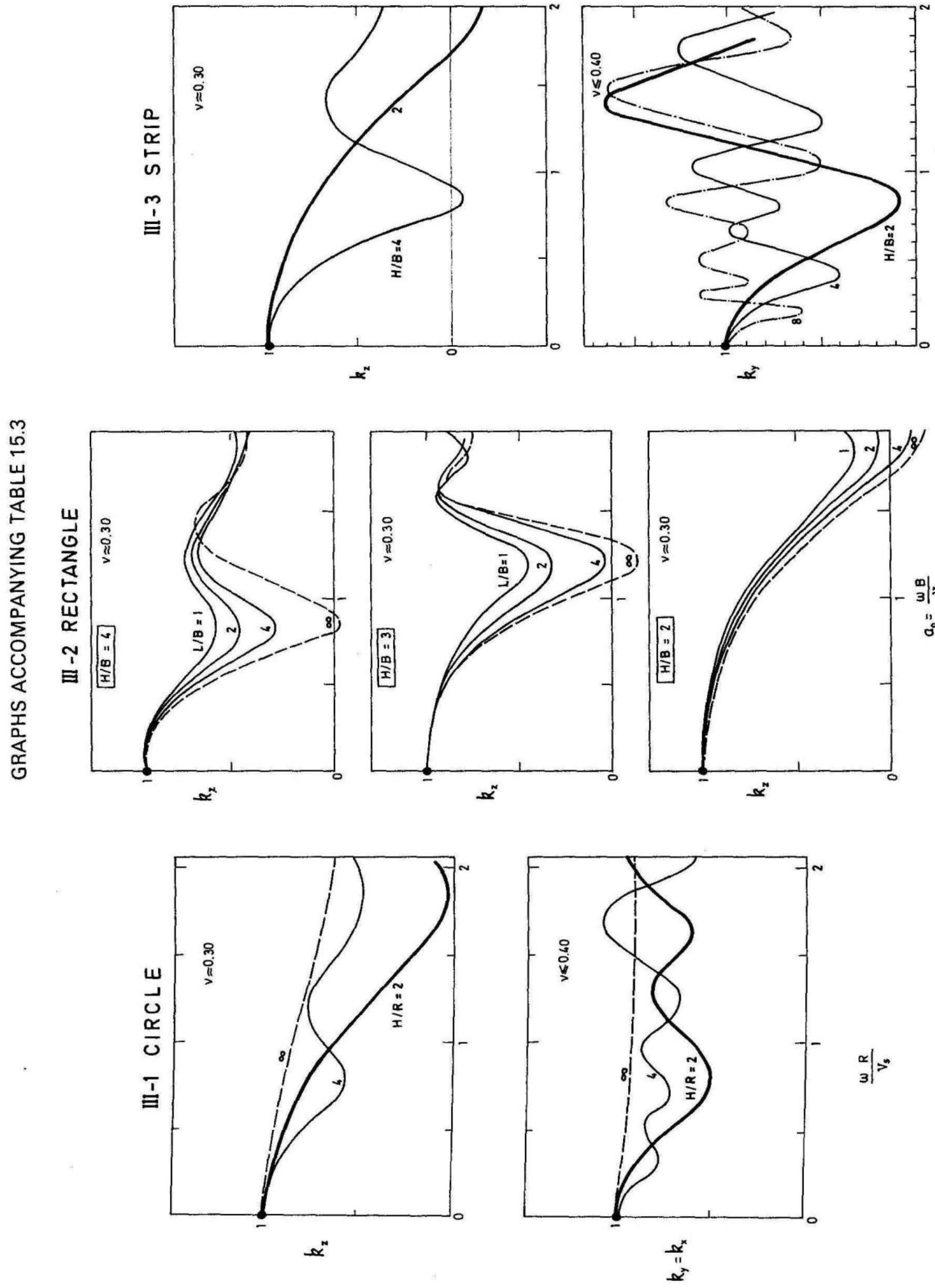

Table A2: Dynamic stiffness's and dashpot coefficients for arbitrarily shaped foundation on the surface of a homogeneous half space.

Vibration Mode	Dynamic Stiffness $\bar{K} = K \cdot k(\omega)$ — Static Stiffness K — General Shape (foundation–soil contact surface is of area A_b and has a circumscribed rectangle $2L$ by $2B$; $L > B$)*	Square $L = B$	Dynamic Stiffness Coefficient k (General shape; $0 \leqslant a_0 \leqslant 2$)†	Radiation Dashpot Coefficient C (General Shapes)
Vertical, z	$K_z = \frac{2GL}{1-\nu}(0.73 + 1.54\chi^{0.75})$ with $\chi = \frac{A_b}{4L^2}$	$K_z = \frac{4.54GB}{1-\nu}$	$k_z = k_z\left(\frac{L}{B}, \nu; a_0\right)$ is plotted in Graph a	$C_z = (\rho V_{La} A_b) \cdot \tilde{c}_z$ $\tilde{c}_z = \tilde{c}_z(L/B, \nu; a_0)$ is plotted in Graph c
Horizontal, y (in the lateral direction)	$K_y = \frac{2GL}{2-\nu}(2 + 2.50\chi^{0.85})$	$K_y = \frac{9GB}{2-\nu}$	$k_y = k_y\left(\frac{L}{B}; a_0\right)$ is plotted in Graph b	$C_y = (\rho V_s A_b) \cdot \tilde{c}_y$ $\tilde{c}_y = \tilde{c}_y(L/B; a_0)$ is plotted in Graph d
Horizontal, x (in the longitudinal direction)	$K_x = K_y - \frac{0.2}{0.75-\nu} GL\left(1 - \frac{B}{L}\right)$	$K_x = K_y$	$k_x \simeq 1$	$C_x \simeq \rho V_s A_b$
Rocking, rx (around longitudinal x axis)	$K_{rx} = \frac{G}{1-\nu} I_{bx}^{0.75}\left(\frac{L}{B}\right)^{0.25}\left(2.4 + 0.5\frac{B}{L}\right)$ with $I_{bx}(I_{by})$ area moment of inertia of the foundation–soil contact surface around the $x(y)$ axis	$K_{rx} = \frac{3.6GB^3}{1-\nu}$	$k_{rx} \simeq 1 - 0.20a_0$	$C_{rx} = (\rho V_{La} I_{bx}) \cdot \tilde{c}_{rx}$ $\tilde{c}_{rx} = \tilde{c}_{rx}(L/B; a_0)$ is plotted in Graphs e and f
Rocking, ry (around lateral axis)	$K_{ry} = \frac{G}{1-\nu} I_{by}^{0.75}\left[3\left(\frac{L}{B}\right)^{0.15}\right]$	$K_{ry} = K_{rx}$	$\nu < 0.45$: $k_{ry} \simeq 1 - 0.30a_0$ $\nu \simeq 0.50$: $k_{ry} \simeq 1 - 0.25a_0\left(\frac{L}{B}\right)^{0.30}$	$C_{ry} = (\rho V_{La} I_{by}) \cdot \tilde{c}_{ry}$ $\tilde{c}_{ry} = \tilde{c}_{ry}(L/B; a_0)$ is plotted in Graph g
Torsional	$K_t = GJ_b^{0.75}\left[4 + 11\left(1 - \frac{B}{L}\right)^{10}\right]$ with $J_b = I_{bx} + I_{by}$ being the polar moment of the soil–foundation contact surface	$K_t = 8.3GB^3$	$k_t \simeq 1 - 0.14a_0$	$C_t = (\rho V_s J_b) \cdot \tilde{c}_t$ $\tilde{c}_t = \tilde{c}_t(L/B; a_0)$

* Note that as $L/B \to \infty$ (strip footing) the theoretical values of K_z and $K_y \to 0$; the values computed from the two given formulas correspond to a footing with $L/B \approx 20$.
† $a_0 = \omega B / V_s$.

Graph A2: Accompanying table A2.

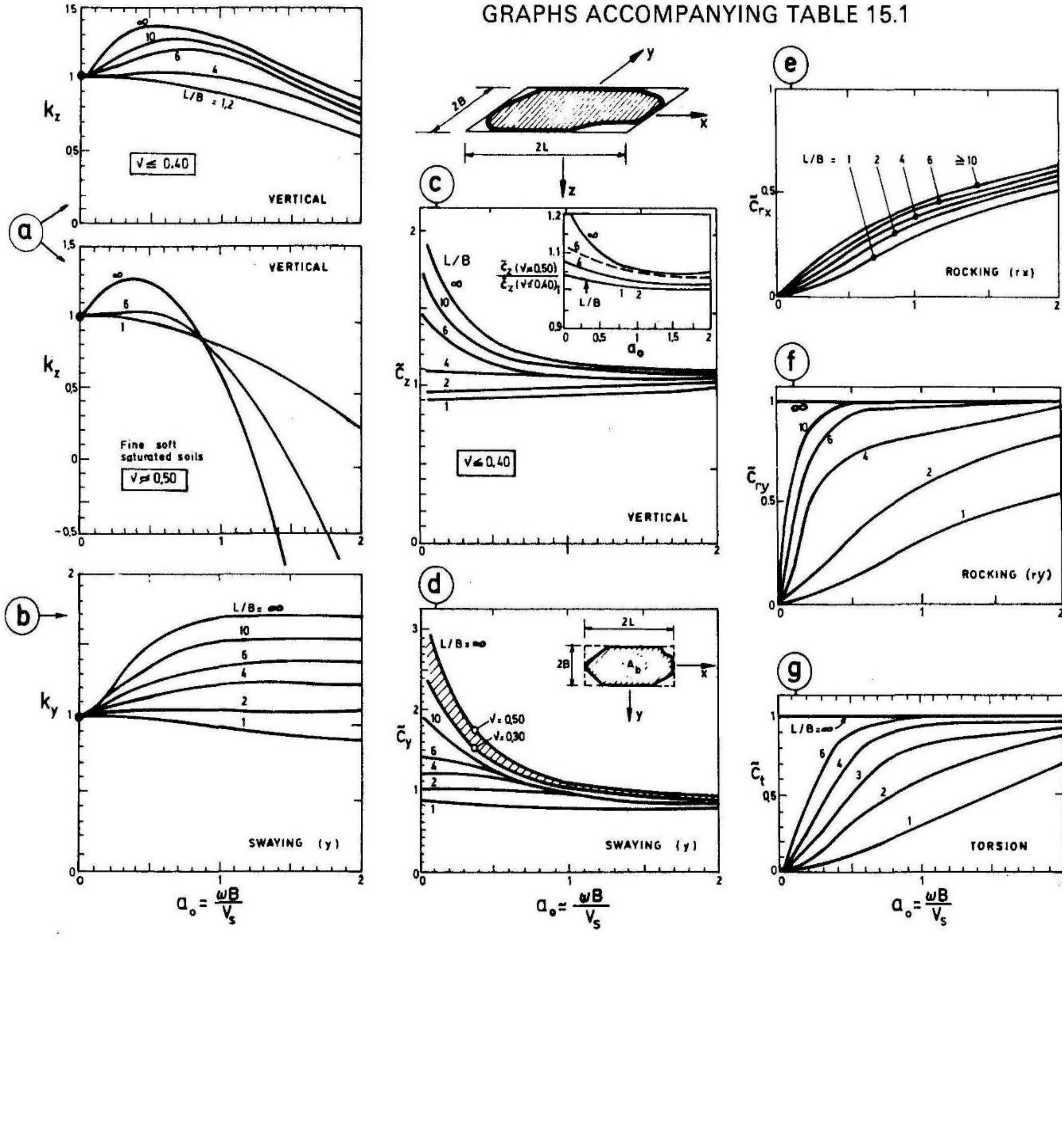

Table A3: Dynamic stiffness's and dashpot coefficients for arbitrarily shaped foundation embedded in of a homogeneous half space.

Vibration Mode	Dynamic Stiffness $\bar{K}_{emb} = K_{emb} \cdot k_{emb}(\omega)$		Radiation Dashpot Coefficient $C_{emb}(\omega)$	
	Static Stiffness K_{emb} For foundations with arbitrarily-shaped basemat A_b of circumscribed rectangle $2L$ by $2B$; total sidewall–soil contact area A_w (or constant sidewall–soil contact height d)	Dynamic Stiffness Coefficient $k_{emb}(\omega)$ $0 < a_0 \leqslant 2$	General Foundation Shape	Rectangular Foundation $2L$ by $2B$ by d
Vertical, z	$K_{z,emb} = K_{z,sur}\left[1 + \frac{1}{21}\frac{D}{B}(1 + 1.3\chi)\right] \times \left[1 + 0.2\left(\frac{A_w}{A_b}\right)^{2/3}\right]$ $K_{z,sur}$ obtained from Table 15.1 A_w = actual sidewall–soil contact area; for constant effective contact height d along the perimeter $A_w = (d) \times (\text{Perimeter}), \chi = A_b/4L^2$	$\nu \leqslant 0.40$: Fully embedded: $k_{z,emb} \simeq k_{z,sur}\left[1 - 0.09\left(\frac{D}{B}\right)^{3/4} a_0^2\right]$ In a trench: $k_{z,tre} \simeq k_{z,sur}\left[1 + 0.09\left(\frac{D}{B}\right)^{3/4} a_0^2\right]$ Partially embedded: estimate by interpolating between the two $\nu \approx 0.50^-$: Fully embedded, $L/B = 1\text{–}2$ $k_{z,emb} \simeq 1 - 0.09(D/B)^{3/4} a_0^2$ Fully embedded, $L/B > 3$ $k_{z,emb} \simeq 1 - 0.35(D/B)^{1/2} a_0^{3.5}$	$C_{z,emb} = C_{z,sur} + \rho V_s A_w$ with $C_{z,sur}$ and $\tilde{c}_z$ according to Table 15.1	$C_{z,emb} = 4\rho V_{La} B L \tilde{c}_z + 4\rho V_s (B + L) d$
Horizontal, y or x	$K_{y,emb} = K_{y,sur}\left(1 + 0.15\sqrt{\frac{D}{B}}\right) \times \left[1 + 0.52\left(\frac{h}{B}\frac{A_w}{L^2}\right)^{0.4}\right]$ $K_{y,sur}$ obtained from Table 15.1 $K_{x,emb}$ similarly computed from $K_{x,sur}$	$k_{y,emb}$ and $k_{x,emb}$ can be estimated in terms of $L/B, D/B$, and d/B for each value of a_0 from the graphs accompanying this table	$C_{y,emb} = C_{y,sur} + \rho V_s A_{w_s} + \rho V_{La} A_{wce}$ $A_{w_s} = \sum(A_{wi} \sin \vartheta_i)$ = total effective sidewall area shearing the soil $A_{wce} = \sum(A_{wi} \cos \vartheta_i)$ = total effective sidewall area compressing the soil ϑ_i angle of inclination of surface A_{wi} from loading direction $C_{y,sur}$ obtained from Table 15.1 $C_{x,emb}$ similarly computed from $C_{x,sur}$	$C_{y,emb} = 4\rho V_s B L \tilde{c}_y + 4\rho V_s B d + 4\rho V_{La} L d$ $\tilde{c}_y$ according to Table 15.1

Rocking, rx (around the longitudinal axis) Rocking, ry (around the lateral axis)	Expressions valid for any basemat shape but constant effective contact height d along the perimeter $K_{rx,emb} = K_{rx,sur} \cdot \left\{1 + 1.26\frac{d}{B}\left[1 + \frac{d}{B}\left(\frac{d}{D}\right)^{-0.2}\sqrt{\frac{B}{L}}\right]\right\}$ $K_{ry,emb} = K_{ry,sur} \cdot \left\{1 + 0.92\left(\frac{d}{L}\right)^{0.6}\left[1.5 + \left(\frac{d}{L}\right)^{1.9} \times \left(\frac{d}{D}\right)^{-0.6}\right]\right\}$	$k_{rx,emb} \simeq k_{rx,sur}$ $k_{ry,emb} \simeq k_{ry,sur}$	$C_{rx,emb} = C_{rx,sur} + \rho V_{La} I_{wce}\tilde{c}_1 + \rho V_s\left(J_{ws} + \sum_i [A_{wcei}\Delta_i^2]\right)\tilde{c}_1$ $\tilde{c}_1 = 0.25 + 0.65\sqrt{a_0}\left(\frac{d}{D}\right)^{-a0/2} \times \left(\frac{D}{B}\right)^{-1/4}$ I_{wce} = total moment of inertia about their base axes parallel to x of all sidewall surfaces effectively compressing the soil Δ_i = distance of surface A_{wcai} from the x axis J_{ws} = polar moment of inertia about their base axes parallel to x of all sidewall surfaces effectively shearing the soil $C_{ry,emb}$ is similarly evaluated from $C_{ry,sur}$ with y replacing x and, in the equation for c_1, L replacing B	$C_{rx,emb} = \frac{4}{3}\rho V_{La} B^3 L\tilde{c}_{rx} + \frac{4}{3}\rho V_{La} d^3 L\tilde{c}_1 + \frac{4}{3}\rho V_s Bd(B^2 + d^2)\tilde{c}_1 + 4\rho V_s B^2 dL\tilde{c}_1$ with $\tilde{c}_1$ as in the preceding column and $\tilde{c}_{rx}$ according to Table 15.1
Coupling term Swaying–rocking (x, ry) Swaying–rocking (y, rx)	$K_{xry,emb} \simeq \frac{1}{3}dK_{x,emb}$ $K_{yrx,emb} \simeq \frac{1}{3}dK_{y,emb}$	$k_{rxy,emb} \simeq k_{yrx,emb} \simeq 1$	$C_{xry,emb} \approx \frac{1}{3}dC_{x,emb}$ $C_{yrx,emb} \approx \frac{1}{3}dC_{y,emb}$	as in the previous column
Torsional	$K_{t,emb} = K_{t,sur} \times \left[1 + 1.4\left(1 + \frac{B}{L}\right)\left(\frac{d}{B}\right)^{0.9}\right]$	$k_{t,emb} \simeq k_{t,sur}$	$C_{t,emb} = C_{t,sur} + \rho V_{La} J_{wce}\tilde{c}_2 + \rho V_s \sum [A_{wi}\Delta_{zi}^2]\tilde{c}_2$ $\tilde{c}_2 \approx \left(\frac{d}{D}\right)^{-0.5} \cdot \frac{a_0^2}{a_0^2 + \frac{1}{2}(L/B)^{-1.5}}$ J_{wce} = total moment of inertia of all sidewall surfaces effectively compressing the soil about the projection of the z axis onto their plane Δ_{zi} = distance of surface A_{wi} from the z axis	$C_{t,emb} = \frac{4}{3}\rho V_s BL(B^2 + L^2)\tilde{c}_t + \frac{4}{3}\rho V_{La} d(L^3 + B^3)\tilde{c}_2 + 4\rho V_s dBL(B + L)\tilde{c}_2$ with $\tilde{c}_2$ as in the preceding column and $\tilde{c}_t$ according to Table 15.1

NOTE: $V_{La} = \frac{3.4}{\pi(1 - \nu)} V_s$ is the apparent propagation velocity of compression–extension waves.

Graph A3: Accompanying table A2 and table A3.

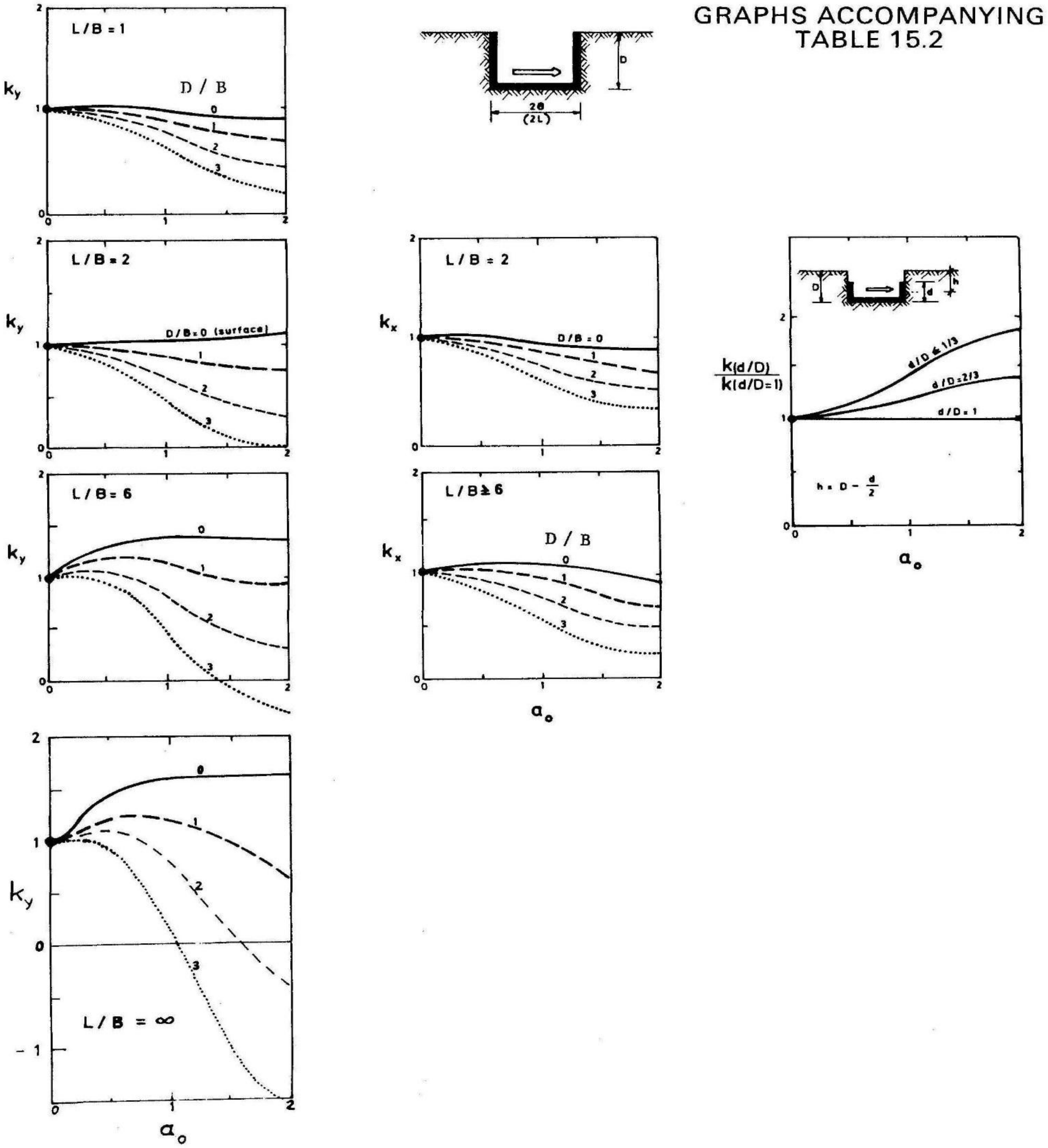

APPENDIX B

Table: B1ground type.

Ground type	Description of stratigraphic profile	Parameters		
		$v_{s,30}$ (m/s)	N_{SPT} (blows/30cm)	c_u (kPa)
A	Rock or other rock-like geological formation, including at most 5 m of weaker material at the surface.	> 800	–	–
B	Deposits of very dense sand, gravel, or very stiff clay, at least several tens of meters in thickness, characterized by a gradual increase of mechanical properties with depth.	360 – 800	> 50	> 250
C	Deep deposits of dense or medium-dense sand, gravel or stiff clay with thickness from several tens to many hundreds of meters.	180 – 360	15 - 50	70 - 250
D	Deposits of loose-to-medium cohesionless soil (with or without some soft cohesive layers), or of predominantly soft-to-firm cohesive soil.	< 180	< 15	< 70
E	A soil profile consisting of a surface alluvium layer with v_s values of type C or D and thickness varying between about 5 m and 20 m, underlain by stiffer material with v_s > 800 m/s.			
S_1	Deposits consisting, or containing a layer at least 10 m thick, of soft clays/silts with a high plasticity index (PI > 40) and high water content	< 100 (indicative)	–	10 - 20
S_2	Deposits of liquefiable soils, of sensitive clays, or any other soil profile not included in types A – E or S_1			

Table B2: Tensile requirement for PLS 2

(1)	(2)		(3)		(4)		(5)		(6)
	Yield Strength, Minimum		Yield Strength, Maximum[b]		Ultimate Tensile Strength, Minimum		Ultimate Tensile Strength, Maximum[c]		Elongation in 2 in. (50.8 mm), Minimum, Percent
Grade	psi	MPa	psi	MPa	psi	MPa	psi	MPa	
B	35,000	(241)	65,000[d]	(448)	60,000	(414)	110,000	(758)	a
X42	42,000	(290)	72,000	(496)	60,000	(414)	110,000	(758)	a
X46	46,000	(317)	76,000	(524)	63,000	(434)	110,000	(758)	a
X52	52,000	(359)	77,000	(531)	66,000	(455)	110,000	(758)	a
X56	56,000	(386)	79,000	(544)	71,000	(490)	110,000	(758)	a
X60	60,000	(414)	82,000	(565)	75,000	(517)	110,000	(758)	a
X65	65,000	(448)	87,000	(600)	77,000	(531)	110,000	(758)	a
X70	70,000	(483)	90,000	(621)	82,000	(565)	110,000	(758)	a
X80	80,000	(552)	100,000[e]	(690)	90,000	(621)	120,000	(827)	a

APPENDIX C

VALIDATION OF FINITE ELEMENT BASED SOFTWARE/ ABAQUS

Large span pipeline structures can be analyzed more easily using a finite element software tool. These pipeline structures have uniform cylindrical shape supported by special materials in order to accommodate the thermal effect.

As a common rule, FEA results such as displacements, stresses, reaction forces, etc., should be compared with experimental testing and other classical numerical method in order to evaluate if the numerical solutions correlate with the response of the physical structure. Of many other methods of comparison, experimental testing is one of the ideal forms of comparison. However, experiments generally are expensive and lengthy [2].

In the scope of the study, the model verification is based on a cantilever beam model and compare the results from analytical approached/numerical method using simple hand calculation with SCILAB matrix solver tool aid against the finite element-based ABAQUS/CAE software

The result used for comparison purpose are the natural frequency of the beam and the tip displacement as concentrated mass is applied at the end of the cantilever beam. The initial parameters chosen for the numerical model-dimensions of the cantilever beam and other data is shown in Table. C1.

Table C1: Model-dimension parameters of 2D cantilever beam.

Parameter	**Notation**	**Value**
Length (m)	L	1.3
Width (m)	b	0.06
Height (m)	h	0.004
Young modulus (N/m^2)	E	$210x10^9$
Density (kg/m3)	ρ	$7.850x10^3$
Concentrated mass at free end	Kg	0.5

For the purpose of numerical method finite element approach is selected to analyze cantilever beam structure, by using the data from table 1. Most frequently the natural frequency and mode of a system is obtained by using type of mathematical problem which is called an eigenvalue problem in Eq. C1.

$$([\mathrm{k}] - \omega\mathrm{n}^2[\mathrm{M}]) - \{u\} = 0 \tag{C.1}$$

where k = Assembled stiffness matrix

ωn =Natural circular frequency

M = Assembled mass matrix and

u = Displacement

When solving Eq. C.1, the modal properties of the structure are obtained. These are the natural frequencies-eigenvalues and the displacements-eigenvectors or also called as mode shapes of the structure. Changes in the mass and stiffness matrices cause modal properties to be also changed. Thus, the modal properties can be extracted from the identification of the correct mass and stiffness matrices, which need to be calculated [23].

A stiffness and Mass matrix for the assumed 2D beam is prepared by sub-dividing the structure in to 9 elements to get acceptable level accuracy. If further division applied, better accurate results would be expected. However, for the prismatic cantilever structure considered here 9 elements give acceptable accuracy [23].

Each element has two nodes, each of them with three degrees of freedom (DOF): two translational DOF horizontal and vertical and one rotational DOF, as shown in Fig. 26. A SCILAB software tool code is prepared (appendix) by applying the boundary condition for cantilever beam considered.

Figure 42: Presentation of 2D beam-element

Considering 2D Euler-Bernoulli beam element, whose cross section is constant and has area A and density ρ along the length of the element L, the consistent element mass matrix is as in Eq. C.2, which is symmetric.

$$M_{ec} = \frac{\rho.A.L}{420}\begin{bmatrix} 140 & 0 & 0 & 70 & 0 & 0 \\ 0 & 156 & 22L & 0 & 54 & -13L \\ 0 & 22L & 4L^2 & 0 & 13L & -3L^2 \\ 70 & 0 & 0 & 140 & 0 & 0 \\ 0 & 54 & 13L & 0 & 156 & -22L \\ 0 & -13L & -3L^2 & 0 & -22L & 4L^2 \end{bmatrix} \quad \text{(C.2)}$$

Nevertheless, the consistent mass matrix tends to overestimate the natural frequencies of the beam [23]. Moreover, it is normally a full matrix. In order to solve these problems, a lumped mass matrix is created. For the 2D Euler-Bernoulli beam, each matrix element is obtained by assigning half the element mass to each of the translational degrees of freedom and the moment of inertia of half the beam element about the respective nodes to the rotational degrees of freedom, as in Fig. 27.

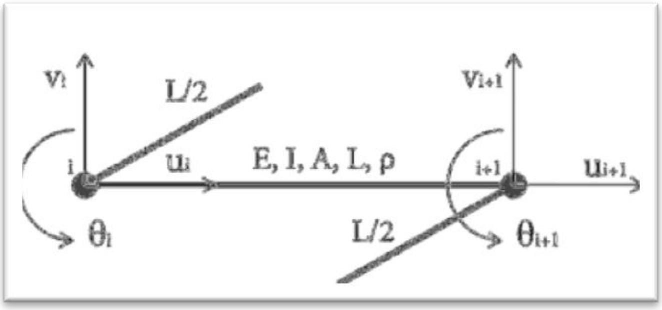

Figure 43: The lumped element mass matrix.

$$M_{el} = \frac{\rho.A.L}{2}\begin{bmatrix} 1 & 0 & 0 & 0 & 0 & 0 \\ 0 & 1 & 0 & 0 & 0 & 0 \\ 0 & 0 & L^2/12 & 0 & 0 & 0 \\ 0 & 0 & 0 & 1 & 0 & 0 \\ 0 & 0 & 0 & 0 & 1 & 0 \\ 0 & 0 & 0 & 0 & 0 & L^2/12 \end{bmatrix} \quad \text{(C.3)}$$

The lumped mass matrix (Eq. C.3) is a diagonal, simpler matrix. On the other hand, it tends to underestimate the natural frequencies of the beam [23]. In order to palliate the errors from both mass matrix formulations, a linear combination of these two matrices is carried out in Eq. C.4.

$$\mathrm{M_e} = (1-\beta) \times \mathrm{M_{el}} + \beta \times \mathrm{M_{ec}} \quad \text{(C.4)}$$

If $\beta = 0.5$ the mass matrix is called “average mass matrix”.

In order to obtain the element stiffness matrix, two effects must be considered separately: axial and bending deformations. The formulation of the first one involves the area of the section and the second one the moment of inertia. For homogeneous isotropic beams, the element stiffness matrix obtained is as in Eq. C.5.

In Eq. C.5 E is the Young’s modulus and $\mathrm{I} = \frac{\mathrm{b}\times\mathrm{h}^3}{12}$ is the bending moment of inertia of the cross section. Here, b is the width of the beam and h its height. Once the element stiffness and mass matrices are obtained, the stiffness and mass matrices of the beam are obtained by an assembly of the element matrices.

$$K_e = \begin{bmatrix} AE/L & 0 & 0 & AE/L & 0 & 0 \\ 0 & 12EI/L^3 & -6EI/L^2 & 0 & -12EI/L^3 & -6EI/L^2 \\ 0 & -6EI/L^2 & 4EI/L & 0 & 6EI/L^2 & 2EI/L \\ AE/L & 0 & 0 & AE/L & 0 & 0 \\ 0 & -12EI/L^3 & 6EI/L^2 & 0 & 12EI/L^3 & 6EI/L^2 \\ 0 & -6EI/L^2 & 2EI/L & 0 & 6EI/L^2 & 4EI/L \end{bmatrix}$$

(C.5)

The assembled mass matrix and the stiffness matrix for this problem is determined in the Appendix C. After running the analysis on SCILAB software tool results are collected. Namely natural cyclic frequency ($\mathrm{f_n}$) and displacement of the free-end from original position before loading to after loading.

For the purpose of this work the first two natural cyclic frequency are obtained both by Numerical method and ABAQUS/CAE.

Table C2: Natural frequency comparison

	Natural frequency		
Mode shape	FEM/Numerical method	ABAQUS/CAE	% Difference
1	1.969	1.977	0.41
2	12.299	12.391	0.75

Table C3: End displacement comparison

End Displacement (mm)		
FEM/Numerical method	ABAQUS/CAE	% Difference
0.152	0.143	5.9

Comparison and conclusion

Based on the analysis conducted results showed in Table. 9 and Table. 10 shows that, the results from the numerical method and the ABAQUS/CAE commercial for displacements and natural frequency are very close. As the result, it is convenient that results from ABAQUS can be used as valid analysis output and it is safe to proceed on analyzing above–ground pipeline structures by ABAQUS/CAE.

APPENDIX D

Scilab code for obtaining the natural frequency and end displacement of cantilever beam

```
//Scilab program for eigen-analysis for cantilever section with concentrated load
at free end.

clear

//m in kg.;

//m=rho*A*L;

rho=7850;

dp=0.004;

wd=0.06;

L=1.3/9;

// A 0.5kg concentrated load is assumed to act at free end.

mcon=0.5

A=wd*dp;

m=rho*A*L;

//consistent mass Mc

Mc=m/420*[280 0      0      70     0      0      0      0      0      0      0      0
       0      0      0      0      0      0      0      0      0      0      0      0
       0      0      0

0      312    0      0      54     -13*L  0      0      0      0      0      0      0
       0      0      0      0      0      0      0      0      0      0      0      0
       0      0

0      0      8*L^2  0      13*L   -3*L^2 0      0      0      0      0      0      0
       0      0      0      0      0      0      0      0      0      0      0      0
       0      0

70     0      0      280    0      0      70     0      0      0      0      0      0
       0      0      0      0      0      0      0      0      0      0      0      0
       0      0

0      54     13*L   0      312    0      0      54     -13*L  0      0      0      0
       0      0      0      0      0      0      0      0      0      0      0      0
       0      0

0      -13*L  -3*L^2 0      0      8*L^2  0      13*L   -3*L^2 0      0      0      0
       0      0      0      0      0      0      0      0      0      0      0      0
       0      0

0      0      0      70     0      0      280    0      0      70     0      0      0
       0      0      0      0      0      0      0      0      0      0      0      0
       0      0
```

```
0       0       0       0       54      13*L    0       312     0       0       54      -13*L   0
        0       0       0       0       0       0       0       0       0       0       0       0
        0       0

0       0       0       0       -13*L   -3*L^2  0       0       8*L^2   0       13*L    -3*L^2  0
        0       0       0       0       0       0       0       0       0       0       0       0
        0       0

0       0       0       0       0       0       70      0       0       280     0       0       70
        0       0       0       0       0       0       0       0       0       0       0       0
        0       0

0       0       0       0       0       0       0       54      13*L    0       312     0       0
        54      -13*L   0       0       0       0       0       0       0       0       0       0
        0       0

0       0       0       0       0       0       0       -13*L   -3*L^2  0       0       8*L^2   0
        13*L    -3*L^2  0       0       0       0       0       0       0       0       0       0
        0       0

0       0       0       0       0       0       0       0       0       70      0       0
        280     0       0       70      0       0       0       0       0       0       0       0
        0       0       0

0       0       0       0       0       0       0       0       0       0       54      13*L    0
        312     0       0       54      -13*L   0       0       0       0       0       0       0
        0       0

0       0       0       0       0       0       0       0       0       0       -13*L   -3*L^2  0
        0       8*L^2   0       13*L    -3*L^2  0       0       0       0       0       0       0
        0       0

0       0       0       0       0       0       0       0       0       0       0       0       70
        0       0       280     0       0       70      0       0       0       0       0       0
        0       0

0       0       0       0       0       0       0       0       0       0       0       0       0
        54      13*L    0       312     0       0       54      -13*L   0       0       0       0
        0       0

0       0       0       0       0       0       0       0       0       0       0       0       0
        -13*L   -3*L^2  0       0       8*L^2   0       13*L    -3*L^2  0       0       0       0
        0       0

0       0       0       0       0       0       0       0       0       0       0       0       0
        0       0       70      0       0       280     0       0       70      0       0       0
        0       0

0       0       0       0       0       0       0       0       0       0       0       0       0
        0       0       0       54      13*L    0       312     0       0       54      -13*L   0
        0       0

0       0       0       0       0       0       0       0       0       0       0       0       0
        0       0       0       -13*L   -3*L^2  0       0       8*L^2   0       13*L    -3*L^2  0
        0       0

0       0       0       0       0       0       0       0       0       0       0       0       0
        0       0       0       0       0       70      0       0       280     0       0       70
        0       0
```

```
0       0       0       0       0       0       0       0       0       0       0       0       0
        0       0       0       0       0       0       54      13*L    0       312     0       0
        54      -13*L

0       0       0       0       0       0       0       0       0       0       0       0       0
        0       0       0       0       0       0       -13*L   -3*L^2  0       0       8*L^2   0
        13*L    -3*L^2

0       0       0       0       0       0       0       0       0       0       0       0       0
        0       0       0       0       0       0       0       0       70      0       0
        140     0       0

0       0       0       0       0       0       0       0       0       0       0       0       0
        0       0       0       0       0       0       0       0       0       54      13*L    0
        156+mcon/(m/420)    22*L

0       0       0       0       0       0       0       0       0       0       0       0       0
        0       0       0       0       0       0       0       0       0       -13*L   -3*L^2  0
        -22*L   4*L^2];

//E=210Gpa;

E=210*10^9;

I=wd*dp^3/12;

//k in N/m;

K= [2*A*E/L  0       0       A*E/L   0       0       0       0       0       0       0       0
        0       0       0       0       0       0       0       0       0       0       0       0
        0       0       0

0       24*E*I/L^3      0       0       -12*E*I/L^3     -6*E*I/L^2      0       0       0       0
        0       0       0       0       0       0       0       0       0       0       0       0
        0       0       0       0       0

0       0       8*E*I/L         0       6*E*I/L^2       2*E*I/L         0       0       0       0
        0       0       0       0       0       0       0       0       0       0       0       0
        0       0       0       0       0

A*E/L   0       0       2*A*E/L         0       0       A*E/L   0       0       0       0       0
        0       0       0       0       0       0       0       0       0       0       0       0
        0       0       0

0       -12*E*I/L^3     6*E*I/L^2       0       24*E*I/L^3      0       0       -12*E*I/L^3     -
6*E*I/L^2       0       0       0       0       0       0       0       0       0       0       0
        0       0       0       0       0       0       0

0       -6*E*I/L^2      2*E*I/L         0       0       8*E*I/L         0       6*E*I/L^2
        2*E*I/L         0       0       0       0       0       0       0       0       0       0
        0       0       0       0       0       0       0       0

0       0       0       A*E/L   0       0       2*A*E/L         0       0       A*E/L   0       0
        0       0       0       0       0       0       0       0       0       0       0       0
        0       0       0

0       0       0       0       -12*E*I/L^3     6*E*I/L^2       0       24*E*I/L^3      0       0
        -12*E*I/L^3     -6*E*I/L^2      0       0       0       0       0       0       0       0
        0       0       0       0       0       0       0
```

```
0	0	0	0	-6*E*I/L^2	2*E*I/L	0	0	8*E*I/L	0
	6*E*I/L^2	2*E*I/L	0	0	0	0	0	0	0	0
	0	0	0	0	0	0	0

0	0	0	0	0	0	A*E/L	0	0	2*A*E/L	0	0
	A*E/L	0	0	0	0	0	0	0	0	0	0	0
	0	0	0

0	0	0	0	0	0	0	-12*E*I/L^3	6*E*I/L^2	0
	24*E*I/L^3	0	0	-12*E*I/L^3	-6*E*I/L^2	0	0	0	0
	0	0	0	0	0	0	0	0

0	0	0	0	0	0	0	-6*E*I/L^2	2*E*I/L	0	0
	8*E*I/L	0	6*E*I/L^2	2*E*I/L	0	0	0	0	0
	0	0	0	0	0	0	0

0	0	0	0	0	0	0	0	0	A*E/L	0	0
	2*A*E/L	0	0	A*E/L	0	0	0	0	0	0	0
	0	0	0	0

0	0	0	0	0	0	0	0	0	0	-12*E*I/L^3
	6*E*I/L^2	0	24*E*I/L^3	0	0	-12*E*I/L^3	-6*E*I/L^2	0
	0	0	0	0	0	0	0	0

0	0	0	0	0	0	0	0	0	0	-6*E*I/L^2
	2*E*I/L	0	0	8*E*I/L	0	6*E*I/L^2	2*E*I/L	0
	0	0	0	0	0	0	0	0

0	0	0	0	0	0	0	0	0	0	0	0
	A*E/L	0	0	2*A*E/L	0	0	A*E/L	0	0	0	0
	0	0	0	0

0	0	0	0	0	0	0	0	0	0	0	0	0
	-12*E*I/L^3	6*E*I/L^2	0	24*E*I/L^3	0	0	-12*E*I/L^3	-
6*E*I/L^2	0	0	0	0	0	0

0	0	0	0	0	0	0	0	0	0	0	0	0
	-6*E*I/L^2	2*E*I/L	0	0	8*E*I/L	0	6*E*I/L^2
	2*E*I/L	0	0	0	0	0	0

0	0	0	0	0	0	0	0	0	0	0	0	0
	0	0	A*E/L	0	0	2*A*E/L	0	0	A*E/L	0	0
	0	0	0

0	0	0	0	0	0	0	0	0	0	0	0	0
	0	0	0	-12*E*I/L^3	6*E*I/L^2	0	24*E*I/L^3	0	0
	-12*E*I/L^3	-6*E*I/L^2	0	0	0

0	0	0	0	0	0	0	0	0	0	0	0	0
	0	0	0	-6*E*I/L^2	2*E*I/L	0	0	8*E*I/L	0
	6*E*I/L^2	2*E*I/L	0	0	0

0	0	0	0	0	0	0	0	0	0	0	0	0
	0	0	0	0	0	A*E/L	0	0	2*A*E/L	0	0
	A*E/L	0	0

0	0	0	0	0	0	0	0	0	0	0	0	0
	0	0	0	0	0	0	-12*E*I/L^3	6*E*I/L^2	0
	24*E*I/L^3	0	0	-12*E*I/L^3	-6*E*I/L^2
```

```
0      0      0      0      0      0      0      0      0      0      0      0      0
       0      0      0      0      0      0      -6*E*I/L^2    2*E*I/L      0      0
       8*E*I/L      0      6*E*I/L^2    2*E*I/L

0      0      0      0      0      0      0      0      0      0      0      0      0
       0      0      0      0      0      0      0      0      A*E/L  0      0
       A*E/L  0      0

0      0      0      0      0      0      0      0      0      0      0      0      0
       0      0      0      0      0      0      0      0      0      -12*E*I/L^3
       6*E*I/L^2    0      12*E*I/L^3   6*E*I/L^2

0      0      0      0      0      0      0      0      0      0      0      0      0
       0      0      0      0      0      0      0      0      0      -6*E*I/L^2
       2*E*I/L      0      6*E*I/L^2    4*E*I/L];

M=Mc

[a,b,f]=spec(K,M)

w2=a./b;

w=sqrt(w2)

Freq=(1/(2*%pi))*w

//To find the displacement the force vector is prepared by considering own weight of the members

//and additional weight is applied at free end which is 0.5kg.Thus F vector is the resulting force vector.

//Weight per meter of the member is given as rho*A=wtpm

Wtpm=rho*A;

//Equivalent joint load from distributed own weight and concentrated load at 9th node is included in F vector from reduced matrix based the boundary condition.

F=[0   wtpm*L 0      0      wtpm*L 0      0      wtpm*L 0      0      wtpm*L 0      0
       wtpm*L 0      0      wtpm*L 0      0      wtpm*L 0      0      wtpm*L 0      0
       wtpm*L/2+0.5*9.81   0]'

D=inv(K)*F
```